Insights into the Origin of the CNS: Early Development of Aminergic Neurons in Molluscs

by

Griffin A. Beach

Submitted in partial fulfilment of the requirements
for the degree of Master of Science

at

Dalhousie University
Halifax, Nova Scotia
April 2022

Dedicated to all who struggled with uncertainty during the covid-19 pandemic,
and those among us who chose to spread kindness and compassion over hate and fear

TABLE OF CONTENTS

LIST OF TABLES

LIST OF FIGURES

ABSTRACT

Advances in molecular approaches over the last few decades have offered new insights into animal phylogeny, revitalizing discussions on the origin of the central nervous system (CNS). Evidence of conserved developmental genes over this time has led many to postulate a single origin of the CNS. However, the degree of morphological diversity across the animal kingdom and recent phylogenetic analyses support multiple origins of the CNS. Research on how these conserved genes are structured into gene regulatory networks that lead to morphological change is required to clarify the discrepancy between conserved developmental mechanisms and morphological diversity. The current thesis aims to inform such studies by expanding previous descriptions of larval neurodevelopment in gastropod molluscs, laying the framework for comparative studies among more distant phyla. Among early developmental descriptions, the ontogenesis of serotonergic, FMRFamidergic and catecholaminergic neural elements have been investigated. To expand on these descriptions, techniques were used to investigate the development of histaminergic and octopaminergic neurons in larva of *Ilyanassa obsoleta* and *Aplysia californica*. Results in this thesis reveal early histaminergic labelling of the statocysts forming commissural fibers that could potentially pioneer the development of the cerebral commissure and connectives; this result also suggests early integration and functionality of the statocysts. Additionally, later stages of development revealed histaminergic neural elements that project throughout the posterior loop of the developing CNS with neurons located in nearly every adult ganglion and foot. Based on criteria used in this study, octopamine (OA) was absent in the larval nervous system; however, results confirmed the conservation of dopamine β-hydroxylase (DBH) and its colocalization with OA in adult molluscan neurons. Together the current thesis provides novel descriptions of larval neurotransmitter systems and identifies an antibody that targets a conserved region of DBH making it suitable for comparative developmental studies. Additionally, these results offer insights into aspects of early neurogenesis and neuronal diversity in gastropod molluscs laying the framework for future comparisons among distantly related phyla that can be used to inform evolutionary relationships.

LIST OF ABBREVIATIONS USED

µg	Microgram
µl	Microliter
µm	Micrometer
5-HT	Serotonin
AADC	Aromatic Amino Acid Decarboxylase
AcT	Acetylated Tubulin
BMP4	*Bone morphogenetic protein 4*
BSA	Bovine Serum Albumin
CH_2O	Formaldehyde
CNS	Central Nervous System
DAPI	4',6-diamidino-2-phenylindole
DBH	Dopamine β-Hydroxylase
DDC	DOPA Decarboxylase
DMSO	Dimethylsulfoxide
DNA	Deoxyribonucleic Acid
DOC	sodium deoxycholate
DPO	Days Post Oviposition
dpp	*decapentaplegic*; invertebrate orthologue to *BMP4*
DTB	Deutocerebral-tritocerebral boundary
EDAC	1-Ethyl-3-(3-dimethylaminopropyl)carbodiimide
ems	*empty spiracles*; invertebrate homeobox gene
Emx	*empty spiracles*; vertebrate homeobox orthologue
EX	X% of embryonic development
ey	*eyeless*; *Pax6* invertebrate homologue
FSW	Mixture of Filtered Artificial and Natural Seawater
GABA	γ-Aminobutyric Acid
Gbx	*unplugged*; vertebrate homeobox orthologue
GRN	Gene Regulatory Network
HA	Histamine

$HNaPO_4$	Sodium Phosphate Monobasic
Hox	Homeotic/Homeobox
hr	Hour
kDa	Kilodalton
KLH	Keyhole Limpet Hemocyanin
LIR	Like Immunoreactive
M	Molar
MeOH	Methanol
mg	Milligram
$MgCl_2$	Magnesium Chloride
MHB	Midbrain-Hindbrain Boundary
min	Minute
ml	Milliliter
mM	Millimolar
Na_2PO_4	Sodium Phosphate Dibasic
NaCl	Sodium Chloride
NCBI	National Center for Biotechnology Information
NE	Norepinephrine
NHS	*N*-Hydroxysuccinimide
NIH	National Institutes of Health
OA	Octopamine
^oC	Degrees Celsius
otd	*orthodenticle*; invertebrate homeobox gene
Otx	*othodenticle*; vertebrate homeobox orthologue
PAGE	Polyacrylamide Gel Electrophoresis
Pax	Paired Box
PBS	Phosphate Buffered Saline
PBT	Phosphate Buffered Saline with 0.5% Triton X-100
PFA	Paraformaldehyde
pH	Potential of Hydrogen
PLP	Periodate-Lysine-Paraformaldehyde

RIPA	Radioimmunoprecipitation Assay
rpm	Rotations Per Minute
RT	Room Temperature
SDS	Sodium Dodecyl Sulfate
sog	*short gastrulation*; invertebrate orthologue to *Chordin*
TAC	Transient Anterior Catecholaminergic
TALE	Transcription Activatior-Like Nucleases
TBH	Tyramine β-Hydroxylase
TBST	Tris-Buffered Saline with Tween
TDC	Tyrosine Decarboxylase
TH	Tyrosine Hydroxylase
unpg	*unplugged*; invertebrate homeobox gene

ACKNOWLEDGEMENTS

I am deeply appreciative of my supervisor, Dr. Roger Croll, for his many years of mentorship and support; throughout my undergraduate and graduate degrees he has continued to provide me opportunities to gain experience and develop skills in research, for which I am forever grateful. I sincerely thank the members of my supervisory committee: Dr. Russell Wyeth for managing the scope and feasibility of the proposed study; Dr. Stefan Krueger for technical advice regarding protein extractions and western blots leading to success with probing for low abundant proteins; and Dr. Yassine El Hiani for providing training and supplies related to my success with western blots. All members of my supervisory committee provided thoughtful feedback and discussion over the duration of my degree. Additionally, I would like to thank Christina Irving and Dr. Elizabeth Cowley for training me to perform and providing essential equipment related to western blots and protein concentration assays. I also thank Annette Kolar for technical advice regarding protein extractions and western blots that led to success with probing for low abundant proteins. Additionally, I acknowledge valuable help from the Aquatron Laboratory here at Dalhousie University and the National Resource for Aplysia at the University of Miami: Gillian Tobin-Huxley at the Aquatron Laboratory provided weekly supplies of natural seawater and algae, as well as helpful advice on raising and feeding larvae that was related to success with *I. obsoleta* rearing; and Phillip Gillette and Dr. Michael Schmale at the National Resource for Aplysia supplied staged and fixed *A. californica* larvae. I would also like to thank Brianne Lindsay, Manager at Dalhousie Faculty of Medicine's Cellular and Molecular Digital Imaging (CMDI) Facility, for technical support relating to confocal imaging; and Alexander Goroshkov, Departmental Technician for Dalhousie's Department of Physiology and Biophysics, for helping design and build various apparatuses related to animal rearing. Finally, I thank all the members of my lab for their camaraderie over the duration of my studies: specifically, Jillian Doyle, Alex Young, Marco Turner, Joji Imai, Tanuj Fernando, and Anya Mehta.

Chapter 1: Introduction

Nervous systems across the animal kingdom show a large degree of diversity, which has made the task of determining evolutionary history of the centralized nervous system difficult and controversial. In the simplest form, nervous systems resemble a nerve net, a diffuse epithelial network of interconnected neurons with limited concentrations of nerve cells, such as that found in the cnidarians and ctenophores. In the most complicated form, nervous systems are consolidated into one or more centralized structures consisting of large concentrations of nerve cells; these large concentrations of nerve cells are organized with distributed functions that follow hierarchical processing as found in vertebrates (Northcutt, 2012). In between these two extremes there are examples of various intermediate forms; hemichordates, which contain a nerve net with longitudinal condensations that form both a dorsal and ventral nerve chord; nematodes, planarians, and annelids with anterior condensations of nerve cells (ganglia) with varying forms of longitudinal projections (ventral/dorsal nerve chord with transverse commissures, bilateral longitudinal nerve chords with transverse commissures, and a segmented ventral nerve chord, respectively); arthropods, which develop a consolidated anterior congregation of nerve cells forming a brain and a ventral nerve chord; and finally molluscs that show evidence for peripheral nerve nets with various forms of condensed ganglionic nervous systems including the relatively more complicated cephalic brain structure in the cephalopods. Given the diverse body plans and forms of nervous systems present throughout the animal kingdom, theories around the derivation of the central nervous system (CNS) remain controversial. The following thesis aims to investigate the early larval development of histaminergic and octopaminergic neurons in molluscs in the context of the evolutionary history of the CNS; the introduction will start with a brief review of opposing arguments surrounding the origin of the CNS and the importance of larval development comparisons in the elucidation of evolutionary history. The following chapters, Chapter 3 and Chapter 4, will provide a more focused review of what is known about the form and function of histaminergic and octopaminergic neurons throughout the animal kingdom.

1.1 Origin of the central nervous system

The origin of the CNS and the evolutionary history leading to the centralization of vertebrate and invertebrate nervous systems has long been debated. The earliest published comparison of nervous systems between phyla was by Étienne Geoffroy Saint-Hilaire in 1822 (cited in Strausfeld and Hirth, 2015) where he compared the vertebrate CNS with that of a lobster proposing the homology of the vertebrate and arthropod CNS, however noting that the vertebrate CNS was upside down. Saint-Hilaire's claim was controversial at a time prior to Charles Darwin's publication "*On the origin of species by means of natural selection, or the preservation of favoured races in the struggle for life*", which was published in 1859, and remained controversial for many years after; however, Saint-Hilaire's ideas eventually picked up steam and recent advances in molecular techniques have provided evidence in support of his claim (reviewed in Strausfeld and Hirth, 2015), as detailed below. Despite recent molecular evidence, there is still considerable debate over the origin of the CNS. Although, the single origin hypothesis of the CNS is favoured by many today, the alternative hypothesis is that the nervous system became centralized independently in multiple phyla. The following discussion aims to provide a review of theories and evidence pertaining to the single and multiple origin hypotheses.

In accordance with Saint Hilaire's early speculations, a dominant view is that centralized nervous systems throughout Bilateria are homologous, meaning that the common ancestor to all bilateral animals had a rudimentary centralized nervous system that was further refined and/or reduced as evolution occurred. The hypothesis of the single origin of the CNS is driven by evidence over the past few decades indicating the conservation of developmental genes that regulate/pattern the body plan, including the nervous system (Arendt & Nübler-Jung, 1994, 1997; De Robertis & Sasai, 1996; Denes et al., 2007; Holley et al., 1995; Kimelman & Martin, 2012; Urbach & Technau, n.d.).

Developmental genes code for transcription factors/morphogens that regulate cellular specification and body patterning. The transcription of developmental genes creates varying concentration gradients of morphogens that influence cellular specification through concentration-dependent changes in gene transcription (Gurdon & Bourillot, 2001; Phillips, 2008). Through complex interactions, the concentration-dependent nature of gene transcription produces spatially and temporally organized

regions of gene expression that lead to the development of different body segments and, therefore, the three bilaterian body axes: Anterior-posterior, medial-lateral, and dorsal-ventral. Surprisingly, there is a striking degree of similarity in the expression of developmental genes among bilateral animals.

Evidence indicates that anterior-posterior body axis/neurodevelopment of bilaterians is regulated by cephalic gap, homeotic/homeobox (Hox), and paired box (Pax) genes (Kammermeier & Reichert, 2001; Lichtneckert & Reichert, 2005). Cephalic gap genes in *Drosophila* pattern the anterior brain and are named for the gap-like phenotype generated when any particular gene is inactivated, thus resulting in missing head segments (Lichtneckert & Reichert, 2005). Orthologues for the cephalic gap genes *empty spiracles* (*ems*) and *orthodenticle* (*otd*) have been identified in mice with similar roles in patterning the anterior brain. Mice have two orthologues for both *Drosophila* genes, *ems* and *otd*, which are *Emx1*/*Emx2* and *Otx1*/*Otx2*, respectively. These orthologous genes share similarities in their expression patterns, especially *otd*/*Otx*. They also share similar functions in early neuroectoderm and cellular specification, as well as brain regionalization; overexpression of orthologues has been shown to rescue mutant phenotypes (reviewed in Lichtneckert & Reichert, 2005). Another set of developmental regulating genes that pattern the posterior brain and spinal cord are the Hox genes.

Hox genes were first discovered in *Drosophila* (Lewis, 1978) and are important in regulating the anterior-posterior segmentation of the hindbrain and nerve cord across many phyla. Hox genes encode transcription factors that contain a DNA binding motif called the homeodomain. In bilaterians, Hox genes are clustered in varying numbers on chromosomes; the number of clusters in extant species is associated with gene duplication events (Kammermeier & Reichert, 2001; Lappin et al., 2006; Lichtneckert & Reichert, 2005). Characteristics of Hox clusters believed to be shared among all bilaterians are “spatial and temporal collinearity” and “phenotypic suppression”, also referred to as “posterior prevalence”. Spatial and temporal collinearity refers to the phenomenon that the relative position of genes in a cluster along chromosomes are correlated with said genes’ spatial and temporal expression; that is to say that the order of genes expressed from anterior to posterior within the body axis are spatially arranged from 3’ to 5’ within the Hox cluster. Phenotypic suppression and/or posterior prevalence

refers to the fact that genes expressed more posteriorly, closer to the 5' end of the chromosome, are functionally dominant over the more anteriorly expressed genes meaning that posteriorly expressed genes suppress the expression of anterior genes. The striking similarity in Hox gene expression patterns and function in forming discrete segments of the developing nerve cords (neuromeres/rhombomeres) and proper axonal guidance cues between vertebrates and arthropods offer a convincing argument for a single origin of a CNS. Some researchers have gone further to say that the conservation and expression patterns of the aforementioned genes in addition to Pax genes (specifically *Pax2/5/8*) indicate that the last common ancestor to all bilaterians contained a complex central nervous system consisting of a tripartite organization (Hirth, 2010; Hirth et al., 2003).

The tripartite brain hypothesis poses that the last common ancestor to all of Bilateria had a complex nervous system consisting of a tripartite organization (i.e. Forebrain, midbrain, and hindbrain/spinal cord) that was subsequently reduced and/or lost throughout evolutionary history, which led to the loss of the CNS in certain extant species observed today (Hirth, 2010; Hirth et al., 2003; Lichtneckert & Reichert, 2005). This theory stems from evidence indicating conservation of anterior-posterior patterning, specifically *otd*/*Otx2*, *Pax2*/*5*/*8*, *unpg* (*unplugged*)/*Gbx2*, and *hox1* that show a pattern of expression that overlaps with divisions in the vertebrate and *Drosophila* brain (Lichtneckert & Reichert, 2005). The anterior patterning genes *otd*/*Otx2*, previously described, overlap with the vertebrate forebrain and midbrain (proto/deutocerebrum in *Drosophila*). Posteriorly, *otd*/*Otx2* border with *unpg*/*Gbx2* and their antagonistic interaction is believed to lead to the positioning of the midbrain-hindbrain boundary (MHB; also known as deutocerebral-tritocerebral boundary, DTB, in *Drosophila*). Further, positioned between *otd*/*Otx2* and *unpg*/*Gbx2* and overlapping with the MHB are *Pax2*/*5*/*8* regulatory genes (Lichtneckert & Reichert, 2005). The expression of these conserved genes seems to overlap with important brain divisions shared between vertebrates and insects (Hirth, 2010; Hirth et al., 2003; Wurst & Bally-Cuif, 2001), while similar gene expression showed overlap with potential rudimentary neural structures in other chordates (amphioxus and larval ascidians; Wada et al., 1998; Wada & Satoh, 2001) and hemichordates (Lowe et al., 2003), giving support to the tripartite brain

hypothesis. Along with the striking conservation of antero-posterior patterning genes, it has also been found that dorsal-ventral patterning genes are largely conserved, further favouring the single origin hypothesis (Arendt & Nübler-Jung, 1994, 1997; De Robertis & Sasai, 1996; Holley et al., 1995).

Dorsal-ventral body/CNS patterning is regulated by antagonizing effects of *bone morphogenetic protein 4* (*BMP4*) by *Chordin* in vertebrates, and the homologous genes *decapentaplegic* (*dpp*) and *short gastrulation* (*sog*), respectively, in *Drosophila* (Arendt & Nübler-Jung, 1994; Holley et al., 1995; Urbach & Technau, n.d.; Watanabe et al., 2009). Evidence indicates that *BMP4* signalling is an ectodermal signal, therefore, in absence of inhibiton from *Chordin*, *BMP4* signalling induces the formation of non-neural ectoderm (reviewed in Watanabe et al., 2009). Thus, the antagonizing effects of *Chordin*/*sog* on *BMP4*/*dpp* enables the formation of neural tissue (Urbach & Technau, n.d.; Watanabe et al., 2009). Interestingly, the expression of homologous genes *Chordin*/*sog* on *BMP4*/*dpp* show opposite expression patterns on the dorsal-ventral axis. In vertebrates, *Chordin* is expressed dorsally whereas its homolog *sog* is expressed ventrally in invertebrates, both leading to the development of the dorsal and ventral nerve chords, respectively (Arendt & Nübler-Jung, 1994; Lacalli, 1995; Lichtneckert & Reichert, 2005). The difference in expression of dorsal-ventral patterning genes in accordance with the location of the dorsal spinal cord and ventral nerve cords have led single origin theorists to propose a dorsal-ventral body inversion, which would explain this difference while maintaining that all bilaterian nervous systems are homologous. The idea of a dorsal-ventral body inversion has been difficult to explain and has brought about some interesting theories on how this could have occurred during evolution (Holland, 2015; Holland, 2003). Some theories describe a hypothetical larval ancestor containing ciliated bands that through subsequent evolution fused along the longitudinal midline either dorsally or ventrally in lineages leading to vertebrates/invertebrates (Nielsen, 1985, 1999, 2018; Nielsen & Norrevang, 1985); others reimagine how the development of the through-gut from a blastopore could have led to either a dorsal or ventral nerve cord (Holland, 2003; Nielsen et al., 2018). However, an alternative view proposes that the high degree of developmental gene conservation could reflect ancestral mechanisms used to pattern the body axes prior to the origin of the CNS, which then could have co-opted

independently numerous times for the role of nervous system centralization and patterning (Erwin, 2020; Erwin & Davidson, 2009; Hejnol & Lowe, 2015; Holland & Short, 2008; Moroz, 2009; Northcutt, 2012).

Evidence suggests that many conserved developmental genes used for cell specification and organization of the body axes predate the centralization of the nervous system (Erwin, 2020; Marlow et al., 2009, 2014; Ryan & Baxevanis, 2007; Watanabe et al., 2009). For example, a single homeobox gene, TALE, has been determined to have a common origin among unicellular eukaryotes, plants and animals (Holland, 2013). The number of Hox genes increased independently in both plants and animals with duplication events throughout subsequent evolution; the origin of Hox clusters in animals is thought to occur after the divergence from sponges (Holland, 2013; Lappin et al., 2006; Larroux et al., 2007). In fact, homologs for numerous developmental genes with similar expression patterns have been identified in a sister group to Bilateria, the Cnidarians; these homologs include genes relating to neuroectoderm/neural cell type specification, sensory system development, and axon guidance that are shared between Bilateria and Cnidaria, thus suggesting that the basic framework for centralization was in place in the last common ancestor (Marlow et al., 2009, 2014; Watanabe et al., 2009). The presence of these genes in clades that split prior to Bilateria considered to have diffuse nervous systems, indicates that the identification of conserved genes involved with regulating neurodevelopment and patterning the CNS across Bilateria is not sufficient to indicate morphological homology; the diversity of morphological features across Bilateria given the largely conserved developmental genes, raises questions on how gene-regulatory networks evolve and contribute to morphological complexity (Erwin, 2020; Erwin & Davidson, 2009; McCune & Schimenti, 2012; Moroz, 2009; Northcutt, 2012; Wagner, 2007).

Gene-regulatory networks (GRNs) comprise complex interactions involving transcription factors and signalling molecules that, individually, play roles in numerous different regulatory pathways and it remains unclear how mutations/changes in these networks are converted into phenotypic novelties in morphological features (Erwin, 2020; Erwin & Davidson, 2009; McCune & Schimenti, 2012; Wagner, 2007). Research has indicated that morphological characteristics/traits believed to be homologous because

of conserved genes can be derived from developmental regulatory networks that, despite indication of conserved components, are structurally non-homologous(McCune & Schimenti, 2012; Wagner, 2007). An example of this is found when comparing the insect and vertebrate eyes. Initially when *Pax6* and its homologue *eyeless* (*ey*) were found to be involved in the morphogenesis of vertebrate and insect eyes, respectively, it was believed that this indicated homology of these sensory organs; however, when the gene regulatory networks that controlled their development were analysed in detail it became clear that the two developmental programs were regulated by non-homologous genes (reviewed in Wagner, 2007). It is now believed that conserved regulatory genes involved in the regulatory networks that give rise to eyes in vertebrates and insects were differentially co-opted during the independent evolution of these convergent sensory structures (McCune & Schimenti, 2012). The gene-regulatory networks involved in body patterning and neurodevelopment still require scrutinous research to elucidate the genes and complex interactions involved in the development of species in different phyla, which can be used to compare developmental programs and how differences in divergent regulatory networks contribute to phenotypic/morphological expression (Erwin, 2020; Hejnol & Lowe, 2015). In fact, one proposition for the emergence of complex body morphology is the evolution of GRNs into complex hierarchical networks through the independent co-option of existing developmental genes in different animal lineages (Erwin, 2020). Thus, the current understanding of GRNs and how they contribute to morphological traits is insufficient for claiming a single origin of the CNS and studies performing cladistic and phylogenetic analyses, including both current morphological and genetic data, indicate that the CNS likely originated numerous times (Hejnol & Lowe, 2015; Moroz, 2009; Northcutt, 2012).

As Northcutt (2012) and Erwin (2020) discuss, investigations into the evolutionary origins of the CNS requires an accurate and well supported understanding of phylogeny. Genetic and molecular data inform phylogeny and in recent years have improved phylogenetic analyses. Morphological and molecular data analysed separately give conflicting phylogenetic results and combined analyses using methods of maximum parsimony are prone to artifacts (i.e. long branch attractions; Glenner et al., 2004); however, new approaches using Bayesian inference have enabled a statistical method for

cladistic analysis of evolutionary relationships using the combined molecular and morphological data, which shows an improved cladogram with substantial congruency between morphological and molecular data analysed by Bayesian methods (Glenner et al., 2004). Outgroup analyses of nervous system characteristics, that define nervous systems as either diffuse, ganglionated, or consisting of a brain, using a modified version of the combined cladogram from Glenner et al. (2004) indicate that a CNS consisting of a complex brain evolved at least four times (Northcutt, 2012). Other analyses indicate that centralization of the nervous system occurred at least five to seven times (Moroz, 2009); alternatively, under a single origin theory the CNS would have been reduced/simplified at least 11 times (Northcutt, 2012). As noted by other researchers (Hejnol & Lowe, 2015), further research comparing morphological characteristics and genetic mechanisms of brain development broadly across the animal kingdom will inform current phylogenies and improve our understanding of nervous system evolution.

The following thesis looks to contribute to the conversation by describing the development of neurotransmitter systems that express markers characteristic of histaminergic and octopaminergic neurons in early molluscan larval development, thus laying the framework for comparisons in species across the animal kingdom. Once neurotransmitters are established in a specific function and/or regulatory system, that function generally persists; examples can be found in the use of serotonin in the control of cilia across phyla (Braubach et al., 2006; Byrne et al., 2007; Croll & Dickinson, 2004; Goldberg et al., 1994; Koss et al., 2003; Satterlie & Andrew Cameron, 1985) and epinephrine in the regulation of the sympathetic nervous system among vertebrates (Romero & Gormally, 2019). However, there are a few instances where functions are controlled by different neurotransmitters between vertebrates and invertebrates representing targets of evolutionary divergence. Some examples are found in the control of muscle contraction at the neuromuscular junction where acetylcholine is used in vertebrates (Rudolf & Straka, 2019) while arthropods use glutamate (Bicker et al., 1988; Smarandache-Wellmann, 2016); additionally, vertebrates use glutamate as a sensory neurotransmitter (Fernández-Montoya et al., 2018) whereas histamine and dopamine are prevalent in sensory signalling in invertebrates (Buchner et al., 1993; Carrigan et al., 2015; Wyeth & Croll, 2011). More evidence for divergence is evident when comparing

the function of octopamine (OA) and norepinephrine (NE) among invertebrates and vertebrates where it has been suggested that OA could function as the invertebrate analogue to NE in regulating the sympathetic nervous system/stress response (Roeder, 1999, 2020). Therefore, histamine and octopamine are neurotransmitters that represent targets of evolutionary divergence; investigating the phenotypic expression and function of these neurotransmitters could inform morphological differences among nervous systems and in conjunction with molecular studies offer insights into evolutionary relationships and how GRNs influence phenotypic expression of morphological differences.

Molluscs are an important facet in the conversation around evolution of diverse body plans and the centralization of the nervous system; their importance is derived from the large degree of diversity within this single phylum and morphological variations compared among other protostomes and/or deuterostomes (Wanninger & Wollesen, 2019). Interestingly, there are studies that show differences in Hox gene expression with evidence indicating loss of co-linearity in some molluscan species (Samadi and Steiner, 2010; Salamanca-Diaz et al., 2021) whereas others show the conserved colinear expression of Hox genes (Fritsch et al., 2015). Therefore, investigating morphological differences within the molluscan phylum will help build the framework for understanding how changes in GRNs lead to changes in morphology and the identification of commonalities among diverse species within the molluscan phylum will help identify basal traits to all of Mollusca that could be used to inform cross phyla comparisons.

1.2 Larval Nervous Systems

The majority of phyla across Bilateria exhibit indirect development, a form of growth where the organism has a post-embryonic intermediate larval stage prior to metamorphosis into an adult form (Sly et al., 2003; Young, 2003); marine larval organisms contain many similarities. In fact, there is strong support for theories that postulate that the ancestral bilaterian was a larva-like ancestor that later evolved a new life stage in which extant adult forms were eventually derived (Nielsen, 1985; Nielsen & Norrevang, 1985). These theories originate from Haeckel's (1874) theory of animal evolution centered on the idea that developmental schemes recreate the evolutionary

history of a species or as he put it “ontogeny recapitulates phylogeny” (cited in Sly et al., 2003). However, Haeckel’s theory in the strict sense has not held up to time and the larva-like Bilaterian ancestor remains up for debate with some arguing that larva-like features evolved in early developmental stages of a bilaterian-like adult (Sly et al., 2003). Regardless of the opposing theories, marine larvae present a relatively simple body plan with ciliary bands and morphological features that are easily comparable across many phyla; just as early developmental mechanisms inform evolutionary relationships, comparisons of early larval morphological and functional development can offer novel insights into phylogeny. In this section, I will describe in general the commonalities among marine larval nervous systems pertinent to this thesis and what is known about larval neurodevelopment in the gastropod molluscs, *Ilyanassa obsoleta*, *Aplysia californica*, and a direct developer, *Lymnaea stagnalis*.

Common among most marine invertebrates is a ciliated-larval stage with some aspect of an apical sensory organ (apical tuft or apical ganglion) used for integrating environmental cues to effect behaviour (Marlow et al., 2014; Nielsen, 2004, 2005; Young, 2003). The apical organ is perhaps most prevalent in species categorized into Spiralia (Hindinger et al., 2013; Lacalli, 1981; Nielsen, 2004, 2005; Rawlinson, 2010) but is also found in species of deuterostomes such as echinoderms (Byrne et al., 2007) and hemichordates (Miyamoto et al., 2010; Nielsen, 2005); additionally, this sensory structure is found in the planula larvae of cnidarians (Arendt et al., 2016; Chia & Koss, 1979; Marlow et al., 2009; Sinigaglia et al., 2015), a sister group to Bilateria, making it a possible ancestral trait among bilaterian organisms (Nielsen, 2005). Interestingly, evidence suggest conservation of developmental regulation of ciliated larva and apical organ development (Arendt et al., 2016; Marlow et al., 2014). This conserved sensory structure has been suggested to be chemo- and/or mechanosensitive consisting of an apical tuft, a collection of long cilia at the apical pole, with sensory-neurosecretory cells along the base and has most prominently been associated with control of locomotive ciliary beating (Braubach et al., 2006; Croll & Dickinson, 2004; Goldberg et al., 1994; Koss et al., 2003; Satterlie & Andrew Cameron, 1985) and settlement/metamorphoses (Conzelmann et al., 2013; Hadfield et al., 2000; Kempf et al., 1997; Rentzsch et al., 2008; Voronezhskaya et al., 2004; Voronezhskaya & Khabarova, 2003).

Although nearly ubiquitous among marine larvae, the organization and features of the apical organ is highly variable among extant species. The cnidarian apical organ comprises sets of columnar cells with long cilia that are twisted to form the apical tuft (Chia & Koss, 1979); these columnar cells are positioned above a neural plexus but seem to lack distinct nerve cells (Chia & Koss, 1979; Sinigaglia et al., 2015). In comparison, the apical organs of annelid and molluscan species comprise apical tuft cells surrounded by flask-like or ampullary cells positioned above a neural plexus (Bonar, 1978; Croll & Dickinson, 2004; Kempf et al., 1997; Lacalli, 1981; Nielsen, 2004); the number of cells that form the apical organ in gastropod molluscs can range up to 25 cells (Bonar, 1978; Croll & Dickinson, 2004; Kempf et al., 1997). In terms of the deuterostome apical organ, there is relatively little literature on the general structure, however, a common feature is bilateral serotonergic ganglia in close association with larval bands (Byrne et al., 2007). In fact, the presence of serotonergic nerve cells seems to be a conserved characteristic of the apical organ among Bilaterians (Byrne et al., 2007; Chia & Koss, 1979; Croll & Dickinson, 2004; Hindinger et al., 2013; Kempf et al., 1997; Marlow et al., 2014; Nielsen, 2004, 2005; Page & Parries, 2000; Santagata, 2011; Voronezhskaya et al., 2004; Voronezhskaya & Khabarova, 2003; Wanninger, 2009; Wollesen et al., 2007). However, serotonergic elements are not restrained to the apical organ throughout larval development.

Pertinent to this thesis, serotonergic cells in *I. obsoleta* arise in the apical organ during the embryonic trochophore stage of development with early development revealing processes extending to the vela and foot (Dickinson & Croll, 2003); however, as the larvae develop to metamorphic competence, serotonergic neurons are evident in nearly all ganglia of the adult CNS (Dickinson & Croll, 2003). Similar observations have been made in other gastropod larvae (Croll, 2006; Dickinson et al., 1999, 2000; Kempf et al., 1997; Page & Parries, 2000; Wollesen et al., 2007).

In addition to descriptions of serotonergic cells among marine larvae, other common neurotransmitters that have been identified broadly are catecholamines and various neuropeptides such as FMRFamide (Croll et al., 1997; Croll & Dickinson, 2004; Dickinson & Croll, 2003; Hay-Schmidt, 1990b, 1990a; Marlow et al., 2014; Voronezhskaya et al., 1999; Wollesen et al., 2007). The characterization and comparison

of these neurotransmitter systems have provided good context for comparing form and function of larval stages among diverse animal phyla and have been well described during gastropod larval development (Braubach et al., 2006; Croll, 2006; Dickinson et al., 1999, 2000; Dickinson & Croll, 2003; Voronezhskaya & Elekes, 1996; Wollesen et al., 2007).

Previous studies in gastropod neurodevelopment have observed the early appearance of FMRFamide in the embryonic trochophore (Croll, 2006; Dickinson et al., 1999, 2000; Dickinson & Croll, 2003). In *I. obsoleta*, FMRFamide develops first with a cell in the posterior region and two flask-shaped cells anteriorly in the apical organ; as the animal develops, these cells send processes toward the midline forming an anterior to posterior projection of fibers that becomes the posterior loop of the developing adult nervous system (Dickinson & Croll, 2003). This early development of anterior-posterior FMRFamidergic axons has been described in numerous gastropod larvae and has been proposed to function as pioneering fibers laying the framework for future neurite growth in the developing CNS (Croll & Dickinson, 2004; Dickinson et al., 1999, 2000; Voronezhskaya & Elekes, 1996). Much like the development of serotonergic elements described earlier, observations in *I. obsoleta* (Dickinson & Croll, 2003) and other gastropods (Croll, 2006; Dickinson et al., 1999; Wollesen et al., 2007) reveal an elaborate network of FMRFamidergic neurons in the developing adult ganglia by metamorphic competence.

Another class of neurotransmitters that has been described in developing gastropod larvae is the catecholamines (Croll, 2006; Dickinson et al., 1999, 2000; Dickinson & Croll, 2003). These studies typically use a formaldehyde-glutaraldehyde histofluorescent protocol (Furness et al., 1977) or antibodies raised against tyrosine hydroxylase, the rate limiting enzyme for catecholamine synthesis, as a general label for catecholamines. In *I. obsoleta*, the first catecholaminergic cells appear in the velar lobe and throughout development were found to be associated with the developing cerebral ganglia, vela, foot, mouth and tentacles (Dickinson & Croll, 2003); at metamorphic competence, cells were also observed in the osphradium (Dickinson & Croll, 2003). Interestingly, studies describing catecholaminergic elements of some other gastropod

larvae, such as *A. californica* (Dickinson et al., 2000), only found cerebral cells with innervation in the foot and mouth (Dickinson et al., 1999).

Most of this section has been focused on marine larva with indirect development, which have a distinct post-embryonic intermediate stage prior to metamorphosis into an adult (Sly et al., 2003; Young, 2003); however, *L. stagnalis* is one of the many gastropods that develop through direct development and experiences a truncated larval development with metamorphosis occurring within an egg capsule (Nielsen, 2004). Despite this, evidence from *L. stagnalis* still show remnants of an apical organ identified with catecholaminergic labelling of the transient anterior catecholaminergic (TAC) cells (Voronezhskaya et al., 1999; Young et al., 2022). Additionally, the development of serotonergic (Diefenbach et al., 1998; Koss et al., 2003; Marois & Croll, 1992) and FMRFamidergic (Voronezhskaya & Elekes, 1996) neural elements have been described in *L. stagnalis* and related species, showing reduced but comparable staining patterns.

The following thesis aims to expand on this body of research by investigating histaminergic and octopaminergic elements in early larval development with a focus on *I. obsoleta*, including brief descriptions and comparisons using *A. californica* and *L. stagnalis*. Improving our understanding of early neurodevelopment in larva through comparative approaches could help elucidate the evolutionary history of the nervous system and inform research investigating how developmental genes and GRNs influence phenotypic expression. Results from this thesis can provide a framework for research investigating distantly related and diverse organisms, which inform approaches used to deduce evolutionary relationships and thus improve our understanding of phylogeny.

Chapter 2: Methods

2.1 Animal Subjects

Ilyanassa obsoleta (previously classified as *Tritia obsoleta*) were collected from the Bay of Fundy in late February. *I. obsoleta* were kept at 4ºC and oviposition was induced by transferring animals to saltwater aquaria where water reached room temperature (RT; ~ 21ºC). Adult *I. obsoleta* were fed fish protein pellets (Fluval, Tropical Fish Pellets) in combination with potato, carrot, and/or lettuce slices. Water for saltwater aquaria was mixed from that collected directly from either the Northwest Arm (Halifax, NS, Canada), or sand filtered by the Aquatron Laboratory (Dalhousie University, Halifax, NS, Canada) or was mixed using Crystal Sea Marine salts (Marine Enterprises International, Baltimore, MD, USA) to obtain a specific gravity of approximately 1.023 g/cm^3.

Aplysia californica were obtained from NIH's National Resource for Aplysia at the University of Miami (Key Biscayne, Florida, USA); larvae arrived staged and fixed according to antibody specific protocols (see section 2.4.3 Fixations), whereas juveniles were dissected within hours of arrival.

Freshwater snails, *Biomphalaria alexandrina* and *Lymnaea stagnalis* were maintained in ongoing laboratory colonies at 20–25°C under a 10/14 hr dark/light cycle. Snails were reared with continuously aerated, carbon-filtered tap water that was conditioned with 600 mg/L sea salts (Crystal Sea, Baltimore, MD, USA) and 26.4 mg/L sodium bicarbonate. Approximately 10–20% of the aquarium water was drained and replaced with freshly conditioned water every 2 weeks and supplemented with crushed, chicken eggshells and/or chalk as an additional calcium source. Snails were fed romaine lettuce and carrots ad lib. All animal care and use were approved by the University Committee on Laboratory Animals at Dalhousie University.

2.1.1 Veliger Rearing

Once *I. obsoleta* began spawning, egg masses were collected every 2-3 days, sorted by date and reared in aerated 500 ml plastic beakers. During the initial collection, egg masses were rinsed thoroughly using a mixture of filtered artificial and natural

seawater (FSW) in a custom sieve comprising a 250 ml plastic cylinder with the bottom removed and replaced with 596 µm Nitex mesh (pore size = 408 µm). Natural seawater was acquired regularly from local sources as described in section 2.1 (Animal Subjects) and filtered using grade 415 filter paper (Cat # 28320, VWR) before being adjusted to a specific gravity between 1.021 and 1.025 g/cm^3 using artificial seawater (Crystal Sea, Baltimore, MD, USA). Once hatched veligers were observed at about seven days post oviposition (DPO), they were fed daily with either *T. Isochrysis* cultures received from the Aquatron Laboratory or Shellfish Diet 1800 (Reed Mariculture, Campbell, CA, United States), the latter containing a mixture of marine microalgae that could support the developmental ranges of *I. obsoleta* veligers.

Finally, cultures of hatched veligers were rinsed every 1-2 days and transferred to new beakers with fresh FSW; transferring and rinsing of the veligers was performed using a series of custom sieves containing different size Nitex mesh: 596, 275 and 245 µm containing 408, 190, 150 µm pore size, respectively. The 596 µm sieve was used to filter out any large debris such as empty egg capsules, aggregated algae and other detritus. The 245 µm sieve was used to catch the veligers and allow smaller debris to be rinsed out of the cultures and discarded, such as shells from dead veligers and waste products; as the veligers developed and grew, the catch sieve was swapped with the 275 µm Nitex mesh to allow clearance of larger waste products. Early during veliger rearing the beakers were aerated using air pumps and the transfer and rinsing of veligers to new beakers was performed every 2-3 days. Eventually, it became evident that the older cultures were crashing; therefore, instead of constantly aerating beakers, cultures were transferred and rinsed daily to limit stress to the animals. All rinsing was performed with FSW.

2.2 Sequence Alignments

Sequence alignments were performed to verify sequence homology of vertebrate dopamine β-hydroxylase (DBH) and invertebrate tyramine β-hydroxylase (TBH); additionally, to test the validity of the DBH antibody used in this study (Cat # ab189991, Abcam), DBH/TBH sequences were aligned to the synthetic human DBH target sequence corresponding to amino acids 437-448 (DNHYSPHFQEIR).

Alignments were performed using full length protein sequences retrieved from the National Center for Biotechnology Information (NCBI)'s database. Protein sequences for alignments were chosen by running a BLASTp search using the human DBH protein sequence provided on the antibody product page (Accession # NP_000778.3) and selecting the top TBH/DBH matches for *L. stagnalis* (Accession # BAM35937.1), *B. glabrata* (Accession # 013081477.1), and *A. californica* (Accession # XP_035825847.1); unfortunately, no matches could be found for *I. obsoleta*. BioEdit (RRID: SCR_007361) sequence analysis tool was then used to perform Clustal Omega multiple sequence alignments (Madeira et al., 2019) and create a graphical representation of the alignments; full length DBH/TBH protein alignments against the human DBH precursor protein (Accession # NP_000778.3) and the DBH antibody target sequence (DNHYSPHFQEIR), were performed separately.

2.3 Western Blots

Western blots were performed to characterize and validate the dopamine β-hydroxylase (DBH) antibody. Western blots enabled the comparison between the molecular weight of the antigen(s) with the expected molecular weight of the target enzyme and provides information on the number of possible antigens present in the tissue, which relates to the specificity of the antibodies. Western blots were performed using tissue from *I. obsoleta*, *A. californica*, *L. stagnalis*, and *B. alexandrina*.

2.3.1 Protein Extraction

Proteins were extracted from homogenates of isolated central nervous systems (CNSs; see 2.4.2 Adult CNS Dissections). After dissections, nervous tissue was freshly washed and homogenized in a radioimmunoprecipitation assay (RIPA) buffer (150 mM NaCl, 1% Triton X-100, 0.5% sodium deoxycholate [DOC], 0.1% sodium dodecyl sulfate [SDS], and 25 mM Tris, pH 7.4) containing protease inhibitor (Cat # A32955, ThermoFisher Scientific) at a ratio of 30 µl of buffer for every 1 mg of tissue. Homogenization occurred on ice with intermittent grinding using a glass rod modified to work as a pestle in a 1.5 ml microvial, followed by continuous pipetting for approximately 1 hr to help further disrupt the tissue. The pipetting occurred sequentially

starting with 200 µl pipette tips followed by 25- and then 27-gauge needles, drawing homogenate in and out of pipette tips/syringes. Then the homogenized tissue was placed on a shaker at 4ºC for 30 min to allow for detergent in the lysis buffer to act on the tissue and maximize solubilization of proteins. The resultant homogenate was centrifuged at 5000 rpm for 30 min and then again at 12000 rpm for 30 mins, both at 4ºC, using a Sorvall™ ST 8R centrifuge (ThermoFisher Scientific). The supernatant was transferred to a new tube and the pellet was discarded. The protein concentrations of tissue homogenates were then assessed using a Micro BCA™ Protein Assay Kit (Cat # 23235, ThermoFisher Scientific; see section 2.6 Protein Assay).

2.3.2 Gel Electrophoresis/Transfer

Samples were prepared with 2x Laemmli sample buffer (Cat # 1610747EDU, BioRad) diluted one to one with CNS protein extract; up to 40 µl of each sample was loaded for sodium dodecyl sulfate polyacrylamide gel electrophoresis (SDS-PAGE) using 10% acrylamide resolving gels with a 4% stacking gel and 1x running buffer (35 mM SDS, 250 mM Tris, 192 mM glycine in dH_2O). Precision Plus Protein™ All Blue Standard (7 µl; Cat # 1610373, BioRad) with the molecular weight markers ranging from 10 to 250 kDa was added to one lane of each gel prior to the loading of the protein samples and electrophoresis proceeded for 30 min at 70 V followed by approximately 1.5 hr at 100 V. Protein samples were later transferred onto 0.22 µm nitrocellulose membranes for 80 min in 1x transfer buffer (25 mM Tris, 192 mM glycine, and 20% methanol in dH_2O) at 100 V.

2.3.3 Blot Incubations

After protein samples were transferred onto a nitrocellulose membrane, the membrane was incubated in blocking buffer containing 5% non-fat dry milk (Cat # 1706404, BioRad) in Tris-buffered saline with Tween (TBST; 137 mM NaCl, 2.7 mM KCl, 19 mM Tris-base, 0.1% Tween 20) either overnight at 4°C or for 1 hr at RT. The membranes were then incubated with, or without, the primary DBH antibody (Cat # ab189991, Abcam, Toronto, ON, Canada) at a dilution of 1:1000 or primary acetylated tubulin (AcT) antibody (Cat # T7451, MilliporeSigma) at a dilution of 1:5000 with Tris-

buffered saline (TBS; 137 mM NaCl, 2.7 mM KCl, 19 mM Tris-base) containing 5% non-fat dry milk (Cat # 1706404, BioRad) for 1 hr at RT. After incubation in the primary antiserum, the membranes were rinsed in TBS, followed by three 15 min washes in TBST and a final 15 min wash in TBS. Then the membranes were incubated with either a donkey anti-goat (Cat # ab6885, Abcam) or donkey anti-mouse secondary antibody conjugated to horseradish peroxidase (HRP; Cat # ab6820, Abcam) at a dilution of 1:5000 in TBST containing 5% non-fat dry milk for 2 hrs at RT on a shaker. After the membranes were washed three times for 15 min each with TBST followed by a 15 min wash with TBS. The blots were analysed using an enhanced chemiluminescence assay (Cat # 1705060, Biorad) and were viewed using the Bio-Rad ChemiDoc XRS+; exposure times varied between 26 to 210 seconds.

2.3.4 WB Controls

To validate the protein extraction protocol, AcT¸ an abundant protein previously examined through western blot analysis in various *L. stagnalis* tissues (Jackson et al., 1995), was probed using a monoclonal antibody (Cat # T7451, MilliporeSigma). Specificity of the secondary antibody was tested by following the antibody incubation protocol while omitting the primary antibody from the primary incubation media (TBS with 5% non-fat dry milk); the immunoblot in the primary omission control was exposed for 82, 180 and 300 sec all showing no protein bands.

Additionally, to test specificity of the DBH antibody, a commercially available isolated DBH protein (Cat # ab202616, Abcam) was purchased and used to perform a preadsorption control. Experimental and control conditions were performed concurrently using protein extractions from the four species used throughout the study. The primary DBH antibody solution was prepared as described in the western blotting section under antibody incubations except solutions were prepared with and without 250 µg/µl of DBH blocking protein (Cat # ab202616, Abcam) for the control and experimental conditions, respectively. Antisera were prepared at least 24 hrs in advance to allow blocking peptides to bind to the DBH antibodies prior to incubation of the nitrocellulose membrane.

2.4 Immunohistochemistry

2.4.1 Specimen Collection/Staging

Embryos and veligers were collected and fixed at various stages so that neuroanatomical descriptions of specific transmitter systems could be performed providing insight into their development.

2.4.1.1 Ilyanassa obsoleta. Embryonic stages were collected from between 3-7 days post oviposition (DPO) by the manual use of forceps to break egg capsules. From >7 DPO, veligers were collected every 2-3 days after rinsing (see section 2.1.1 Veliger Rearing for details on rinsing); once veligers were concentrated in the catch sieve, the sieve was resuspended in FSW and a glass pipette was used to select healthy swimming specimen into microvials. Retrieved embryos and veligers were then anaesthetized with isotonic 0.36 M $MgCl_2$ in preparation for fixation. Various fixatives were used depending on the specific antibody protocol (see section 2.4.3 Fixations). After fixation, veligers were stored at 4^{o}C in PBS containing 0.01% sodium azide. For developmental descriptions, *I. obsoleta* veligers were staged based on days post oviposition (DPO) and descriptions by Dickinson and Croll (2003).

Hundreds of *I. obsoleta* specimens were collected and fixed at 23 separate time points between 4 and 27 DPO. Specimens from each point were processed separately for each of the antibodies used: octopamine (OA), DBH, histamine (HA), and HA/AcT double labels. To collect specimen for processing, a glass pipette was used to randomly draw 20 – 100 specimens from the storage vials. After processing no fewer than three samples from each time point were observed and photographed in an appropriate orientation to determine anatomical and developmental descriptions; however, numerous additional samples that showed positive labelling were also observed to be consistent with those photographed for this study.

2.4.1.2 Aplysia californica. All larval *A. californica* samples were collected and fixed at National Institutes of Health (NIH)'s National Resource for Aplysia at the University of Miami (Key Biscayne, Florida, USA). Embryonic stages were retrieved from days 3-8 in 1 cm egg mass segments. Both embryonic samples and Stage 6 veligers

were gathered into separate 1.5 ml microvials and fixed using various fixatives dependent on the specific antibody protocol (see section 2.4.3 Fixations).

2.4.1.3 Freshwater Species. Embryonic *B. alexandrina* and *L. stagnalis* were collected at approximately 55% of embryonic development (E55), just as the eyes were beginning to develop, by manually breaking open egg capsules and using a 200 µl pipette to gather them into 500 µl microvials for fixation. Specimen were then fixed using specific antibody dependent protocols (see section 2.4.3 Fixations).

2.4.2 Adult CNS Dissections

To dissect adult CNSs, animals were first anaesthetized with magnesium chloride ($MgCl_2$); freshwater snails and marine specimen were anaesthetized with 0.05 M and 0.36 M $MgCl_2$ in dH_2O, respectively. To properly anaesthetize animals, *A. californica* were injected with 0.36 M $MgCl_2$, whereas the rest of the specimen were anaesthetized sequentially in $MgCl_2$ baths; shelled animals were placed in beakers containing anaesthetic for about 30 mins and then removed from their shells and placed in a second beaker of $MgCl_2$ for another 30 mins. Once relaxed, specimen were pinned to dissection trays starting with the anterior end and then stretched longitudinally with a pin placed in the posterior end; then a longitudinal cut was made and the body wall to either side of the incision was pinned laterally. At this point the buccal mass was pinned anteriorly to expose the CNS (Note: nervous tissue dissected for protein extractions was removed at this point by cutting all peripherally projecting nerves); then peripherally projecting nerves were carefully cut to keep them long enough to easily pin for fixation. To properly pin out the nervous tissue so that it was fixed flat, either the cerebral commissure or pedal commissure had to be cut so the associated ganglia could be pinned laterally (Beach et al., 2019). Once the isolated CNSs were pinned flat in a Sylgard-lined (Dow-Corning, Midland, MI, USA) Petri dish, preparations were ready for antibody dependent fixation protocols.

2.4.3 Fixations

2.4.3.1 Octopamine (OA). Samples destined to be incubated with antibodies raised against octopamine were fixed using a solution that contained 4% paraformaldehyde (PFA) in PBS overnight (OVN).

2.4.3.2 Dopamine β-Hydroxylase (DBH). Samples prepared for DBH labelling were fixed using a solution that contained either 4% paraformaldehyde in PBS or was comprised of nine parts methanol and one part formaldehyde (9 MeOH: 1 CH2O; Wyeth & Croll, 2011), for 15 to 30 min. Samples prepared for double labelling with OA were fixed according to section 2.4.3.1 Octopamine (OA).

2.4.3.3 Histamine (HA). Samples processed for incubation with antibodies raised against HA were fixed using a solution containing 2% 1-ethyl-3-(3-dimethylaminopropyl) carbodiimide (EDAC; Cat # E7750, MilliporeSigma) and 0.4% *N*-hydroxysuccinimide (NHS; Cat # 130672, MilliporeSigma) in PBS for 3 hrs. Then samples were further fixed overnight at 4ºC with 1% paraformaldehyde (PFA) in PBS. This fixation protocol will be referred to henceforth as EDAC fixation.

2.4.3.4 Acetylated Tubulin (AcT). An antibody raised against AcT (see Table 1 for details) was used to orient novel labelling and improve descriptions. The AcT antibody was determined to show binding affinity with either 4% PFA, EDAC or nine parts methanol and one part formaldehyde (9 MeOH: 1 CH_2O) fixations, which allowed double labels to be performed with any of the other antibodies used in this study.

2.4.4 Antibody Incubations

Antibody incubations were performed at 4ºC while the subsequent washes occurred at RT; all incubations were carried out with gentle agitation using a rotary shaker. After fixation, samples were rinsed two times and then washed with phosphate buffered saline (PBS; 100 mM $HNaPO_4/Na_2PO_4$ buffer, 140 mM NaCl, pH 7.4) with two changes over 1 hr. The tissues were then either stored in PBS containing 0.01% sodium azide for future antibody incubations or processed immediately.

Once ready for antibody incubations, marine veligers >8 DPO and freshwater specimen were treated with a solution of 80% 0.23 M ethylenediaminetetraacetic acid (EDTA) and 20% 0.1 M sodium acetate in dH_2O for approximately 5 min to decalcify and remove shells. Marine veligers 7 DPO and younger were not subjected to decalcification. Next the samples were treated with 2% Triton X-100 in PBS for 2 hrs, followed by a rinse with PBS and wash in blocking medium containing 0.1% Triton X-100, 2% dimethylsulfoxide (DMSO), 1% normal donkey serum and 1% bovine serum albumin (BSA) in PBS, for 30 to 60 mins at RT or overnight at 4°C. After blocking, tissues were incubated in a solution containing one or two primary antibodies in blocking medium (see Table 1) for three days. Tissues were then rinsed with PBT (0.5% Triton X-100 in PBS) and washed for four changes over 2 hrs in PBT; they were subsequently incubated for 30 min in blocking medium alone before incubation in blocking medium containing one or two secondary antibodies (see Table 2) for two days. The tissues were then rinsed with PBT and washed for four changes over 2 hrs with PBT. Finally, the tissues were cleared overnight in CUBIC-1 (Susaki et al., 2014) at 4°C. In some experiments 2 ug/ml 4',6-diamidino-2-phenylindole (DAPI) was added to CUBIC-1 for visualization of cell nuclei. Samples were then mounted on glass slides with CUBIC-1.

Table 1. Primary antibodies, their dilutions and supplier information. All antibodies were diluted in blocking medium (OA, octopamine; BSA, bovine serum albumen; DBH, dopamine β-hydroxylase; sDBH protein seq, synthetic DBH protein sequence; HA, histamine; KLH, keyhole limpet hemocyanin; AcT, acetylated tubulin).

Label	Immunogen	Host	Dilution (µl)	Supplier/location	Catalog #
OA	OA-BSA conjugate	Rabbit	(1:100)	MoBiTec, Göttingen, DE	1003GE
DBH	sDBH protein seq	Goat	(1:100)	Abcam, Toronto, ON, CA	ab189991
HA	HA-KLH conjugate	Rabbit	(1:100)	Immunostar, Hudson, WI, USA	22939
AcT	Acetylated tubulin	Mouse	(1:200)	MilliporeSigma, Oakville, ON, CA	T6793

Table 2. Secondary antibodies used in association with each primary label including dilutions and catalog numbers (OA, octopamine; HA, histamine; DBH, dopamine β-hydroxylase; AcT, acetylated tubulin). All secondary antibodies were purchased from Life Technologies (Burlington, ON, CA).

Label	Secondary Antibody	Fluorophore	Dilution (µl)	Catalog #
OA/HA	Donkey anti-rabbit	Alexa Fluor® 555	(1:200)	A-31572
	Donkey anti-rabbit	Alexa Fluor® 488	(1:200)	A-21206
DBH	Donkey anti-goat	Alexa Fluor® 555	(1:200)	A-21432
AcT	Donkey anti-mouse	Alexa Fluor® 488	(1:200)	A-21202

2.4.5 IHC Controls

To test the specificity of the experimental antibodies, raised against HA and OA, preadsorption controls were performed. Since HA and OA protein conjugates were not commercially available, HA-BSA and OA-BSA protein conjugates had to be synthesized (see section 2.5 Protein Conjugations). The same procedure described above, in section 2.4.4 Antibody Incubations, was followed for preparing and incubating tissue samples except that the primary antisera were prepared at least 24 hrs in advanced of primary antibody incubations and samples were incubated in blocking medium during this same duration. Antisera and blocking media prepared for preadsorption controls consisted of 654 µg/ml and 588 µg/ml of blocking proteins for the HA-BSA and OA-BSA preadsorption, respectively. Primary antibodies were diluted at 1:300 in blocking medium, with and without blocking proteins for experimental and control conditions, respectively. The secondary antibodies were diluted at 1:200 in blocking medium.

In addition, it has been shown that antibodies raised against hapten-protein conjugates can have binding affinity to epitopes generated from the carrier protein (Beach et al., 2019). The HA antibody was raised using HA conjugated to KLH, and therefore preadsorption controls were performed by preincubating tissue and antisera with 200 µg/ml KLH protein (Cat # H7017, MilliporeSigma) added to both the blocking medium and antiserum (Beach et al., 2019; Wyeth and Croll, 2011); this preadsorption tested whether there was any binding to epitopes generated by the KLH portion of the HA-KLH

conjugate. The OA antibody was raised using OA conjugated to BSA, which was already controlled for since the generic blocking medium contained 1% BSA.

Further testing of the specificity for the antibody targeting the synthetic enzyme DBH was performed using western blots (see section 2.3.4 WB Controls).

2.4.6 Imaging

Samples were initially viewed using a Leica DM4000B fluorescent microscope. After which selected samples were imaged using a Zeiss LSM 510 confocal microscope equipped with Zen 2009 software. Confocal stacks were then processed using ImageJ (Schindelin et al., 2012; https ://fiji.sc/) and Photoshop CS2 (Adobe Systems, Inc., San Jose, CA, USA); whole image adjustments in contrast and brightness were made to achieve consistency within plates.

2.5 Protein Conjugation

Hapten to protein conjugations were performed to generate blocking peptides to use for preadsorption controls, which test the specificity of the OA and HA antibodies. The antibodies were raised against either an OA-BSA or HA-KLH conjugate that was synthesized with glutaraldehyde and EDAC, respectively. Since different fixatives behave differently and can introduce different epitopes for antibodies to recognize, two different conjugation protocols were used to match the appropriate fixative with the conjugate initially used in the creation of the antibody.

2.5.1 HA-BSA EDAC Conjugation

The HA-BSA conjugation was performed using EDAC as described in Scaros et al., (Scaros et al., 2020). Conjugation started by mixing a solution of 20 mg/ml histamine dihydrochloride (Cat # 150625000, ThermoFisher) in 1.5 mL phosphate buffer (pH 7.4). Then, 50 mg of BSA was added making a concentration of 33 mg/ml BSA. Next, 0.5 ml of 4.6 mg/ml EDAC was added and the solution was protected fromf light and incubated at RT for 18 hrs. After the incubation with EDAC, 2.0 ml of 1 M hydroxylamine (Cat # 159417, MilliporeSigma) was added and incubated for an additional 5 hrs. All incubations were performed on a stir plate with gentle stirring. Finally, the HA-BSA

conjugate solution was dialyzed with PBS using Slide-A-Lyzer™ Dialysis Cassettes (Cat # 66380, ThermoFisher) with a 10 kDa molecular weight cut off. Dialysis occurred with four changes of PBS over 24 hrs at RT.

2.5.2 OA-BSA Glutaraldehyde Conjugation

The protocol used for OA-BSA conjugation was adapted from various sources (Carter, 1996; Lemus & Karol, 2008) using glutaraldehyde. Conjugation started by mixing a solution of 2 mg/ml BSA in 3 mL PBS. After which, 2 mg of octopamine hydrochloride (Cat # O0250, MilliporeSigma) was added giving a molar ratio of 116:1 hapten to protein. Then, sodium borohydride (Cat # S9125, MilliporeSigma) was added to a concentration of 10 mg/ml and the solution was cooled to 4ºC. Finally, 1 ml of 1% glutaraldehyde in dH_2O was added dropwise over 2 mins while gently mixing and the solution then continued to mix for another 1 hr. After the conjugation was complete, the OA-BSA conjugate solution was dialyzed with 0.1 M PBS using Slide-A-Lyzer™ Dialysis Cassettes with a 10 kDa molecular weight cut off. Dialysis occurred with four changes of PBS over 24 hrs at RT.

2.6 Protein Assay

The protein concentrations of tissue homogenates used for western blot analysis and protein conjugates used for preadsorption controls were determined using Micro BCA™ Protein Assay Kit (Cat # 23235, ThermoFisher Scientific). Following the instructions provided for performing protein assays in a 96-well microplate, the linear working range was 2-40 ug/ml; therefore, tissue homogenates and protein conjugates had to be diluted to give concentrations within this range.

To acquire concentrations within the proper range, samples were prepared using serial dilution with each sample having three replicates. In the first set of samples, dilution factors used for all tissue homogenates were 100x, 200x, and 500x in PBS. Based on the initial spectrophotometric data, a subsequent protein assay was performed using dilution factors of 200x and 400x in PBS. When testing protein conjugates, protein concentrations were estimated based on calculations done using conjugation protocols (estimated OA-BSA = 2 mg/ml; estimated HA-BSA = 12.5 mg/ml); therefore, OA-BSA

conjugates were diluted 75x, 150x, and 300x and HA-BSA conjugates were diluted 300x, 400x, and 500x in PBS. Tissue homogenate and protein conjugate samples were measured for optical density at 562 nm wavelength using the AD 340C Absorbance Detector (Beckman Coulter, Fullerton, CA) and associated AD/LD Analysis Software (Beckman Coulter, Fullerton, CA). These data were compared to a standard curve created using the BSA standard provided with the Micro BCA™ Protein Assay Kit (Cat # 23235, ThermoFisher Scientific) and diluted to a series of concentrations within the working linear range of the method: 0, 0.5, 1, 2.5, 5, 10, 20 and 40 µg/ml.

Protein concentrations were determined using Microsoft Excel to generate a standard curve and then convert the optical density measurement into protein concentration. The standard curve was generated using the BSA standard described above where the optical density measurement from the blank wells (0 µg/ml BSA) was subtracted from all standard and experimental measurements. This standard curve was generated against the second order polynomial best fit line as recommended in the assay kit. Therefore, the equation of the best fit line followed the quadratic polynomial equation ($y = ax^2 + bx + c$). To solve for protein concentration of experimental samples, the quadratic equation was used:

$$x = \frac{-b \pm \sqrt{b^2 - 4a(c - y)}}{2a}$$

where x is protein concentration and y is optical density. The “LINEST()” function on excel was used to extract a, b, and c values from the line of best fit.

Chapter 3: Octopamine

Octopamine (OA) is a neurotransmitter that shows divergent evolution among vertebrate and invertebrate phyla. Evidence has suggested that the octopaminergic signalling system in invertebrates is analogous to the noradrenergic signalling observed in vertebrate species with little if any evidence for physiological roles for norepinephrine (NE) in invertebrates or for OA in vertebrates (Axelrod & Saavedra, 1977; Bauknecht & Jékely, 2017; David & Coulon, 1985; Roeder, 1999). Although OA receptors have not been identified in vertebrates, recent research indicates that at least two receptor types each for OA (octopamine α and β receptors) and NE (adrenergic α1 and α2 receptors) coexist in certain extant deuterostomes and protostomes (Bauknecht & Jékely, 2017). Based on this evidence, the authors suggest that these two signalling systems likely coexisted in an ancestral species with potentially redundant and overlapping functions; subsequent evolution led to differential loss of OA and NE receptors in protostomes and deuterostomes independently (Bauknecht & Jékely, 2017). Interestingly, in addition to overlapping functions, OA and NE share similar and somewhat intertwined synthetic pathways that could have facilitated their evolution and subsequent divergence.

The similarities between OA and NE synthesis may not come as a surprise when one considers that structurally the only difference is an extra hydroxyl group on the benzene ring in NE (Roeder, 1999). Both OA and NE synthesis start with the amino acid tyrosine (Broadley, 2010). NE is part of the catecholaminergic synthetic pathway, which starts with the conversion of tyrosine to L-DOPA by tyrosine hydroxylase followed by a conversion to dopamine by DOPA decarboxylase (DDC; Broadley, 2010). In OA synthesis, tyrosine is converted into tyramine by tyrosine decarboxylase (TDC; Broadley, 2010). Both DDC and TDC are distinct but evolutionarily related aromatic amino acid decarboxylases (AADC; Nagy & Hiripi, 2002; Sandmeier et al., 1994); however, recent research indicates that TDC can still bind and convert L-DOPA to dopamine (van Kessel et al., 2019; Zhu et al., 2016) indicating possible non-specific binding affinity between these AADCs. The final step in both NE and OA synthesis is the conversion of dopamine and tyramine into NE and OA, respectively, by a shared homologous enzyme; this enzyme is referred to as dopamine β-hydroxylase (DBH) and tyramine β-hydroxylase

(TBH) in vertebrate and invertebrate species, respectively. In addition to the traditional synthetic pathways, a major cytochrome P450 isoform, CYP2D6, has been shown to convert tyramine and OA into dopamine and NE, respectively (Hiroi et al., 1998; Wang et al., 2014). These observed interactions between OA and NE synthesis complicated early studies on OA biosynthesis (Axelrod & Saavedra, 1977; David & Coulon, 1985) and even led some to believe that OA evolved as a "metabolic mistake" (Evans, 1978).

In terms of physiological roles, OA was first identified in acetone extracts from the salivary glands of the octopus, from which it was named, and was found to exhibit adrenergic-like effects on blood pressure, small intestines, and hearts of various vertebrate species (Erspamer, 1948). Further research in vertebrates identified that OA was present in trace amounts at the nerve terminals of sympathetic neurons and the organs that they innervate, where OA was shown to be co-released with NE (Axelrod & Saavedra, 1977; Broadley, 2010; David & Coulon, 1985; Ibrahim et al., 1985; Robertson, 1981). Ultimately, OA signalling was revealed to mimic the effects of NE in vertebrates and given the colocalization, co-release, relative abundance and synthetic pathways of these biogenic amines, OA was largely regarded as a false or pseudo-transmitter (Axelrod & Saavedra, 1977; Evans, 1978; Pflüger & Stevenson, 2005); however, recent research into trace amines suggests that OA could act to modify NE signalling (Axelrod & Saavedra, 1977; Broadley, 2010). The opposite could be said in terms of OA and NE prevalence in invertebrate physiology.

In contrast to vertebrates, OA is a prominent signalling molecule in invertebrates believed to be analogous to the vertebrate adrenergic system with neurohormonal, neuromodulatory and direct neurotransmitter effects involved with regulating energy mobilization and stress (Adamo, 2012; Axelrod & Saavedra, 1977; David & Coulon, 1985; Pflüger & Stevenson, 2005; Roeder, 1999, 2020). Most extensively studied in the arthropods, OA has been shown to be involved in a broad range of behavioural and physiological processes; these functions include modulation of muscle contractions, such as increased heart rate (Chowański et al., 2017; Papaefthimiou & Theophilidis, 2011) or regulation of energy metabolism and activation of flight muscles (Duch & Pflüger, 1999; Goosey & Candy, 1982; Orchard & Lange, 1984). OA has also been implicated in neurohormonal release of adipokinetic hormone from the corpus cardiaca and medial

neurohemal tissues involved with energy mobilization (Antemann et al., 2018; Evans, 1978; Goosey & Candy, 1982). Additionally, evidence suggests a role for OA in modulating sensitivity to various sensory stimuli with implications in food and mate seeking behaviours (Farooqui, 2007; Hillier & Kavanagh, 2015; Jung et al., 2013; Mercer & Menzel, 1982); in food seeking behaviour, evidence is controversial with results showing a role for OA in starvation-induced hyperactivity (Yang et al., 2015) but also arrest of odour tracking and possible initiation of feeding (Sayin et al., 2019).

Although not as extensively studied, other phyla that OA has been described in are the nematodes (Churgin et al., 2017), platyhelminthes (El-Sakkary et al., 2018), annelids (Barna et al., 2001; Crisp et al., 2002; Crisp & Mesce, 2003) and molluscs (Elekes et al., 1993, 1996; Hiripi et al., 1998; Juorio & Molinoff, 1974; Pryce et al., 2015; Saavedra et al., 1974; Vehovszky et al., 1998). Evidence from nematodes, platyhelminthes and annelids indicate that OA modulates muscle contractions and stimulates excitatory locomotory activity (Barna et al., 2001; Churgin et al., 2017; Crisp & Mesce, 2003; El-Sakkary et al., 2018). In molluscs, research has provided evidence for stress-related responses such as increased heart rate and neurohormonal release in bivalves (Dougan & Wade, 1985; Pryce et al., 2015); however, most studied is the role of OA in modulating feeding behaviour and aversive taste conditioning in *L. stagnalis* (Aonuma et al., 2017; Vehovszky et al., 1998, 2005). In *L. stagnalis*, OA containing cells have been described in the buccal ganglia that interact and modulate neurons associated with the feeding network; pharmacological or electrical stimulation of these buccal OA cells activated feeding whereas antagonists injected into intact snails decreased instances of feeding (Hiripi et al., 1998; Vehovszky et al., 2005). In terms of conditioned taste aversion, it seems that high levels of OA, which are associated with food deprivation, block the learned taste aversion whereas low levels of OA enable conditioned taste aversion (Aonuma et al., 2017). Altogether, it has been proposed that a prominent role of invertebrate OA is to coordinate whole body physiological processes to prepare for heightened activity (Roeder, 2020).

Despite the extensive research exploring OA localization and function in adult arthropods and molluscs, relatively few studies describe early development and or function in larvae (Crisp et al., 2002; Elekes et al., 1996; Goodman & Spitzer, 1979;

Python & Stocker, 2002; Schneider et al., 1996). With regard to arthropods, research in *Drosophila melanogaster* larvae has revealed limited OA labelling in the subesophageal ganglion suggested to modulate olfactory processing (Python & Stocker, 2002); developmental studies on the grasshopper identified the emergence of OA in the dorsal unpaired neurons on day 13 of embryonic development (Goodman & Spitzer, 1979); and evidence indicates the developmental appearance of octopaminergic neurons in the lobster, *Homarus americanus*, at E43 (43% of embryonic development; Schneider et al., 1996). In an annelid, medicinal leech, octopaminergic elements became apparent on embryonic day 20 with all OA neurons present by the juvenile stage (Crisp et al., 2002). The only molluscan developmental study was performed on *L. stagnalis*, a gastropod with direct development, which showed the appearance of OA positive neurons at E85 (Elekes et al., 1996); this developmental stage is associated with post-metamorphosis of an indirect developing marine gastropod (Raven, 1966). Expanding on these early descriptions by looking at OA development in a broader variety of organisms within and across phyla will help elucidate the evolutionary relationship of OA signalling among invertebrates and provide possible insights into the evolutionary divergence of OA and NE signalling among vertebrate and invertebrate phyla.

The present chapter expands on this previous work by investigating the development of octopaminergic neuronal elements in larval stages of indirect developing marine gastropods, *Ilyanassa obsoleta* and *Aplysia californica*. Given past evidence suggesting the homology of DBH and TBH enzymes, I use the comparison of antibodies raised against DBH and OA as a conservative control to confirm the presence of neuronal OA during larval development; therefore, either overlapping staining patterns or, when possible, co-localization of antibodies was used to indicate true OA positive cells.

To show proof of concept, I first verified sequence homology among human and invertebrate DBH and TBH enzymes with Clustal Omega multi-sequence alignments (Madeira et al., 2019) using sequences retrieved from the National Center for Biotechnology Information (NCBI)'s database. I then characterized a DBH antibody using sequence alignments and western blots, including preadsorption controls. Finally, I performed immunohistochemistry on adult dissected CNSs from *A. californica* and *L. stagnalis* and showed co-localization of OA and DBH antibodies. Results from this study

provide information on OA during development of gastropods and lay the framework for future comparisons among more distantly related phyla; thus, informing our understanding of the evolutionary history of OA in the nervous system.

3.1 Results

3.2.1 Antibody Specificity Analysis

To evaluate the applicability of the DBH antibody as a marker to confirm the validity of OA-LIR and DBH-LIR labelling in gastropod molluscs, I first performed protein alignments to show the homology of DBH and TBH enzymes and the conservation of the DBH target sequence used to raise the antibody. Next, I performed western blots to test specificity and characterize target antigens. Finally, I performed immunohistochemistry on adult specimens of freshwater and marine species to confirm the potential for co-localization of DBH with OA.

3.2.1.1 Dopamine β-Hydroxylase Sequence Analysis. Since the criteria used to indicate the presence of octopaminergic neural elements in this study was the colocalization of DBH with OA immunoreactivity, protein alignments were performed to verify sequence homology among human DBH and molluscan tyramine β-hydroxylase (TBH)/DBH. *Lymnaea stagnalis* TBH (Accession # BAM35937.1), *Biomphalaria alexandrina* DBH (Accession # 013081477.1), and *Aplysia californica* DBH (Accession # XP_035825847.1) sequences were aligned to a human DBH precursor sequence (Accession # NP_000778.3) demonstrating a high degree of conservation (Fig 1). As shown in figure 1, sections of the four aligned sequences between amino acids 198 to 314 (aa198-314) and aa349-480 were nearly identical. The percent identity matrix shows that *L. stagnalis* TBH, *B. alexandrina* DBH, and *A. californica* DBH were 47.14 %, 44.77 %, and 44.27 % identical to the human DBH precursor sequence, respectively. The highest degree of similarity was indicated between the two freshwater gastropods *L. stagnalis* and *B. alexandrina* (Percent identity = 68.38 %; Table 3). Unfortunately, no TBH or DBH sequence could be found for *Ilyanassa obsoleta* on NCBI's (National Center for Biotechnology Information) database.

In addition to the alignments of the full DBH/TBH synthetic enzymes, the aforementioned protein sequences were aligned to the synthetic human DBH target sequence corresponding to amino acids 437-448 (DNHYSPHFQEIR), which was used to raise the DBH antibody (Cat # ab189991, Abcam). Results showed near identical alignments between amino acids 444 to 455 among human and molluscan sequences with the DBH target sequence (Fig 2); the only exceptions were a change in *B. glabrata* at amino acid position 447 (aa447) from tyrosine (Y) to phenylalanine (F) and two changes in *A. californica* at aa445 and aa449 with changes from asparagine (N) to lysine (K) and proline (P) to glutamine (Q), respectively. Despite these differences, only the amino acid change at aa449 in *A. californica* resulted in an amino acid with different properties, thus indicating the Abcam DBH antibody as a strong candidate for comparative studies.

Table 3. Percent identity matrix showing the percent of identical amino acids compared among the entire dopamine β-hydroxylase (DBH) and tyramine β-hydroxylase (TBH) sequences among species investigated (see Fig 1 for alignment).

Dopamine β-hydroxylase Sequence	Human (NP_000778.3)	*Aplysia califonica* (XP_035825847.1)	*Lymnaea stagnalis* (BAM35937.1)	*Biomphalaria alexandrina* (XP_013081477.1)
Human (NP_000778.3)	100.00	-	-	-
Aplysia califonica (XP_035825847.1)	44.27	100.00	-	-
Lymnaea stagnalis (BAM35937.1)	47.14	57.89	100.00	-
Biomphalaria alexandrina (XP_013081477.1)	44.77	57.11	66.38	100.00

3.2.1.2 Western Blot Analysis. In addition to protein sequence analyses, western blots were performed to test the specificity and validity of the DBH antibody. Protein extraction and western blot protocols were developed using *L. stagnalis* nervous tissue and results revealed two strong bands and a relatively faint band between 50 and 75 kDa and a fourth faint band between 37 and 50 kDa (Fig 3; $n = 2$). Comparing the Abcam antibody (Cat # ab189991) with a second DBH antibody from Immunostar (Cat # 22806)

revealed matching strong bands between 50 and 75 kDa (Fig 3, solid arrows; $n = 1$) and a matching faint band between 37 and 50 (Fig 3, open arrowhead). These bands were consistent with evidence suggesting a membrane-bound and cytosolic isoform of DBH and potential degradation products produced by detergent-based protein extraction protocols (Joh & Hwang, 1987; Lewis & Asnani, 1992). Additionally, the protein band representing the largest molecular weight matched the expected molecular weight of 66 kDa generated from *L. stagnalis* sequence data (TBH, accession # BAM35937.1). Extraneous to the shared protein bands, the Immunostar DBH antibody revealed four faint bands between 75 and 250 kDa that were absent when probed using the Abcam DBH antibody (Fig. 14); these bands are likely generated by non-specific binding of the polyclonal antibody, as compared to the more specific binding generated from the affinity purified Abcam antibody. To demonstrate reliability of the protein extraction procedure, a western blot was performed using an antibody raised against acetylated-tubulin (Cat # T6793, MilliporeSigma) revealing a single protein band near the 50 kDa ladder marker (Fig 3), matching the expected molecular weight of 55 kDa. These results revealed the applicability of DBH antibodies for studies in molluscs, and the general protocols for protein extraction and western blots to successfully probe for multiple proteins using different antibodies (see Young et al., 2022).

After these protocols were established, I performed western blots using tissue homogenates generated from dissected adult central nervous systems (CNSs) from every organism investigated in this study: *L. stagnalis*, *B. alexandrina*, *A. californica*, and *I. obsoleta*. Results showed labelling of the same two bands between 50 and 75 kDa across all species (Fig 4; $n = 2$). Preadsorption of primary antisera with DBH blocking peptides showed a decrease in signal, further supporting specificity of the primary DBH antibody used in this study (Fig 4; $n = 2$). No attempt was made to titrate antibody and blocking peptide concentrations to achieve complete pre-adsorption of antibodies; interestingly, bands from *B. alexandrina* and *A. californica* homogenates were blocked preferentially, which could reflect mutations in the corresponding epitope within their DBH sequences (Fig. 2).

3.2.1.3 Co-localization in Adult Specimen. To test the application of OA and DBH antibodies in immunohistochemistry protocols and test the hypothesis that octopaminergic neurons would also contain DBH, adult freshwater gastropods, *L. stagnalis* and *B. alexandrina*, were processed and analyzed. Both *L. stagnalis* and *B. alexandrina* showed positive immunoreactivity to OA and DBH antibodies with double labels revealing colocalization, which supports the criteria used herein for determining true OA positive labelling. Additionally, OA-LIR labelling matched a subset of cells described previously using a different OA antibody in adult *L. stagnalis* providing further confidence (Elekes et al., 1993).

Results in dissected central ganglia of *L. stagnalis* revealed OA and DBH positive labelling in the buccal, cerebral and pedal ganglia with some degree of colocalization occurring in each ganglion (Fig 5; $n = 3$). The buccal ganglia showed colocalization of asymmetrically positioned cells with a single cell visible in the left ganglion (Fig 5A-C, solid arrowhead) and two cells in the right ganglion (Fig 5A-C, open arrowheads); however, DBH-LIR cells that were negative for OA immunoreactivity were also found along the lateral anterior/dorsal edges (Fig 5A-C, arrows). The pedal ganglia showed colocalization of immunoreactivities within two paired bilateral cells (Fig 5D-F, solid arrowhead) and some fibers in the neuropil (Fig 5D-F, open arrowhead); the DBH-LIR labelling showed more extensive staining in the neuropil and two extraneous cells not labelled with OA along the lateral edge (Fig 5D-F, arrows). Although not shown, colocalization of OA and DBH could be found in a cell along the lateral edge of the cerebral ganglia positioned between the cerebral-pedal and cerebral-pleural connectives. In addition to the three samples processed for this thesis, isolated *L. stagnalis* CNSs were processed as part of a collaboration by Alex Young and Dr. Roger Croll (unplublished), which reveal corroborating results. Similar staining as described here was also observed in *B. alexandrina*, with more detailed descriptions part of a collaborative project (Imai et al., unpublished).

Like the freshwater gastropods, juvenile *A. californica* showed evidence for DBH and OA colocalization (Fig 6). Since both the OA and DBH antibodies worked optimally using different fixation protocols, double-labels were not initially performed; however, the striking similarity of the OA and DBH-LIR labelling in post-metamorphic animals

suggested that these cells were in fact OA neurons and further supports the use of DBH and OA colocalization as a control to improve confidence.

Results in post-metamorphic *A. californica* revealed OA (n = 3) and DBH-LIR (*n* = 3) cells in the buccal, cerebral and pedal ganglia. In the buccal ganglia (BG), an asymmetric placement of cells was visible along the medial edges of the ganglia lateral to the buccal commissure (BC), similar to that described in freshwater species (Fig 5A-C), with a single cell in the left ganglion (Fig 6A-A', solid arrowhead) and two cells in the right ganglion (Fig 6A-A', open arrowheads); additionally, fibers could be seen projecting through the neuropil of the BG (Fig 6A-A', arrows). The cerebral ganglia showed labelling of a single cell anteriorly (Fig 6B-B', arrow) and along the medial lateral edge (Fig 6B-B', open arrowhead), as well as a cluster of small cells posteriorly (Fig 6B-B', solid arrowhead). Finally, the pedal ganglia showed relatively large, paired cells along a ventral-lateral lobe (Fig 6C-C', arrows).

3.2.1.4 Octopamine Pre-adsorption Control. The octopamine antibody used in this study has been used to describe octopaminergic neurons in various arthropods (Konings et al., 1988; Sinakevitch et al., 1994); however, to test specificity in molluscan larvae I conjugated OA and bovine serum albumen (BSA) with glutaraldehyde to block HA specific labelling. I tried two different sets of pre-adsorption experiments using *I. obsoleta* at 7 days post oviposition (DPO). In the first experiment, I used a concentration of 196 µg/ml of the OA-BSA conjugate with a 1:100 antibody dilution; in this experiment the pre-adsorption control failed to block labelling. In the second experiment, I used a concentration of 654 µg/ml of the OA-BSA conjugate in the antiserum with a 1:300 antibody dilution; however, in this experiment both the pre-adsorption and experimental control failed to produce any labelling. Therefore, the results of the pre-adsorption attempts were inconclusive.

3.2.2 Embryonic/Larval Development

With the DBH antibody characterized and the rationale behind its applicability to confirm the presence of OA in neuronal elements supported by experimental methods, I

next investigated the presence of OA in early larval development of the marine molluscs, *A. californica* and *I. obsoleta*.

3.2.2.1 Aplysia californica Immunohistochemistry. Specimens of *A. californica at* embryonic days 2, 5 and 7 as well as stage 1 and 6 veligers were fixed and labelled for OA and DBH immunoreactivity. No labelling was observed throughout the embryonic stages of development; however, at stage 1 of larval development (hatchling veliger) indistinct bilateral concentrations of OA-LIR labelling were visible in the cephalopedal region (Fig 7A, brackets; $n = 8$). Once specimens developed to stage 6 (metamorphically competent veliger) OA-LIR labelling revealed a large bilateral structure showing strong immunoreactivity located in a region around the cerebral/pedal ganglia (Fig 7B-B', solid arrowheads; $n = 3$). Additionally, there were at least two potential bilateral cells that exhibit a less intense signal positioned more posteriorly, possibly part of the rudimentary posteriorly developing ganglia (Fig 7B, arrows); these two bilateral cells had faint fiber-like labelling that extended anteriorly connecting to the aforementioned intensely labelled bilateral structures (Fig 7B, open arrowheads). This early labelling of OA was unusual in that the anterior large bilateral structures were larger than larval neurons and the fibers from posteriorly placed cells were faint and exhibited low contrast with background.

DBH-LIR labelling was also not observed at embryonic days 2, 5, or 7; however, DBH did not show overlap with OA-LIR labelling at stage 6. Instead, DBH-LIR labelling showed a bilaterally placed cell along the medial-anterior edge of the developing cerebral ganglia (Fig 8A, open arrowheads; $n = 3$). The cerebral bilateral cells were located along fibers that projected across the cerebral commissure (CeC) and wrapped around to the ventral side of the esophagus (Fig 8A-A'', brackets), presumably through the neuropil of the cerebral and pedal ganglia and across the pedal commissure. Ventral to the esophagus, fibers projected into the footpad (Fig 8B-B') and seemed to branch, forming a nerve-net like plexus with scattered cell bodies (Fig 8C). Additionally, a faintly labelled bilateral cell was evident in the propodium (Fig 8B, solid arrowheads).

3.2.2.2 Ilyanassa obsoleta Immunohistochemistry. Consistent with what was found in larvae of *A. californica*, OA and DBH-LIR labelling in *I. obsoleta* larvae did not

show overlapping staining patterns. Based on the criteria used for this study, these results indicate the absence of true octopaminergic neuronal elements in larval development suggesting that OA lacks a role in early larval behaviour, however, alternative explanations are given in the discussion.

OA-LIR labelling first appeared at 7 days post oviposition (DPO), which corresponded to the late embryonic veliger stage. Labelling resembled bilateral oblong structures that follow along posterior loop fibers (See histamine results, Fig 15; Fig 9A-C) with the left (LPF) and right (RPF) structure following a path that is ventral and dorsal to the esophagus, respectively. The anterior portion of each of these oblong structures showed evidence of branching in regions around the eyes (Fig 9B, solid arrowheads). The labelling sometime resembled net-like superficial labelling along the perimeter of cell membranes similar to a sheath of connective tissue (image not shown). As *I. obsoleta* developed further, the general organization of the labelling stayed consistent but became more extensive with the addition of more oblong cells. By 25 DPO, OA-LIR staining resembled a chain of oblong and irregular shaped cells (Fig 9D-D', arrows) with relative few fiber-like projections (Fig 9D-D', solid arrowheads). Like younger specimen, these 25 DPO veligers showed indications of branching at/or around the eyes.

For DBH-LIR labelling, preliminary results using adult freshwater species, *L. stagnalis* and *B. alexandrina*, and the marine opisthobranch, *A. californica*, showed positive DBH-LIR labelling with either a 9 parts methanol and 1 part formaldehyde or 4% PFA fixation; therefore, larval specimen processed with both fixations were incubated with the DBH antibody for analysis. The 9 parts methanol and 1 part formaldehyde fixative produced staining that was determined to be more consistent, so the full range of developmental stages were analyzed (Fig 10).

DBH-LIR labelling was first observed at around 9 DPO (Fig 10A), corresponding to the hatchling stage, revealing a blebby discontinuous fiber that extended through the apical region (Fig 10A, CeC), dorsal to the mouth (Fig 10A, M) and esophagus. The majority of hatchling specimens solely showed labelling of this rudimentary cerebral commissure (CeC), however, a single sample showed a faintly labelled cell where the right cerebral ganglion is expected to develop (Fig 10A, RCeG). DBH-LIR labelling did not change up to 25 DPO, corresponding to a late-stage free swimming veliger (Fig 10B).

At 25 DPO, specimen still showed a blebby and discontinuous process within the cerebral commissure (CeC) extending dorsal to the esophagus (Eso), however, a bilateral cell was consistently found in the cerebral ganglia (Fig 10B, CeG).

Despite having showed less consistent and less intense labelling than the 9 parts methanol and 1 part formaldehyde fixed specimen, a 4% PFA fixed specimen provided the most extensive labelling (Fig 11). This specimen was around the hatchling developmental stage and showed a large concentration of blebby labelling spanning the apical region, corresponding to the rudimentary cerebral commissure (Fig 11A'-B, CeC). A faintly labelled cell within the cerebral ganglion (CeG) was located medial to the left eye (Fig 11 A'-B, open arrowhead) and connected to the cerebral commissure by a faintly labelled fiber (Fig 11B, arrow). This unilateral cell is likely part of a bilateral pair evident by the symmetry found with the rest of the labelling and matching faint fiber on the right side of the CeC (Fig 11B, arrow); however, the faint and inconsistent labelling produced by the DBH antibody and fixative protocols used in larval stages could have led to incomplete labelling. From the apical labelling, blebby discontinuous processes extended into the foot (Fig 11A', arrows) and along the medial edge of the vela around the dorsal and lateral sides of the mouth (Fig 11A, arrow); the deep labelling with processes into the foot and the superficial labelling were connected by bilateral fibers projecting along the anterior to posterior axis.

3.2 Discussion

Results in this study showed the high degree of sequence homology among human DBH and gastropod TBH enzymes, supporting the concept of using commercial antibodies raised against vertebrate DBH to confirm OA positive labelling in invertebrates. Additionally, results show the characterization of a DBH antibody revealing conservation of its target sequence, estimated molecular weights of different antigen isoforms across four different gastropod species, and its ability to colocalize with an antibody raised against an OA conjugate. These findings provide proof of concept for mapping the co-localization of DBH and OA and suggesting the reliability of a DBH antibody for use in comparative studies across Bilateria. Finally, this study suggests the

absence of octopaminergic neural elements during larval development in both *I. obsoleta* and *A. californica*.

Evidence suggesting the absence of OA during larval development is based on immunohistochemical labelling presented in this study that failed to show colocalization of OA and DBH antibodies during larval stages. OA- and DBH-LIR labelling was revealed but both antibodies showed staining patterns without any overlap. In contrast to the DBH-LIR labelling, OA-LIR labelling in larvae showed structures that were either too large or too irregular to be considered neuronal (see Fig 7 and 9). Previous research has shown that catecholamines and their metabolites can be converted to OA and vice versa (Broadley, 2010; David & Coulon, 1985; Hiroi et al., 1998; Wang et al., 2014), therefore it is possible that OA-LIR larval labelling revealed herein represents the coincidental conversion of monoaminergic metabolites in various tissues. The DBH-LIR labelling did show convincing neuronal labelling of a single bilaterally located cerebral cell with projections that cross the cerebral commissure and into the foot where peripheral cells could be identified (see Figs 8, 10 and 11). These results are consistent with previous descriptions that indicated DBH-LIR labelling that showed either peripheral cells in the foot or fibers that extended across the apical neuropil and into the foot of *I. obsoleta* depending on whether a methanol or 4% PFA fixation was used (Dickinson & Croll, 2003). Based solely on these results, the DBH-LIR labelling could potentially indicate the presence of NE in larval development, or perhaps that the DBH enzyme is expressed in development prior to the availability of tyramine, which would be necessary for traditional OA synthesis. Alternative explanations for independently labelled DBH-LIR neurons are that given the fixation protocols used, the OA antibody was not sensitive enough to detect the relatively low concentrations of OA that could have been present, or that the Abcam DBH antibody non-specifically bound another enzyme among the monooxygenase protein family.

Despite evidence suggesting the absence of neuronal octopaminergic elements in larva, results indicate that neural sources of OA in molluscan gastropods do appear in post-metamorphic stages of development. This is consistent with a developmental study performed in *L. stagnalis* that showed the appearance of OA-LIR elements in specimen developed to E85, corresponding to a post-metamorphic animal prior to hatching (Elekes

et al., 1996). In adults, OA has been shown to be involved in modulating feeding behaviour in *L. stagnalis* (Vehovszky et al., 1998, 2005) and various arthropods (Sayin et al., 2019; Yang et al., 2015). In arthropods, it is believed that OA modulates feeding behaviour and even sensitivity to sensory stimuli in response to their physiological state (Farooqui, 2007; Sayin et al., 2019; Yang et al., 2015); it is likely that OA also modulates feeding in a manner dependent on physiological state in *L. stagnalis* and other molluscs (Aonuma et al., 2017). Given the absence of OA in the planktonic larvae of the marine gastropods, *I. obsoleta* and *A. californica*, it is possible that their physiology is not complex enough to require such state dependent mechanisms. Additionally, this could reflect an evolved life history strategy where a large number of offspring are produced and energy is directed to behaviours that optimize growth and development at the detriment of complex stress responses to ensure the survival of a few offspring to metamorphosis.

Future research should attempt to investigate the nature of single labelled DBH-LIR neurons in the gastropod larvae; among other explanations, these neurons could reflect noradrenergic neurons, or perhaps octopaminergic neurons with OA concentrations too low to be detected by methods used in this study. Additionally, the labelling could indicate non-specific binding to a closely related enzyme from the monooxygenase protein family. One way to investigate these explanations could be to use antibodies that target alternative synthetic enzymes in the catecholaminergic and octopaminergic synthetic pathways such as TDC/DDC, and TH to determine if the necessary precursors are present for NE or OA synthesis. It would also be interesting to expand the approaches in this study to a broad range of invertebrate larvae from both deuterostomes and protostomes to determine the prevalence of OA and NE signalling in larvae across Bilateria. Results from these studies could provide novel perspectives on the evolutionary history of OA and NE signalling.

In conclusion, this study indicates that octopaminergic neural elements do not appear until post-metamorphic developmental stages of gastropod molluscs and also provides evidence supporting an Abcam DBH antibody (cat # ab189991) as a candidate for comparative immunohistochemical studies. These results provide the framework for comparing the localization of OA during development of species across Bilateria. The

absence of OA containing neurons in gastropod larvae could imply that sympathetic-like stress responses do not arise until post-metamorphosis, which could be relevant in terms of the evolution of multicellular stress signalling.

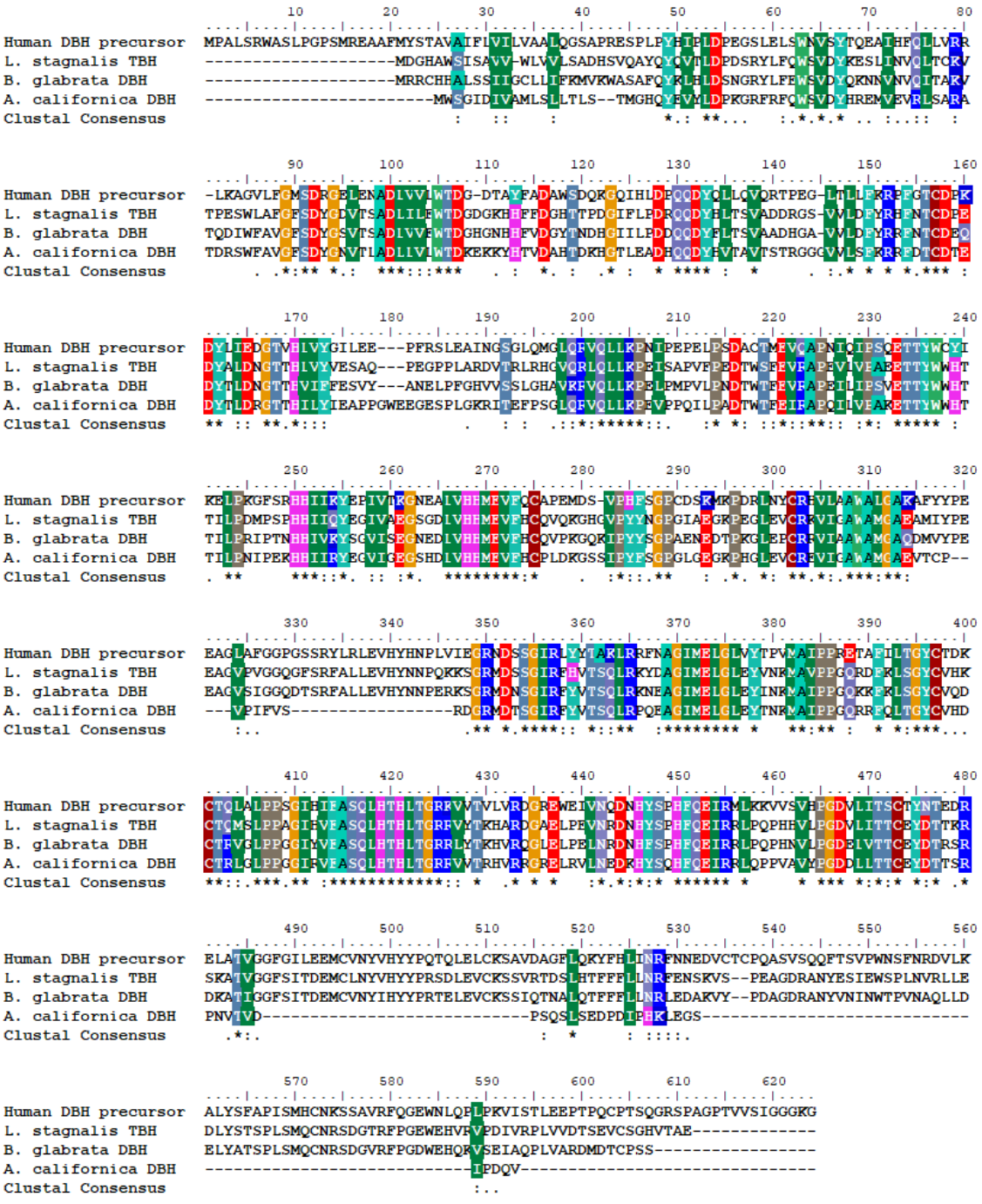
Human DBH precursor
L. stagnalis TBH
B. glabrata DBH
A. californica DBH
Clustal Consensus

Figure 1. Clustal Omega multi-sequence alignment performed and visualized using BioEdit. Tyramine β-hydroxylase (TBH) and dopamine β-hydroxylase (DBH) sequences from *L. stagnalis* (Accession # BAM35937.1), *B. alexandrina* (Accession 013081477.1), # XP_and *A. californica* (Accession # XP_035825847.1) were aligned to a human DBH sequence (Accession # NP_000778.3) showing a large degree of similarity. Clustal consensus sequence indicates aligned amino acids that are identical (asterisk), have strongly similar properties (colon) and have weakly similar properties (period). Identical and similar amino acids were shaded according to the BioEdit color table with the shading threshold set to 100%.

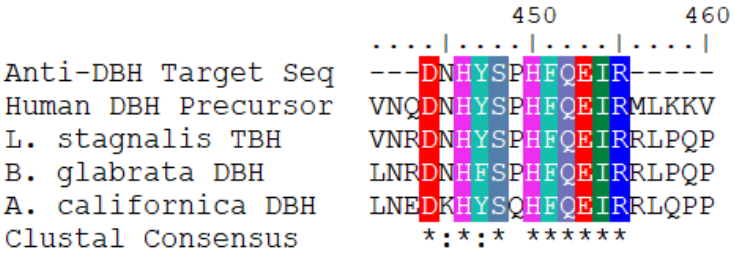
450
460
Anti-DBH Target Seq ---DNHYSPHFQEIR-----
Human DBH Precursor VNQDNHYSPHFQEIRMLKKV
L. stagnalis TBH VNRDNHYSPHFQEIRRLPQP
B. glabrata DBH LNRDNHFSPHFQEIRRLPQP
A. californica DBH LNEDKHYSQHFQEIRRLQPP
Clustal Consensus *:*:* ******

Figure 2. Clustal Omega multi-sequence alignment performed and visualized using BioEdit showing nearly a 100% amino acid sequence match among tyramine β-hydroxylase (TBH) and dopamine β-hydroxylase (DBH) sequences from human (Accession # NP_000778.3), *L. stagnalis* (Accession # BAM35937.1), *B. alexandrina* (Accession # XP_013081477.1), and *A. californica* (Accession # XP_035825847.1) with the synthetic target sequence used to raise the Abcam DBH antibody (Cat # ab189991). Clustal consensus sequence indicates aligned amino acids that are identical (asterisk), have strongly similar properties (colon) and have weakly similar properties (period). Identical and similar amino acids were shaded according to the BioEdit color table with the shading threshold set to 100%.

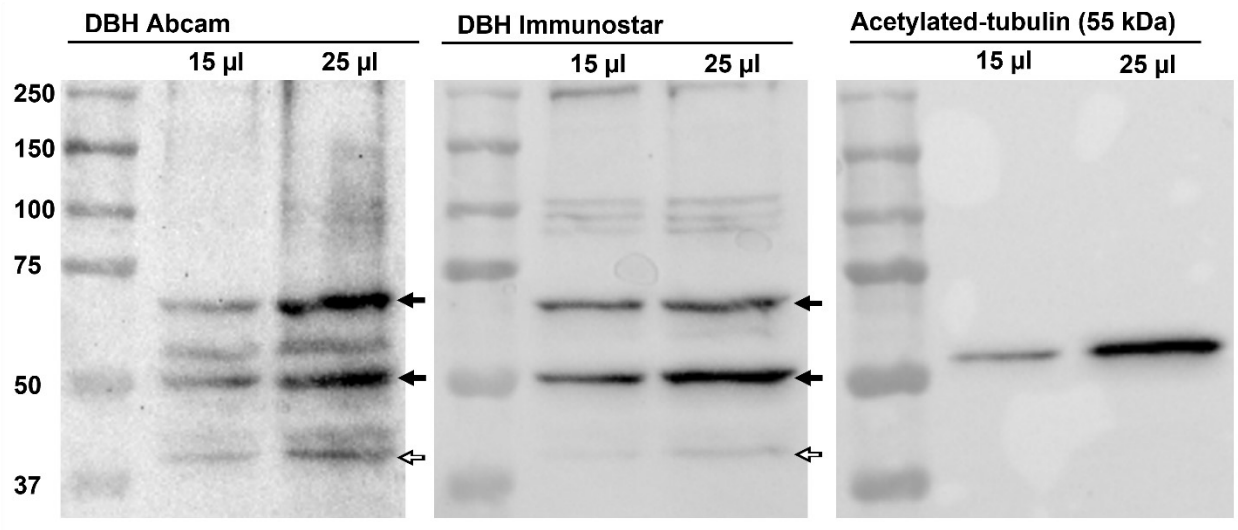
DBH Abcam
15 µl
25 µl
DBH Immunostar
15 µl
25 µl
Acetylated-tubulin (55 kDa)
15 µl
25 µl
250
150
100
75
50
37

Figure 3. Western blot showing the binding specificity of two separate DBH antibodies and an antibody raised against acetylated-tubulin (AcT) in *L. stagnalis* CNS homogenate. Both the affinity purified polyclonal Abcam (Cat # ab189991) and polyclonal Immunostar (Cat # 22806) antibodies showed three matching protein bands; two strongly labelled bands between 50 and 75 kDa (solid arrowheads) and a relatively faint band between 37 and 50 kDa (open arrowhead) indicated by the Precision Plus Protein ™ All Blue Standard molecular weight ladder. These bands are consistent with previous research showing up to three potential bands resulting from membrane-bound and cytosolic isoforms, as well as different degradation products (Joh & Hwang, 1987; Lewis & Asnani, 1992). The largest band reflects the expected molecular weight of 66 kDa generated by a *L. stagnalis* protein sequence (TBH, accession # BAM35937.1). A western blot probing for AcT, which has an expected molecular weight of 55 kDa, was performed to verify the reliability of protein extraction and western protocols; the AcT blot used in this figure was previously published in Young et al. (2022). Two lanes were loaded with protein extract, one with 15 µl (~115 µg) and the other with 25 µl (~190 µg). The exposure times for the Abcam, Immunostar and acetylated-tubulin blots were 83, 26, and 80 seconds, respectively.

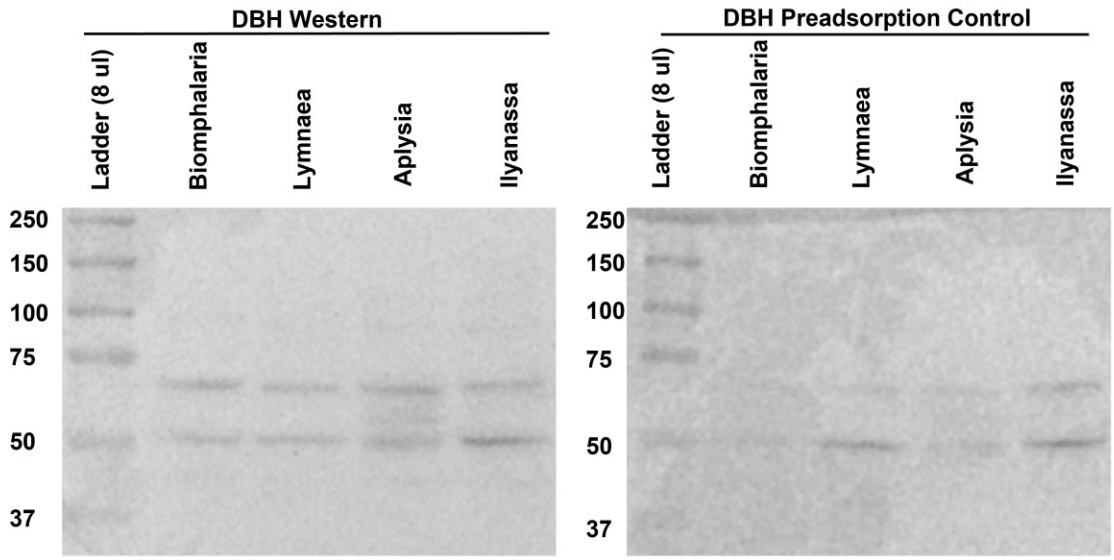
DBH Western
Ladder (8 ul)
Biomphalaria
Lymnaea
Aplysia
Ilyanassa
250
150
100
75
50
37
DBH Preadsorption Control
Ladder (8 ul)
Biomphalaria
Lymnaea
Aplysia
Ilyanassa
250
150
100
75
50
37

Figure 4. Western blots showing the binding specificity of the Abcam DBH antibody (Cat # ab189991) in CNS homogenate from each species investigated: *B. alexandrina*, *L. stagnalis*, *A. californica*, and *I. obsoleta*. Results showed two strong protein bands between 50 and 75 kDa indicated by the Precision Plus Protein ™ All Blue Standard molecular weight ladder, consistent with membrane-bound and cytosolic isoforms. The two labelled protein bands matched across all species with the largest band reflecting the expected molecular weight of 66 kDa generated by a *L. stagnalis* protein sequence (TBH, accession # BAM35937.1), thus indicating the antibody as a good candidate for comparative studies. Each well was loaded with 20 µl of protein extract resulting in total protein content that varied based on the concentration of each extract (*B. alexandrina* = ~110 µg, *L. stagnalis* = ~153 µg, *A. californica* = ~141 µg, and *I. obsoleta* = ~116 µg). Exposure time for both the experimental and pre-adsorption blots was 210 seconds.

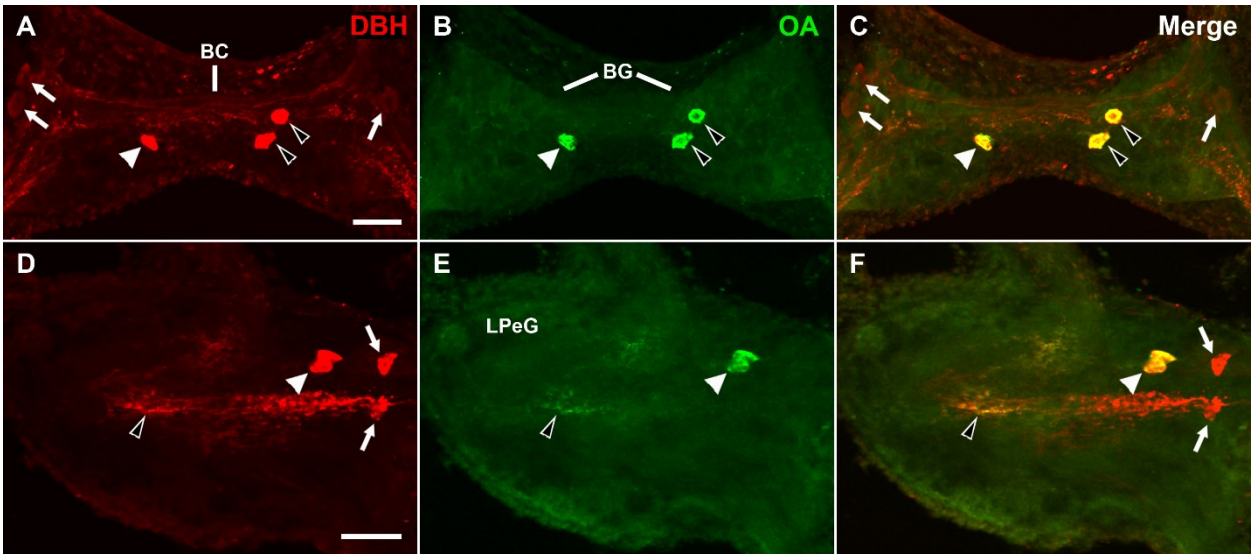
A
DBH
BC
B
OA
BG
C
Merge
D
E
LPeG
F

Figure 5. Micrographs showing double labels of DBH and OA-LIR labelling in ganglia of the central nervous system in adult *Lymnaea stagnalis*. A-C) Caudal perspective of the buccal ganglia (BG) showing an asymmetric placement of cells lateral to the buccal commissure (BC) with a single cell in the left BG (solid arrowhead) and two adjacent cells visible in the right BG (open arrowheads) labelled with both octopamine (OA) and dopamine β-hydroxylase (DBH); additionally, cells labelled solely with DBH are evident along lateral-anterior/dorsal edges (arrows). D-F) Dorsal perspective of the left pedal ganglion (LPeG) showing two lateral cells co-labelled with DBH and OA (solid arrowhead); DBH showed extraneous labelling of cells (arrows) and more extensive labelling of the neuropil (open arrowheads; scale bars = 100 μm).

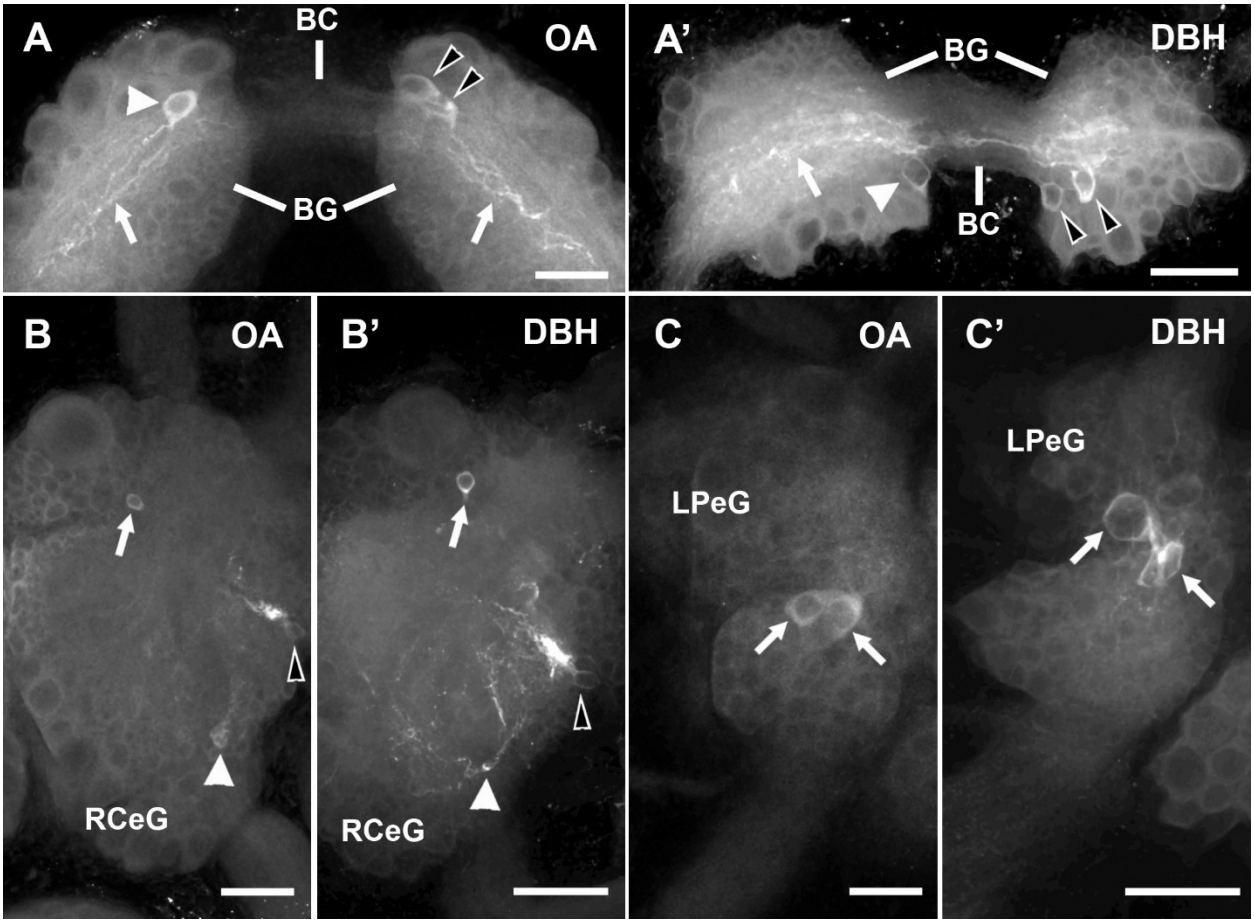
A
BC
OA
BG
A'
BG
DBH
BC
B
OA
RCeG
B'
DBH
RCeG
C
OA
LPeG
C'
DBH
LPeG

Figure 6. Side by side micrographs showing octopamine (OA) and dopamine β-hydroxylase (DBH)-LIR labelling in central ganglia of post-metamorphic, juvenile, *A. californica* revealing similarities in staining pattern. A-A') OA (A) and DBH-LIR (A') labelling in buccal ganglia (BG) viewed from slightly different perspectives showing an asymmetric placement of cells lateral to the buccal commissure (BC) with a single cell in the left BG (solid arrowhead) and two adjacent cells visible in the right BG (open arrowheads); additionally, processes are evident within the neuropil (arrows). B-B') Dorsal perspective of OA (B) and DBH-LIR (B') labelling in the right cerebral ganglia (RCeG) showing the labelling of three cells in the same pattern with a single cell in the anterior half of the ganglion (arrow), along the lateral medial edge (open arrowhead) and in the posterior half of the ganglion (solid arrowhead). C-C') Ventral-lateral perspective of OA (C) and DBH-LIR (C') labelling in the left pedal ganglion (LPeG) showing paired cells (arrows; scale bars = 100 μm).

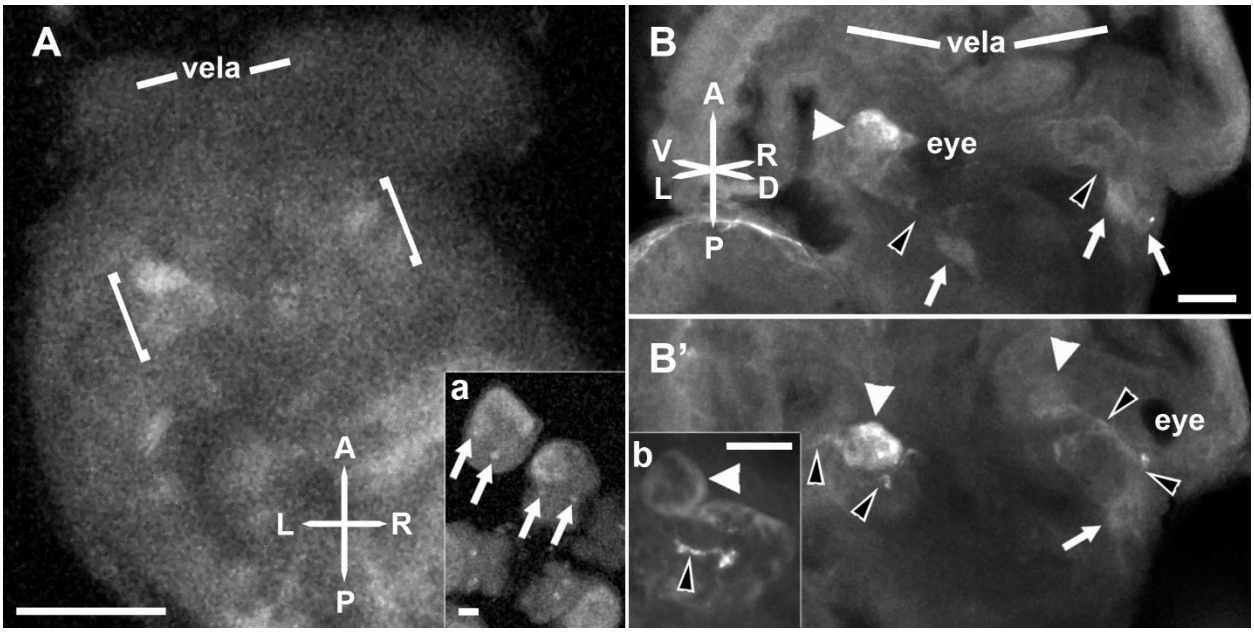
A
vela
A
L
R
P
a
B
vela
A
V
R
L
D
P
eye
B'
b
eye

Figure 7. Micrographs showing OA-LIR labelling in *A. californica* at stage 1 (hatching; A/a) and stage 6 (competent veliger; B/b). A) Dorsal perspective of a stage 1 hatchling showing bilateral concentrations of OA-LIR labelling (brackets); a) inlay showing low magnification of four hatchling veligers all showing this bilateral pattern of labelling (arrows). B-B') Slightly angled dorsal view of a stage 6, competent, veliger showing superficial (B) and deep (B') OA-LIR labelling. B) Strong labelling of an ovular structure resembling a single large cell (solid arrowhead) near the left eye, which evidence suggests has a contralateral counterpart; faint labelling is observed extending posteriorly from the region of intense labelling that is also observed contralaterally (open arrowheads) with potentially two faintly labelled bilateral cells (arrows). B') Clear labelling of strongly labelled cell-like structure on left side of the organism with opposing structure only faintly labelled (solid arrowheads); faint labelling of potential fibers are visible (open arrowheads) with a single faint cell still visible from the superficial labelling (B) along the right side of the organism (arrow); b) inlay showing one of a bilaterally located large single cell (solid arrowhead) and labelled process (open arrowhead) matching that shown in B but from a different perspective (scale bars = 25 μm; orientation labels = A, anterior; P, posterior; V, ventral; D, dorsal; L, left; R, right).

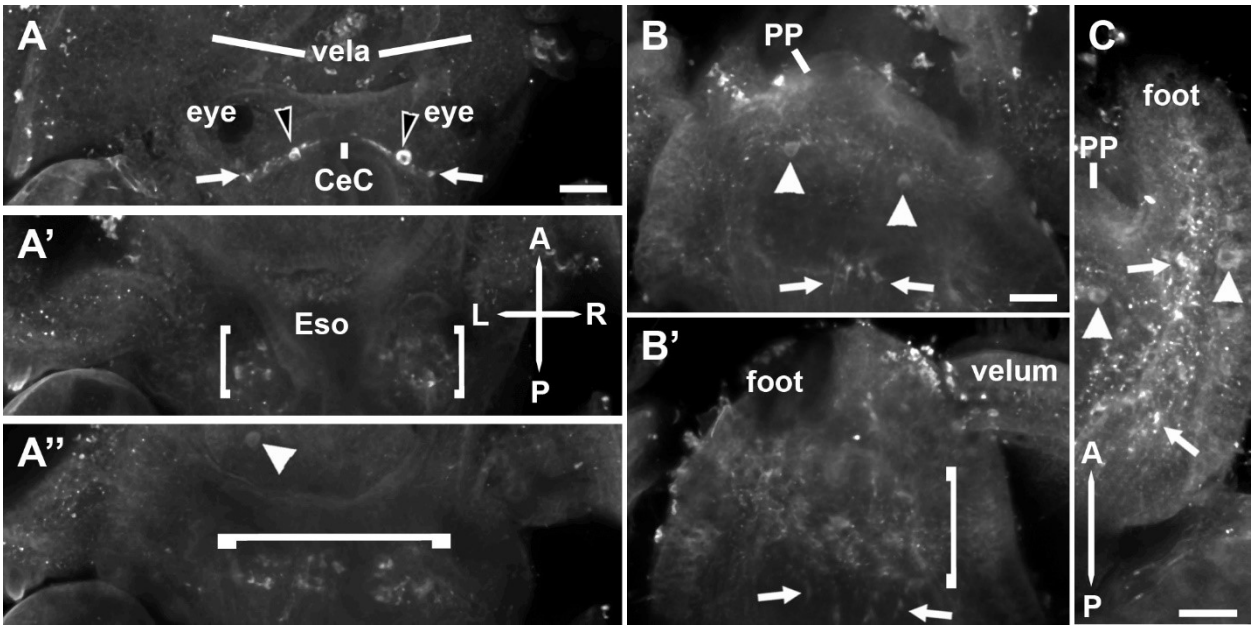
A
vela
eye
eye
CeC
A'
Eso
A
L
R
P
A''
B
PP
B'
foot
velum
C
foot
PP
A
P

Figure 8. Micrographs showing DBH-LIR labelling in *A. californica* stage 6, competent, veligers that were fixed using a solution of 9 parts methanol and 1 part formaldehyde. A-A'') Dorsal perspective showing superficial (A), intermediate (A') and deep (A'') labelling of a single specimen. A) A strongly labelled bilaterally located cell is evident medial to the eyes (open arrowheads) where the cerebral ganglia are expected to develop. These cerebral cells appear along a horizontal, apically spanning fiber herein called the cerebral commissure (CeC); additionally, fragmented blebby processes extend ventral-laterally (arrows). A') Brackets show the continuation of ventral-laterally projecting blebby labelling to either side of the esophagus (Eso). A'') Discontinuous blebby labelling from the cerebral cells extend ventral to the esophagus (bracket) with a faint cell visible in the propodium (solid arrowhead). B-B') Continuation of A showing superficial (B) and deep (B') labelling in the foot. B) Solid arrowheads indicate a faintly labelled bilateral cell located in the propodium (pp); the beginning of four faintly labelled processes extending into the foot are also visible between the arrows. B') Continuation of the four ventrally projecting foot fibers (arrows) and diffuse ambiguous labelling within the center of the footpad (bracket). C) A side perspective of the foot showing punctate labelling of potential fibers with extensive branching (arrows) and relatively faint cells (solid arrowheads; scale bars = 25 μm; orientation labels = A, anterior; P, posterior; L, left; R, right).

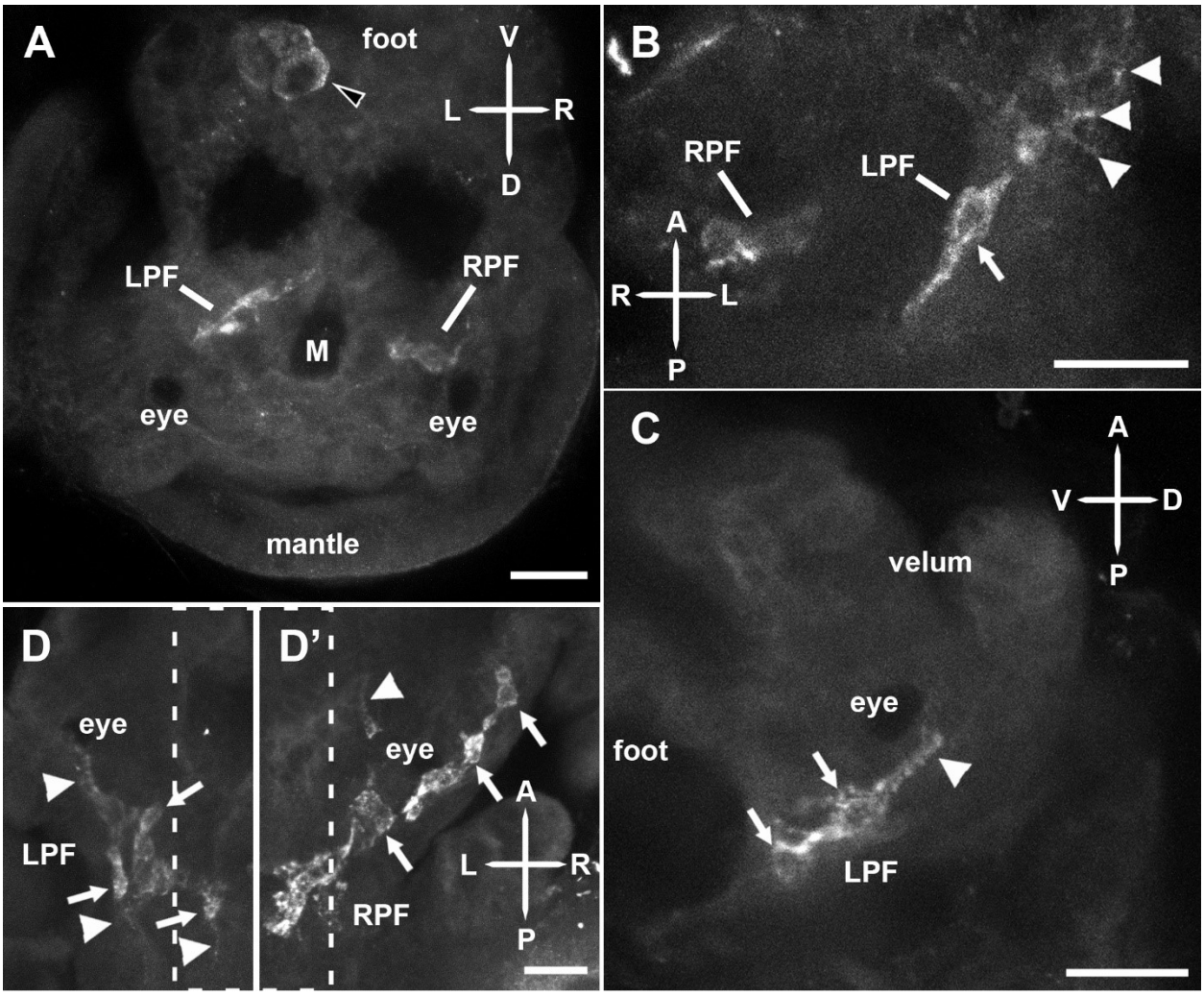
A
foot
V
L
R
D
LPF
RPF
M
eye
eye
mantle
B
RPF
LPF
A
R
L
P
C
A
V
D
P
velum
eye
foot
LPF
D
eye
LPF
D'
eye
A
L
R
RPF
P

Figure 9. Micrographs showing octopamine like immunoreactive (OA-LIR) labelling in the *I. obsoleta* larvae at 9 days post oviposition (DPO; A-C) and 25 DPO (D-D'). A) Anterior perspective showing labelling that follows the left posterior fiber (LPF) extending posteriorly and ventral relative the mouth (M), as well as labelling that follows the right posterior fiber (RPF) extending posteriorly and dorsal relative the mouth (M); the open arrowhead indicates a cluster of three large cell-like structures in the foot that are not routinely labelled. B) Ventral perspective showing close up of the RPF and LPF labelled structures. Both the RPF and LPF structures show bulbous oblong cell-like structures (arrow) and indications of net-like branching with scattered faint labelling that contain sections of relatively high fluorescence (solid arrowheads); this branching occurs in a region around the eyes. C) Side perspective showing the LPF with two oblong cell-like structures (arrows) and apical projection (solid arrowhead). D-D') Dorsal perspective showing deep (D) and shallow (D') labelling of the same specimen at 25 DPO; the region marked by the dashed box represents overlapping sections. At 25 DPO the LPF and RPF labelling is more extensive looking like a chain of bulbous cell-like structures (arrows) with relatively few fiber-like projections (solid arrowheads; scale bars = 25 μm; orientation labels = A, anterior; P, posterior; V, ventral; D, dorsal; L, left; R, right).

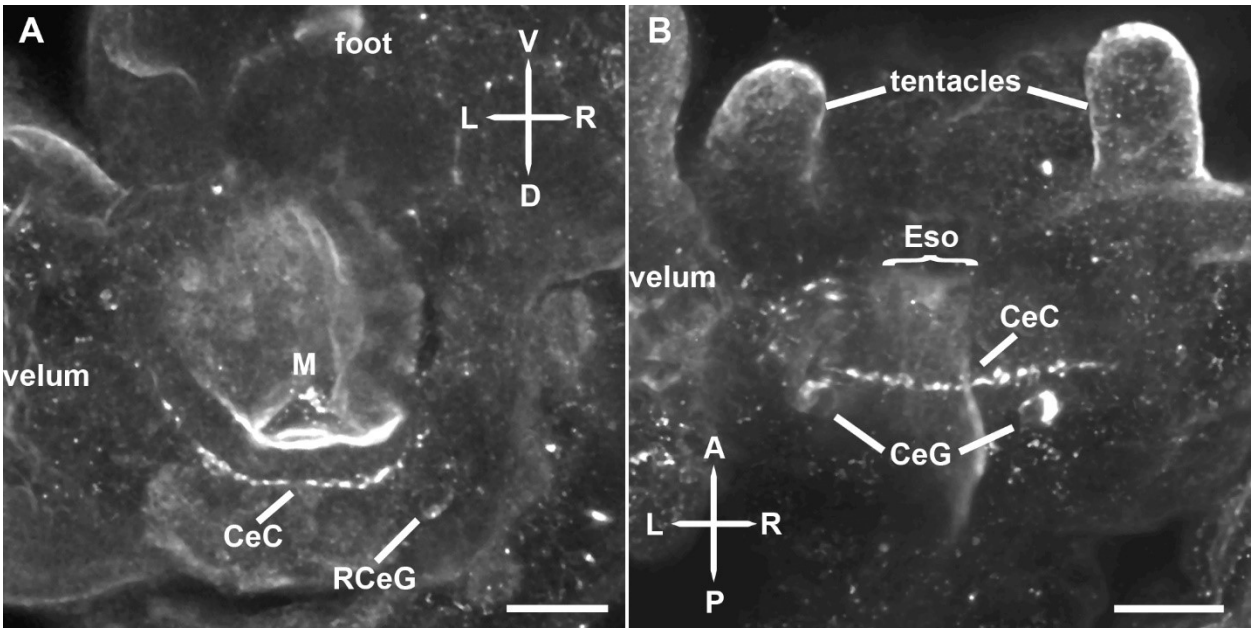
A
foot
V
L
R
D
velum
M
CeC
RCeG
B
tentacles
Eso
velum
CeC
CeG
A
L
R
P

Figure 10. Micrographs showing dopamine β-hydroxylase like immunoreactive (DBH-LIR) labelling in *I. obsoleta* larvae that were fixed using a solution of 9 parts methanol and 1 part formaldehyde at 9 DPO (A) and 25 DPO (B). A) Anterior perspective at 9 DPO showing blebby labelling along a commissure-like structure likely the rudimentary cerebral commissure (CeC) dorsal to the mouth (M); a single faintly labelled cell is evident on the right cerebral ganglion (RCeG). B) Dorsal perspective at 25 DPO showing the cerebral commissure (CeC) positioned dorsal to the esophagus (Eso); a single bilaterally placed cell is evident in the rudimentary cerebral ganglia (CeG; scale bars = 25 μm; orientation labels = A, anterior; P, posterior; V, ventral; D, dorsal; L, left; R, right).

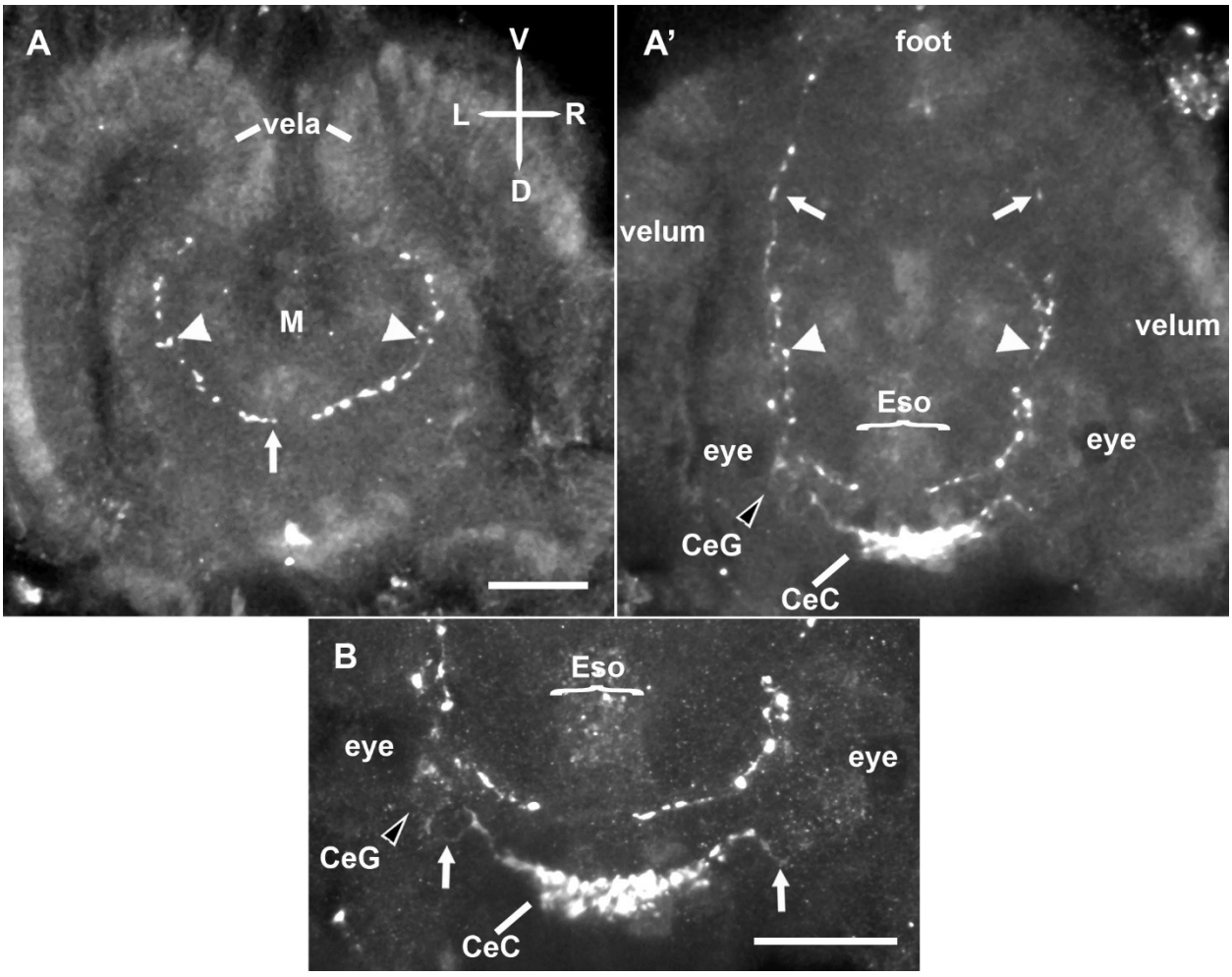
A
V
L
R
D
vela
M
A'
foot
velum
velum
Eso
eye
eye
CeG
CeC
B
Eso
eye
eye
CeG
CeC

Figure 11. Micrographs showing DBH-LIR labelling in a single specimen of *I. obsoleta* larvae that were fixed using 4% paraformaldehyde in 0.1 M PBS at the hatchling stage. A-A') Anterior perspective of a specimen at the same magnification showing superficial (A) and deep (A') labelling; solid arrowheads indicate location of fiber running anterior to posterior between A and A'. A) Blebby discontinuous fiber (arrow) extending along the dorsal and lateral sides of the mouth (M). A') Concentration of blebby labelling along the cerebral commissure (CeC) with a single unilateral cell (open arrowhead) visible to the left of the CeC; blebby discontinuous fibers along the dorsal-ventral access into the foot (arrows). B) High magnification of apical region in A' showing faintly labelled fine processes (arrows) on either side of the CeC connecting to the cerebral ganglion cell (open arrowhead) on the left and presumably a matching cell on the right that did not label (Eso, esophagus; scale bars = 25 μm; orientation labels = V, ventral; D, dorsal; L, left; R, right).

Chapter 4: Histamine

Histamine (HA) is a conserved neurotransmitter prominent in both vertebrate and invertebrate neurophysiology. Investigations looking at HA receptors have shown that H2 metabotropic receptors originated in a prebilaterian ancestor with H1 and H3-4 receptors having appeared as bilaterian novelties with convergent acquisition of HA binding properties (Ravhe et al., 2021). It was originally proposed that invertebrate HA functioned through ionotropic receptors exclusively and that the metabotropic HA receptors evolved independently in vertebrate lineages (Roeder, 2003), however, this is challenged by a recent molecular phylogenetic study (Ravhe et al., 2021). In line with the idea that vertebrate and invertebrates function predominantly through contrasting HA signalling pathways, HA has been shown to perform different functions among vertebrate and invertebrate lineages.

Histamine as a signalling molecule has been shown to have a broad range of roles in vertebrate physiology (Haas et al., 2008); these roles span non-neuronal functions such as gastric acid secretion (Håkanson et al., 1986; Håkanson & Owman, 1967; Prinz et al., 2003), immunomodulation (Jutel et al., 2001; Metcalfe et al., 1997; Thangam et al., 2018), bronchoconstriction (Thangam et al., 2018; Yamauchi & Ogasawara, 2019), and vasodilation (Dacey & Bassett, 1987; Jin et al., 2006). Within the nervous system, histamine acts to maintain wakefulness and attention and has broad neuromodulatory roles affecting homeostatic and higher brain processes involved with circadian (Mochizuki et al., 1992; Strecker et al., 2002; Tuomisto et al., 2001) and feeding rhythms (Ishizuka & Yamatodani, 2012), learning and memory (Brown et al., 1995; Dere et al., 2003; Selbach et al., 1997). These neuromodulatory functions arise from axons originating from the vertebrate tuberomammillary nucleus, which project throughout the whole CNS (Haas & Panula, 2003).

In invertebrates, evidence suggest that HA has some modulatory functions (Alejevski et al., 2019; Chiel et al., 1990; Hamasaka & Nässel, 2006; Hong et al., 2006; Nässel, 1999; Omond et al., 2022; Weiss et al., 1986); however, in contrast to vertebrates, HA has also been found to have a pronounced role in sensory signalling (Buchner et al., 1993; Habib et al., 2015; Hegedűs et al., 2004b; Nässel, 1999; Stuart et al., 2007; Wyeth

& Croll, 2011). Much of our understanding of HA in invertebrates comes from studies on arthropods where HA functions as a neurotransmitter in photoreceptors involved with vision (Stuart et al., 2007) and has been shown to participate in light entrainment of circadian clock neurons (Alejevski et al., 2019; Hamasaka & Nässel, 2006); in addition to light entrainment, other neuromodulatory roles of HA in arthropods are involved with odor processing (Dacks et al., 2010; Sachse et al., 2006), as well as, temperature preference and tolerance (Hong et al., 2006). In molluscs, evidence suggests HA is involved with feeding related arousal (Chiel et al., 1990), respiratory pumping (Elste et al., 1990) and sensory cells of the statocysts (Habib et al., 2015; Hegedűs et al., 2004b). Additionally, numerous histaminergic peripheral sensory cells have been described in cephalic tissues that are proposed to be chemosensory (Habib et al., 2015; Hegedűs et al., 2004b; Scaros et al., 2020; Wyeth & Croll, 2011). Based on this extensive research investigating HA in general physiology and neural signalling, it is evident that some neuromodulatory roles may overlap among vertebrate and invertebrate phyla, however, HA performs novel functions that are distinct to different clades even in terms of the sensory involvement among invertebrates.

The variability in HA function described among different bilaterian clades makes HA a good example of evolutionary divergence among nervous systems, yet relatively little is known about its development or early function in invertebrates. In *Drosophila melanogaster* larvae, HA has been described and proposed to have a role in light entrainment in circadian clocks (Hamasaka & Nässel, 2006; Python & Stocker, 2002), in line with evidence from adults (Alejevski et al., 2019). In larvae of the echinoderms, HA has been found to modulate metamorphic competence and signal metamorphosis (Sutherby et al., 2012; Swanson et al., 2004, 2012). In molluscan larvae, there is weak evidence implicating an HA receptor in regulation of metamorphosis (Joyce & Vogeler, 2018), otherwise descriptions of early embryonic/larval development of histaminergic elements are limited to the freshwater pulmonate snail, *Lymnaea stagnalis* (Hegedűs et al., 2004a). Improving and expanding on these descriptions within and among diverse phyla could provide novel insights into the evolutionary history of histaminergic neurons and phylogenetic relationships among Bilateria.

Given our limited understanding of the development of histaminergic elements in the nervous systems of invertebrates and the relevance of larval physiology in comparative and evolutionary studies (described in Chapter 1), the present chapter aims to provide the framework for comparing histaminergic elements of developing larval nervous systems more broadly across the animal kingdom. To do that, I used immunohistochemistry to describe the early embryonic/larval development of histaminergic elements in the marine caenogastropod, *Ilyanassa obsoleta,* with a brief overview of HA at select developmental stages of three heterogastrpods, *Aplysia californica*, *Biomphalaria alexandrina* and *L. stagnalis*. This research builds upon previous descriptions of serotoninergic, catecholaminergic and peptidergic neural elements in molluscan larvae expanding our understanding of the complexity of larval neurophysiology and behaviour; additionally, results presented in this study form a framework for future comparative studies with potential insights into evolutionary divergence and thus relationships among nervous systems.

4.1 Results

4.2.1 Antibody Specificity

The specificity of the HA antibody used in this study has been tested extensively and used to describe histamine localization in numerous species (Dacks et al., 2010; Wyeth & Croll, 2011). Additionally, HA-LIR staining herein corresponds to labelling described in several adult gastropods (Braubach & Croll, 2004; Habib et al., 2015; Hegedűs et al., 2004b; Ohsuga et al., 2000; Webber et al., 2017); however, the HA antibody was found to produce background noise in early larval development that is potentially generated from non-specific binding (see section 4.2.4 Quality of Labelling).

Since the HA antibody was raised against HA conjugated to keyhole limpet hemocyanin (KLH), a preadsorption control was performed by incubating 200 µg/ml KLH protein in an antibody dilution of 1:100 prior to incubation with the tissue (n = 4). However, preadsorption did not abolish the background labelling or seem to make a noticeable difference compared with samples processed without the KLH preadsorption.

In addition to the KLH preadsorption and past literature describing the specificity of the HA antibody, I conjugated HA and bovine serum albumen (BSA) as a control to block HA specific labelling. The preadsorption experiments used a concentration of 654 µg/ml of the HA-BSA conjugate in an antibody dilution of 1:300, which sufficiently blocked labelling in 16- and 15-days post oviposition (DPO) specimen (n = 2). Labelling was produced in samples processed concomitantly without the HA-BSA blocking conjugate; however, labelling produced at 15 DPO was only faint.

4.2.2 *Ilyanassa obsoleta* Larval Development

Histamine-like immunoreactive (HA-LIR) labelling first appeared in the late trochophore/early embryonic veliger stage between 4 to 5 days post oviposition (DPO). Double labels revealed bilateral structures consisting of 2-3 dimly stained HA-LIR cells surrounding circular concentrations of acetylated-tubulin (AcT)-LIR labelling (Fig 12A-C; Fig 13A'-C' and D-F); this organization was consistent with the organization of the statocysts in which ciliated surfaces of sensory neurons are directed into the lumen of a fluid-filled sac containing a large single statolith or many small stataconia (Braubach & Croll, 2004; Kononenko et al., 2012; Raven, 1966; Wiederhold et al., 1986, 1990; Zaitseva, 2001). Based on this and past research showing the presence of HA in static sensory neurons, the first HA-LIR cells described herein appeared in the statocyst, which encapsulate AcT-LIR cilia (Fig 12A and 13, solid arrowheads). Differential interference contrast (DIC) imaging further supported this interpretation by revealing the colocalization of the AcT-LIR ciliary labelling with an ovular structure indicating the lumen where statoconia would be encased (Fig 12D). The labelling of early HA-LIR cells was generally dim, particularly in double labelled specimen, but then intensified throughout subsequent development; however, early single labelled samples occasionally produced clear and intense labelling (Fig 12E). In addition, cells surrounding the statocyst were difficult to quantify and visualize given that somata were contorted around the ovular sac within the statocysts and well-defined cell perimeters were obstructed.

From the HA-LIR cells in the statocysts, processes that appeared blebby and discontinuous at points, like pearls on a string, extended anteriorly and contralaterally forming a commissural structure, hence forth called the static commissure (Fig 13, SC;

see Fig 14 for schematic overview). The blebby nature of HA-LIR processes could indicate the presence of en passant synapses along the axons where a concentration of HA immunoreactivity would be expected. Alternatively, the discontinuous, fragmented, staining could reflect suboptimal fixation resulting from the EDAC fixative, which is necessary for fixation of HA within the tissue and suggested to have issues with penetration. Under high magnification, faintly labelled HA-LIR fibers could be seen to bifurcate from the static commissure, projecting from the HA-LIR cells of the statocysts (Fig 12A, open arrowheads). Additionally, AcT-LIR cells in the anterior most region that match previous descriptions of leu-enkephalin positive cells in the apical organ (Dickinson and Croll, 2003) were found adjacent to the HA-LIR static commissure, indicating possible interaction with the neuropil of the apical organ (Fig 13A-C and D-F, AO). Extraneous to the static commissure, HA-LIR fibers projected dorsolaterally from the statocysts (Fig 13, open arrowheads); double labels with AcT showed that these projections end lateral to the larval kidneys, which are indicated by AcT labelling of the nephridial duct (Fig 13A'-C', ND; see Figure 3 for schematic). Finally, in addition to the background staining observed, there was a relatively high concentration of HA-LIR labelling that outlined the mouth (Fig 13, dashed outline) matching AcT labelling of oral cilia (Fig 13, OC). It is unclear whether this oral concentration of HA immunoreactivity is nonspecific binding generated by the polyclonal antibody or if it represents a non-neuronal source of HA.

As *I. obsoleta* larvae developed from trochophore/early veliger to embryonic/hatchling veligers (7 DPO), the HA-LIR elements elaborated posteriorly with cells appearing in regions associated with ganglia of the adult nervous system (Fig 15). By the time of hatching, the HA-LIR static commissure takes the form of two distinct parallel fibers that maintain a blebby and discontinuous appearance (Fig 15A-C, SC) with the blebby/punctate labelling more diffuse along the posterior fiber (Fig 15A-C, large open arrowhead) possibly indicating dispersed synaptic endings. It is important to note the SC described here follows the same path as the cerebral commissure (CeC; see Fig 8 and 11) and likely gets incorporated once the cerebral ganglia develop, but herein we continue to call this structure the static commissure for clarity and continuity. In addition to the SC, thin faintly labelled projections extended posteriorly and contralaterally from

the posterior fiber of the static commissure (Fig 15, arrows). The left posterior process (Fig 15; large solid arrowheads) was only weakly and sporadically labelled lacking any cell bodies and following a path that extended ventrally relative to the esophagus. The right posterior process labelled more regularly with brighter fluorescence following a path that extended dorsally relative to the esophagus; two cells were visible along the right posterior projection: a single cell in each the right rudimentary cerebral-pleural ganglion (Fig 15, CePG) and supraintestinal ganglion (Fig 15, SpG). Additionally, a single specimen at this stage was found to contain a HA-LIR cell in the rudimentary right cerebral ganglion at 8 DPO (Fig 15C', CeG).

After hatching at around 11 to 15 DPO, HA-LIR labelling further elaborated with a cell appearing in the subintestinal ganglion (Fig 16A'-B', SbG) including an increased frequency of a cell observed in the right cerebral ganglion (Fig 16A-B, CeG). Variability in staining intensity was observed with cells in the subintestinal ganglion (SbG), right cerebral ganglion (CeG) and the cerebral-pleural ganglion (CePG; compare in Fig 16A-B). Additionally, concentrations of blebby labelling lateral to the statocysts showed potential projections to the vela (Fig 16A-B', open arrowheads); this labelling resembled processes described in the trochophore (4-5 DPO; Fig 13A', open arrowheads), however target structure remained unclear. Finally, among some diffuse labelling in the viscera/mantle of the veliger, there was a concentration of punctate labelling along the left side with two or more cell bodies abutting; this structure was in a region near the mantle cavity associated with the osphradium (Fig 16A-B, Os; see Fig 17 for schematic overview). Cells were difficult to see and therefor quantify with certainty because of the punctate neuropil-like labelling that obscured cell perimeters.

At around 22 DPO, as *I. obsoleta* developed into free-swimming veligers, HA-LIR elements appeared in the pedal ganglia (Fig 18A and C, PeG) and footpad (Fig 18a and B) as well as novel cells in the cerebral ganglia (CeG) and left cerebral-pleural ganglion (LCePG) making the location of HA-LIR cells in the adult ganglia more symmetrical (Fig 18). HA-LIR labelling showed two bilateral cells in each pedal ganglion positioned anteroventral to the statocysts (Fig 18A, LPeG and RPeG; Fig 18C) with faintly labelled processes containing numerous swellings and extending contralaterally across the pedal commissure (Fig 18C, PeC). Double labels with HA and

AcT antibodies confirmed that these bilateral cells were separate from the statocysts (Fig 19A-C, PeG), which at this point contain three HA-LIR cells surrounding the AcT-LIR lumen (Fig 18A and 19A-C), providing confidence that these were pedal cells. In the developing cerebral ganglia (CeG), two bilateral cells were observed in each of the left and right hemispheres (Fig 18A-A', solid arrowheads), which increased from a single cell in the right cerebral ganglion at 15 DPO; these cerebral cells were located along the static commissure (Fig 18, SC). HA and AcT double labels revealed that the HA-LIR static commissural fibers abut the AcT-LIR cells in the apical organ (Fig 19D-F). Additionally, a single cell in the left cerebral-pleural ganglion became evident (Fig 18A, LCePG) matching the earlier developed right cerebral-pleural cell (Fig 18A', RCePG). Outside the development of the adult ganglia, results showed blebby and discontinuous HA-LIR labelling, characteristic of HA-LIR nerve fibers described herein, projecting to/from the developing foot (Fig 18a and B, arrows). At least two bilateral HA-LIR peripheral cells were present (Fig 18B, solid arrowhead) in the footpad. Finally, a concentration of HA-LIR punctate labelling with at least five cell bodies (Fig 18A'', solid arrowheads; Fig 19G-I) first described as the osphradium at 11 DPO persists (Fig 18A'', Os). Double labels with AcT showed the presence of cilia near the HA-LIR osphradial elements (Fig 19G-I).

Once the *I. obsoleta* veligers developed to around 24-27 DPO (late-stage free swimming veliger), HA-LIR labelling maintained a blebby and discontinuous appearance yet was more intense with projections throughout the posterior loop appearing thicker and including cells in nearly all ganglia of the developing adult nervous system (Fig 20; see Fig 21 for schematic overview). In comparison with 22 DPO, there was not any noticeable difference in terms of quantity and locations of cells. Two bilateral HA-LIR cells were located in the left and right cerebral ganglia (Fig 20A and B, CeG) along the static commissure (Fig 20, SC) maintaining symmetry of cerebral cells. The cerebral-pleural ganglia (CePG) also maintained symmetry with a single bilateral cell in both left and right ganglion (Fig 20, CePG). Finally, at least two bilateral HA-LIR cells were identified in the pedal ganglia (PeG; Fig 20A' and c, solid arrowheads), anteroventral to the statocysts, with the two sides connected by a fine faintly labelled fiber with numerous swellings indicating the pedal commissure (Fig 20A' and c, PeC). In addition to the pedal

cells, fine processes extended from the pedal/statocyst complex ventrally (Fig 20B-B', arrows), into the footpad.

4.2.3 *Aplysia californica* Larval Development

Histamine-like immunoreactive (HA-LIR) labelling first appeared at day 5 of embryonic development (E5; $n = 4$). The first cell that appeared was a single bilaterally placed cell located in the cephalopedal anlage (Fig 22A, arrows), likely part of the developing statocyst (St). The bilateral cells had fine tortuous processes that projected apically and contralaterally creating commissural-like fibers likely forming the static commissure (SC; Fig 22A, open arrowheads) previously described in *I. obsoleta*. At day 7 of embryonic development, HA-LIR labelling showed more intense labelling of the static commissure (SC) extending between the statocysts (St; Fig 22B, open arrowheads; $n = 5$). This intense labelling of the SC presented as globular discontinuous fragments that introduced difficulty with discerning cell bodies.

By hatching, stage 1 veliger, HA-LIR elements became more structured (Fig 22C; $n = 6$). Blebby HA-LIR processes resembled a lower case "n" where the ends showed intense bilateral labelling of the statocysts (Fig 22C, St). Similar to E5 specimen, the statocysts fine blebby processes extended anterodorsally where they turn and project contralaterally forming the static commissure (SC; Fig 22, open arrowheads). Along the SC at the point where processes turned toward the midline, intense HA-LIR staining could indicate the rudimentary cerebral ganglia (Fig 22, CeG). However, based on data showing that *Aplysia* larvae have statocysts that measure 16 µm in diameter at hatching (Wiederhold et al., 1990), the combination of structures labelled CeG and St could in fact be cells at either end of the developing statocysts.

Once developed to stage 6 veliger, specimens were capable of undergoing metamorphosis and contained more elaborate nervous systems. HA-LIR labelling at this point was more extensive than during embryonic development and at hatching ($n = 3$). Potentially two cells could be identified in the rudimentary cerebral ganglia (CeG; Fig 22D'') with projections laterally, possibly into the vela (Fig 22D'', open arrowhead). Additionally, there was intense labelling ventral to the esophagus showing at least two bilateral cells, thought to be part of the statocysts (Fig 22D', St). Blebby lateral processes

extended from the region of the statocysts into the foot (Fig 11D', arrows) where three or more putative peripheral sensory cells extended dendrites toward the epithelium (Fig 22E, open arrowheads). Finally, two bilaterally paired cells positioned anterodorsally to the statocysts (Fig 22, solid arrowheads), likely part of the pedal ganglia (Fig 22, PeG), contained faint processes that extended toward the statocysts and contralaterally forming a commissure like structure; given the location of this staining, these fibers likely formed part of the pedal commissure (Fig 22D', PeC; see Fig 23 for schematic overview).

4.2.3 Early Histaminergic Elements in Freshwater Species

To compare the development of the first HA-LIR elements to appear among gastropods, *L. stagnalis* and *B. alexandrina* embryos were fixed at the point where eyes were beginning to appear and processed for HA immunoreactivity. In *L. stagnalis*, results revealed a single bilaterally paired cell that was ciliated (Fig 24D-F, solid arrowhead; n = 3) and therefore likely part of the statocysts (St) with an apical projection that extended contralaterally forming the static commissure (Fig 24A-C, SC). In *B. alexandrina*, there were two bilaterally paired cells (Fig 24G-I; n = 3) where one of them was ciliated and had a faint blebby apical projection consistent with the static commissure (SC; Fig 24G-I, St and solid arrowhead). The additional paired bilateral cell is of unknown origin but could potentially be an early pedal cell (Fig 24G-I, arrow).

4.2 Discussion

The results in this study provide the first descriptions of the development of histaminergic neuronal elements in larvae of indirect developing gastropods, *I. obsoleta* and *A. californica*. Results from *I. obsoleta* showed that the first HA positive cells arise in the late trochophore/early embryonic veliger stage (~4-5 DPO). Based on double-labels with an antibody targeting AcT and the use of DIC imaging, these cells were determined to be part of the statocysts with processes that project apically forming a bundle of commissural fibers herein called the static commissure (SC). As the larvae developed, the appearance of new HA-LIR cells followed an asymmetric sequence with cells forming in the right cerebral and supraintestinal ganglia, followed by the subintestinal ganglion before obtaining symmetry with the appearance of cells in the left

cerebral ganglion. The last ganglia to acquire HA-LIR cells were the pedal ganglia by ~22 DPO, coinciding with the appearance of the pedal commissure and projections to/from peripheral cells in the foot. Results in this study also revealed HA-LIR labelling of a structure along the left mantle appearing at ~11 DPO, presumed to be the osphradium.

Immunoreactivity in both *A. californica* and in the direct developing *L. stagnalis* corroborate results from *I. obsoleta* showing that the first HA-LIR neurons to form are of the statocysts. This is indicated by a similar progression of labelling in *A. californica* with an initial bilateral cell showing anterior-contralateral projections that form a commissure (SC); however, later development shows some divergence likely related to differences in morphology of the *I. obsoleta* and *A. califonica* adult nervous systems. In *L. stagnalis*, early double labels using an antibody against AcT and HA at around 55% of embryonic development showed similar static-like labelling as *I. obsoleta*; this labelling showed an initial bilaterally located ciliated cell at the base of the foot with an anterior projection forming a commissure dorsal to the mouth. This labelling was comparable to descriptions of the statocyst sensory cells and static commissure in *I. obsoleta*.

It is important to note that descriptions in this study were done on clutches of heterogenous stages of developing *I. obsoleta*. Attempts were made to maintain cultures of larvae that were spawned within two to three days; therefore, exact timing of descriptions are estimates based on morphological features (Dickinson & Croll, 2003) and estimated date of oviposition. Although the general sequence and descriptions are accurate, the exact timing will need to be identified through future studies. Furthermore, descriptions of *A. californica* were based on a single shipment of a limited number of larvae (n = 6) and double labels were not performed; interpretation of results was done in comparison to *I. obsoleta* and literature on development of *A. californica* (Coggeshall, 1969; Kriegstein, 1977a, 1977b). Further experiments are required to improve certainty around interpretation of HA-LIR cells described in larval development of *A. californica*.

4.2.1 Statocysts/Static Commissure

The results in this study are consistent with previous research indicating HA-LIR sensory neurons in the statocysts of molluscs. This previous research focused on adult

gastropods and revealed histaminergic sensory neurons as a subset of cells in the statocysts (Braubach & Croll, 2004; Habib et al., 2015; Hegedűs et al., 2004b; Ohsuga et al., 2000; Soinila et al., 1990; Webber et al., 2017); other neurosignalling molecules identified in gastropod statocysts are FMRFamide and small cardioactive peptide B (SCPb; Ohsuga et al., 2000; Webber et al., 2017). Interestingly, there is evidence in cephalopods that indicates that catecholamines and acetylcholine are present and function in the statocysts (Auerbach & Budelmann, 1986; Budelmann & Bonn, 1982; Williamson, 1989). Novel findings in this study represent the first descriptions of HA in the statocysts during embryonic and larval development.

Statocysts are the invertebrate analogue to the human vestibular system and consist of a fluid filled structure containing one or more calcium carbonate stones (statolith or statoconia) encapsulated by ciliated mechanosensitive sensory cells; the function of the statocysts is to detect changes in motion and orientation relative to gravity (Alkon, 1975; Braubach & Croll, 2004; Zaitseva, 2001). Early studies on statocyst organization primarily relied on a combination of light and scanning electron microscopy in conjunction with general histological stains to describe the ultrastructure and development of the statocyst hair cells and statoconia (Atkinson, 1971, 1986; Coggeshall, 1969; Gao et al., 1997; Kononenko et al., 2012; McCain, 1992; Pedrozo et al., 1996; Raven, 1966; Wiederhold et al., 1986, 1990; Zaitseva, 2001). In *I. obsoleta* and *A. californica*, these early studies indicate that the general structure of the statocysts was fully formed in the larvae at hatching (Atkinson, 1971; Kriegstein, 1977b; Wiederhold et al., 1990); however, expression of neurotransmitters and neural projections were not assessed. The early expression of HA indicated by immunoreactive labelling in this study, revealed for the first time HA in larval sensory cells of the statocysts indicating possible early functionality. These early histaminergic cells had processes that projected through the neuropil of the apical organ forming a commissure with numerous blebby swellings; the morphology of the commissure containing numerous swellings just below the apical organ could indicate locations of en passant synapses and integration with the apical organ in larvae.

Behavioural evidence supports the functionality of the statocysts in larvae (Fuchs et al., 2018). In a study on two closely related marine snail, *Ilyanassa trivittata* and *I.*

obsoleta, researchers showed that larvae could detect and respond to different forms of water turbulence enabling the two species to maintain their geographical distribution along the coastline (Fuchs et al., 2018). Both species responded to turbulence and vorticity the same with animals showing increased swimming effort and descent frequency; however, *I. trivittata* responded to wave induced acceleration by powerful upward swimming (Fuchs et al., 2018). The authors suggest that given their contrasting environments, powerful upward swimming along the continental shelf in response to waves would allow the *I. trivittata* larvae to ride the current closer to the shore; this would prevent *I. trivittata* from getting pulled out to sea, whereas sinking in response to vorticity and turbulence would keep *I. obsoleta* larvae along the inlet from crashing into shore (Fuchs et al., 2018).

In addition to function in larval behaviour, the early development of the statocysts in relation to the developing adult nervous system could indicate involvement in pioneering the cerebral commissure as well as pedal-cerebral connectives; in fact, this was suggested by previous authors who described the development of histaminergic elements in *L. stagnalis* (Hegedűs et al., 2004a). In this study, HA-LIR neurons appeared in the statocysts during the late trochophore/early embryonic veliger stage (~4-5 DPO) of *I. obsoleta* development; this early appearance corresponds to the timing of development of FMRFamide containing cells in the supra- and subintestinal ganglia but predates the expression of 5-HT and catecholamines in adult ganglia (Dickinson & Croll, 2003). Previous research on gangliogenesis in *I. obsoleta* only describe the presence of adult ganglia at 6 days post-hatching (Lin & Leise, 1996), although other descriptions have suggested the presence of cerebral and pedal ganglia at hatching (Raven, 1966). In addition, it has been shown that the development of statocysts is independent of proper cerebro-pedal connective development (Raven, 1966). Therefore, it is possible that the development of the statocyst and the static commissure projecting through the neuropil of the apical organ could lay the framework and act as a scaffold for the development of cerebral and pedal ganglia and their projections.

Results in this study also identified early development of HA-LIR cells in *A. californica*, *L. stagnalis* and *B. alexandrina* that are presumed to be part of the statocysts. In *A. californica*, the early labelling pattern at embryonic day 5 matched what was

observed in *I. obsoleta* with a bilateral cell possessing apically projecting fibers that form a commissure; unfortunately, given the limited availability of specimen, double labels were not performed to verify whether these early cells were ciliated and DIC imaging of the statocysts was not evident. Looking into the literature, the statocysts of *I. obsoleta* were amenable to DIC imaging because they contain a single large statolith that has birefringent properties making it easily identifiable under polarised light (Atkinson, 1971; McCain, 1992); this does not seem to be the case for *A. californica*, *L. stagnalis* and *B. glabrata*. However, early bilateral cells in freshwater snails, *L. stagnalis* and *B. alexandrina*, both showed the presence of AcT-LIR cilia at around 55% of embryonic development further supporting the findings that the first HA cells develop in the statocysts of gastropods. However, these results contradict descriptions of HA development in *L. stagnalis* described by Hegedűs et al. (2004a), which showed a different pattern of staining early in development.

Results in Hegedűs et al. (2004a) showed that the first HA cells to appear were in the cerebral ganglia with projections that extended through the cerebro-pedal connectives and across the pedal commissure. These results suggest a staining pattern that is flipped vertically from my description in which a statocyst cell sends projections dorsal-anteriorly forming a commissure dorsal to the mouth, likely to become the cerebral commissure. Further research is needed to clarify these differences in early HA development. Additionally, further research can be performed to further describe neurosignalling molecules in the developing statocysts, functionality in larval behaviour and potential contribution to gangliogenesis of the adult nervous system.

4.2.2 Adult Nervous System

In *I. obsoleta*, the early asymmetric appearance of cells in the developing posterior loop ganglia is consistent with previous literature describing the ganglionic development. Research on gastropod gangliogenesis reveals numerous theories ranging from a single apical ectodermal proliferative zone, in which the cerebral cells form and delaminate with subsequent migration of cells to form other ganglia, to the idea that every ganglion develops from its own ectodermal placode (reviewed in Raven, 1966). In *I. obsoleta*, evidence indicates that the cerebral ganglia develop first followed by the

pedal ganglia, which are both present at hatching (Lin & Leise, 1996; Raven, 1966); the sequence of buccal, pleural and intestinal ganglionic development are less clear. However, evidence suggest that the subintestinal ganglia appear slightly after the supraintestinal ganglia (Lin & Leise, 1996). This corresponds to the development of histaminergic cells reported in this study where the right cerebral-pleural and the supraintestinal ganglion cell developed prior to the subintestinal ganglion, showing an asymmetric sequence of development. In addition, the right cerebral cells developed before the left cerebral cells.

Asymmetries in morphology and development are common in molluscs and is believed to be associated with torsion. It was generally believed that torsion was a consequence of larval retractor muscle contraction during development (Wanninger et al., 2000) but more recently evidence suggests asymmetric cell proliferation along the mantle epithelium plays a role (Kurita & Wada, 2011). Interestingly, this asymmetric proliferation corresponds to the timing of organogenesis with the right tentacle developing prior to the left tentacle (Atkinson, 1971; Render, 1997; Tomlinson, 1987); this also matches the sequence of HA-LIR cerebral cells described in this study. In Atkinson (1971), the author describes the close relationship between the tentacles and the cerebral ganglia indicating that the body of the right tentacle seemed attached to the cerebral ganglion. Given the anatomical proximity and similar timing of development, it is possible that the HA-LIR cerebral cells and the tentacle could be associated. In fact, studies have shown numerous HA-LIR sensory cells in cephalic regions of gastropods (Wyeth and Croll, 2011) and evidence from studies on *A. californica* have implicated HA in feeding related arousal (Chiel et al., 1990; Elste et al., 1990).

In *A. californica*, an extensively characterised histaminergic cerebral cell, C2, has been shown to be involved with food arousal and modulation of feeding motor programs (Chiel et al., 1990). The C2 cell has been shown to receive tactile stimulation from axons in the lips that when exposed to seaweed initiate an excitatory response that leads to feeding, once feeding is initiated a positive feedback loop is initiated from proprioceptive signals to maintain arousal (Chiel et al., 1990). Results at stage 6 of *A. californica* development revealed peripheral cells in the foot with projections that could have extended to the HA-LIR cerebral cells; therefore, it is possible that these descriptions

identify the early establishment of the C2 cerebral neurons and its afferents. Interestingly, a recent study on flatworms showed that whole body application of HA stimulated increased locomotion that they associate with a signal promoting wakefulness, but this could be related more specifically to food related arousal (Omond et al., 2022).

Results in this study also revealed the late development of HA-LIR pedal cells in both *A. californica* and *I. obsoleta*. This late development corresponds to the development of the propodium in preparation for metamorphosis, when the planktonic larval form converts to a benthic adult (Kriegstein, 1977b; Lin & Leise, 1996); therefore, it is possible that these cells are involved with locomotion or sensory processing related to the adult foot. Future research could look at the further development of these cells during metamorphosis and into the juvenile to elucidate possible functions.

4.2.3 Osphradium

Results in this study revealed HA-LIR fibrous/punctate neuropil-like labelling with abutting cells along the left side of the mantle, an area associated with the osphradium in *I. obsoleta* larvae (see Figs1 and 19G-I; Dickinson & Croll, 2003; Lin & Leise, 1996).

The osphradium is a pigmented chemosensory organ that shows large variability among molluscs but is generally positioned within the mantel cavity on or near the gill/pneumostome (Haszprunar, 1985, 1987; Lindberg & Sigwart, 2015). The consensus is that the osphradium functions as a chemosensory organ, however, exact functions range from food/predator/mate detection to monitoring water quality (oxygen, carbon dioxide, dissolved particles, etc.; Lindberg & Sigwart, 2015). In line with the large diversity in body plans among molluscs, the morphology of adult structures varies considerably ranging from just a small pit at the anterior region of the gill to consisting of a ridge that runs parallel to the gill (Haszprunar, 1985, 1987; Nezlin et al., 1994a, 1994b). In terms of characterization of neurotransmitters present in the adult osphradium, evidence for FMRFamide, leucine-enkephalin, 5-HT, and nitric oxide has been reported (Nezlin et al., 1994a, 1994b). Despite the broad morphological comparisons of the osphradium across Mollusca (Haszprunar, 1985, 1987), there is relatively little known about larval osphradial structures.

Previous research on *I. obsoleta* larval development indicates that the osphradial ganglion develops early and is visible at or shortly after hatching (Dickinson & Croll, 2003; Lin & Leise, 1996). Consistent with adults, FMRFamide and 5-HT have also been described in the osphradium of larvae (Dickinson & Croll, 2003). Results in this study add to these previous descriptions indicating HA-LIR labelling of the osphradial ganglion at about 11 DPO. In addition, double labels revealed adjacent AcT-LIR cilia, which is associated with the early gill anlage (Fig 19G-I; Raven, 1966). Based on these previous descriptions, this HA-LIR labelling is likely part of the osphradial ganglion. Therefore, these descriptions represent the first known labelling of HA associated with the osphradium; future research should investigate the prevalence of HA in the adult osphradium.

4.2.4 Quality of Labelling

HA-LIR labelling described in this study showed axons with numerous swellings, often looking blebby and discontinuous at points (see Fig 15). Generally, when viewed under high magnification these fragmented, blebby processes resembled pearls on a string. The blebby nature of the labelling along axons, especially along the static commissure (SC; Fig 15 and 20), could indicate locations of en passant synapses. En passant synapses are swellings along the axons that form synapses other than at the axon terminal (Shen & Cowan, 2010), which are often viewed as blebs when visualized using immunohistochemistry. However, it is also possible that the blebby and sometimes fragmented labelling of neuronal processes was related to inadequate fixation.

In addition to the often-blebby nature of the labelling, there was some variability in the intensity and quality of axonal and cell labelling among preps (see Figs 15 and 16). On occasion one could barely see an axon except for a line of blebs (Fig 16A', solid arrowheads). It is possible that this variability was due to a combination of penetration issues with the HA antibody and sub-optimal fixation produced by the EDAC fixative; although not documented in peer reviewed papers, Andrew Dacks cautioned about penetration issues with the HA antibody and emphasized the importance of a long EDAC fixation in a review submitted on the HA antibody product page (*Histamine Antibody | Immunostar*, n.d.).

Finally, the HA antibody was found to produce high background noise in early larval development potentially generated from non-specific binding. This background noise has been documented in adult freshwater species with mention that it could be minimized with preadsorption using keyhole limpet hemocyanin (KLH; Wyeth and Croll, 2011). For HA antibody synthesis, KLH was conjugated to HA to stimulate an immunogenic response, therefore, preadsorption likely ameliorated the staining by blocking antibodies raised against epitopes on the KLH molecule (Beach et al., 2019); however, KLH preadsorption did not abolish the background noise, which indicated the likelihood for other immunoreactive off-target antibodies present in the anti-HA whole serum. In this study, KLH preadsorption results failed to show a drastic difference and therefore were not performed routinely. Despite these issues, the specificity of the HA antibody used in this study has been tested extensively and used to describe histamine localization in numerous species (Dacks et al., 2010; Wyeth and Croll, 2011).

4.2.5 Conclusion

In conclusion, this study reveals a complex network of HA-LIR neuronal elements in the early larval stages of both *I. obsoleta* and *A. californica*. This labelling reveals the first early descriptions of the expression of HA in the larval statocysts providing histological evidence for larval functionality. The early establishment of the statocyst and associated commissure also indicate a possible role in laying the framework to help guide the development of the adult CNS. In addition to labelling of the statocysts, HA-LIR cells were identified in nearly all developing ganglia except for the visceral. Together, these descriptions contribute to past literature in revealing the complexity of the developing nervous system in molluscan larvae, providing a framework for future comparative studies. Future research describing early histaminergic neuronal development in larvae of other phyla could help elucidate the evolutionary history of HA signalling and inform phylogenetic relationships.

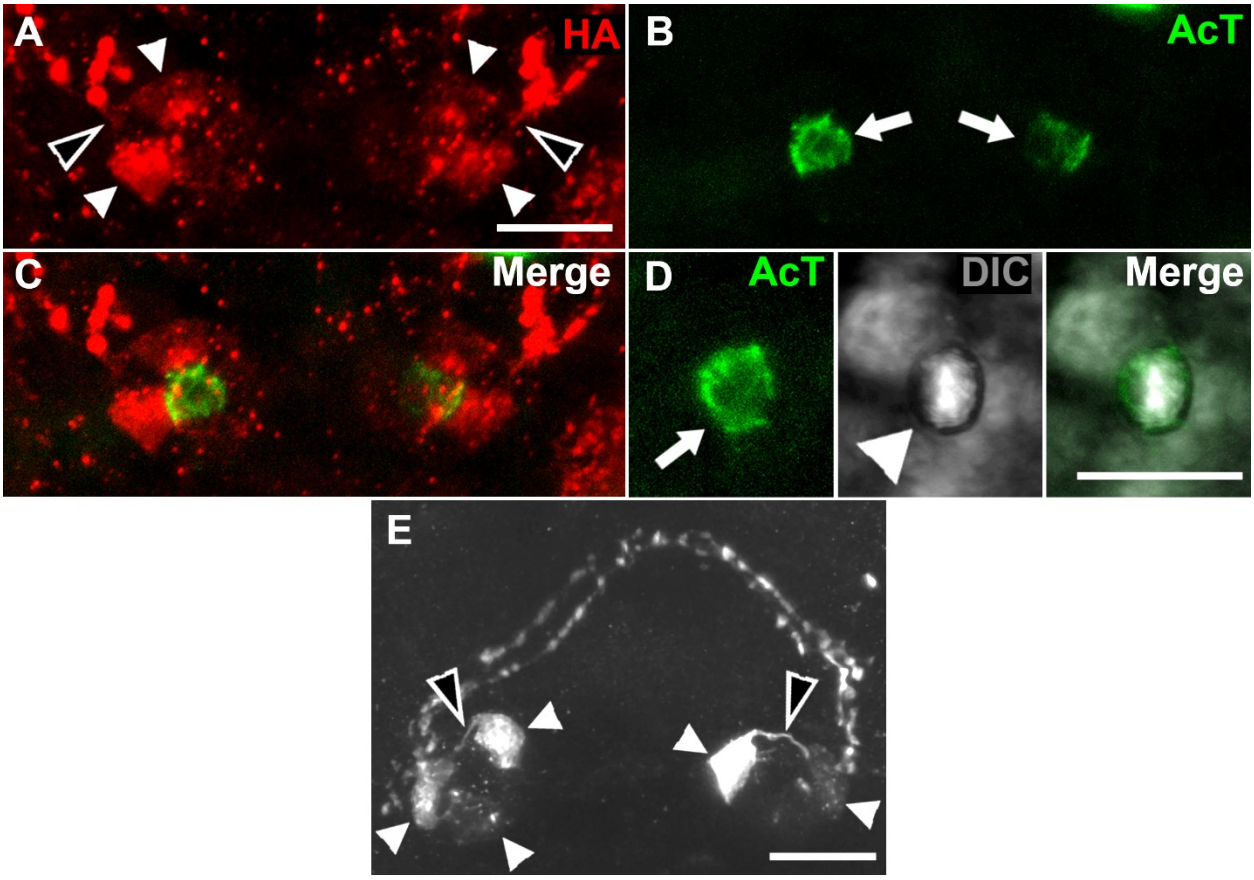
A
HA
B
AcT
C
Merge
D
AcT
DIC
Merge
E

Figure 12. Micrographs showing digital zoom of statocyst labelling in the *Ilyanassa obsoleta* trochophore at 4-5 DPO. A-C) Double label showing HA-LIR (A) and AcT (B) labelling. Arrowheads indicate individual HA-LIR cells surrounding the ciliated lumen (AcT, arrows) of the statocysts with open arrowheads showing faintly labelled processes from the HA-LIR cells joining as they project through the static commissure (Fig 13). D) AcT labelling of cilia (arrow) in conjunction with differential interference contrast (DIC) imaging showing overlap with the lumen of the statocyst (large arrowhead). E) labelling from a slightly older sample that was processed for HA immunoreactivity showing strong labelling of three cells around the statocysts including a couple of dim cells (solid arrowheads); Open arrowheads indicate processes projecting from HA-LIR cells (scale bars = 20 μm).

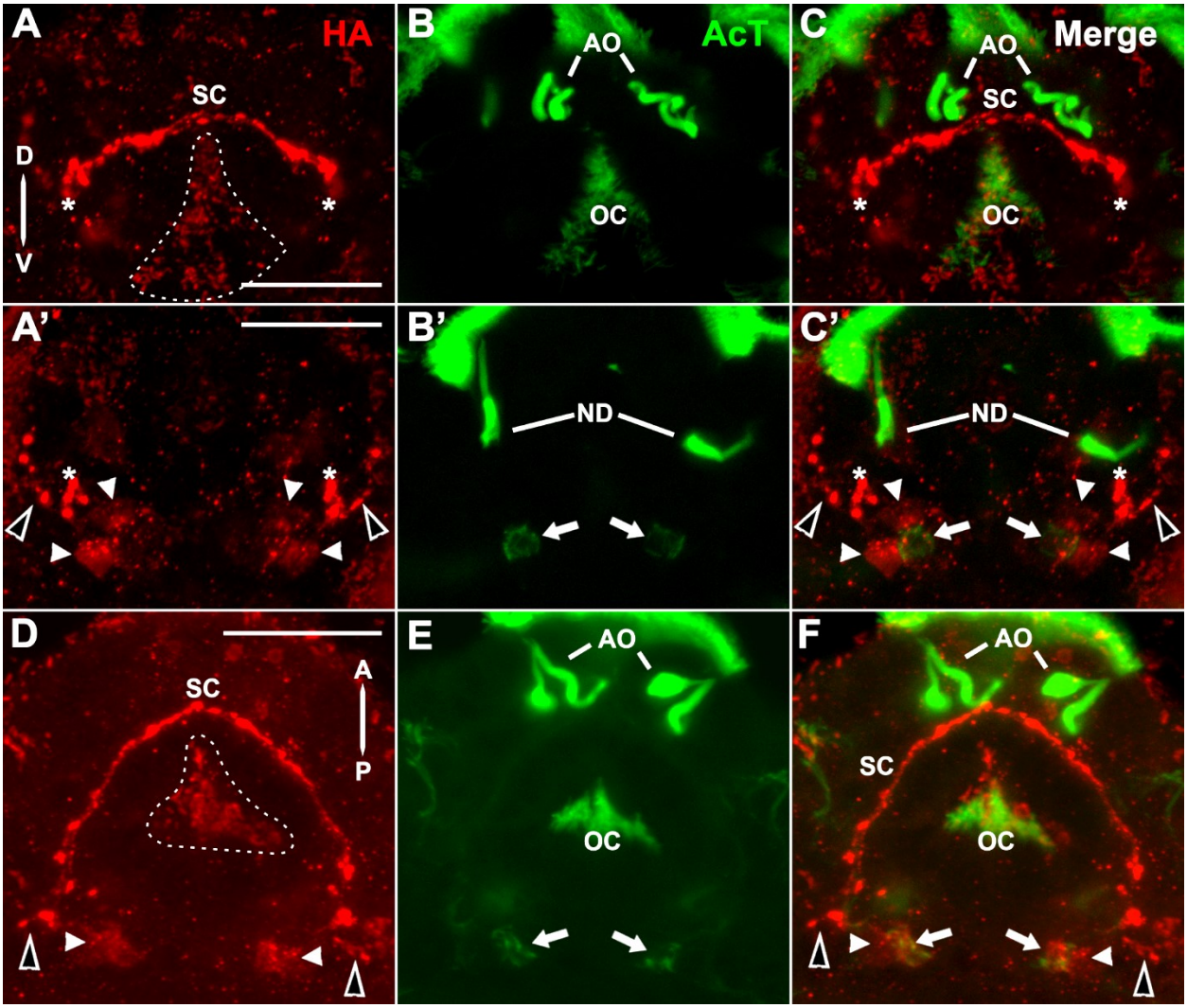
A
HA
SC
D
V
*
*
B
AcT
AO
OC
C
Merge
AO
SC
OC
*
*
A'
*
*
B'
ND
C'
ND
*
*
D
SC
A
P
E
AO
OC
F
AO
SC
OC

Figure 13. Micrographs showing double labels of HA-LIR and acetylated-tubulin (AcT) labelling in the *Ilyanassa obsoleta* trochophore at 4-5 days post oviposition (DPO): A-C) anterior perspective of same specimen where A to C shows superficial labelling and A' to C' shows deep labelling with asterisk indicating point of continuation of the static commissure (SC); G-I) dorsal perspective of a separate sample. Solid arrowheads indicate dim individual HA-LIR cells that surround the AcT labelled lumen (arrows) of the statocysts. Blebby processes project contralaterally from the HA-LIR cells forming a static commissure (SC) that passes just below the apical organ (AO). In addition, HA-LIR fibers project dorsal-laterally from the statocyst/SC (open arrowheads) to a region lateral to the larval kidneys (ND), as indicated by AcT immunoreactive labelling of the nephridial duct (ND; Page, 2003). Finally, a concentration of punctate/blebby HA-LIR labelling is evident surrounding the rudimentary mouth (dashed outline) that follows a similar staining pattern as AcT labelling of oral cilia (OC; D, dorsal; V, ventral; A, anterior; P, posterior; scale bars = 40 μm).

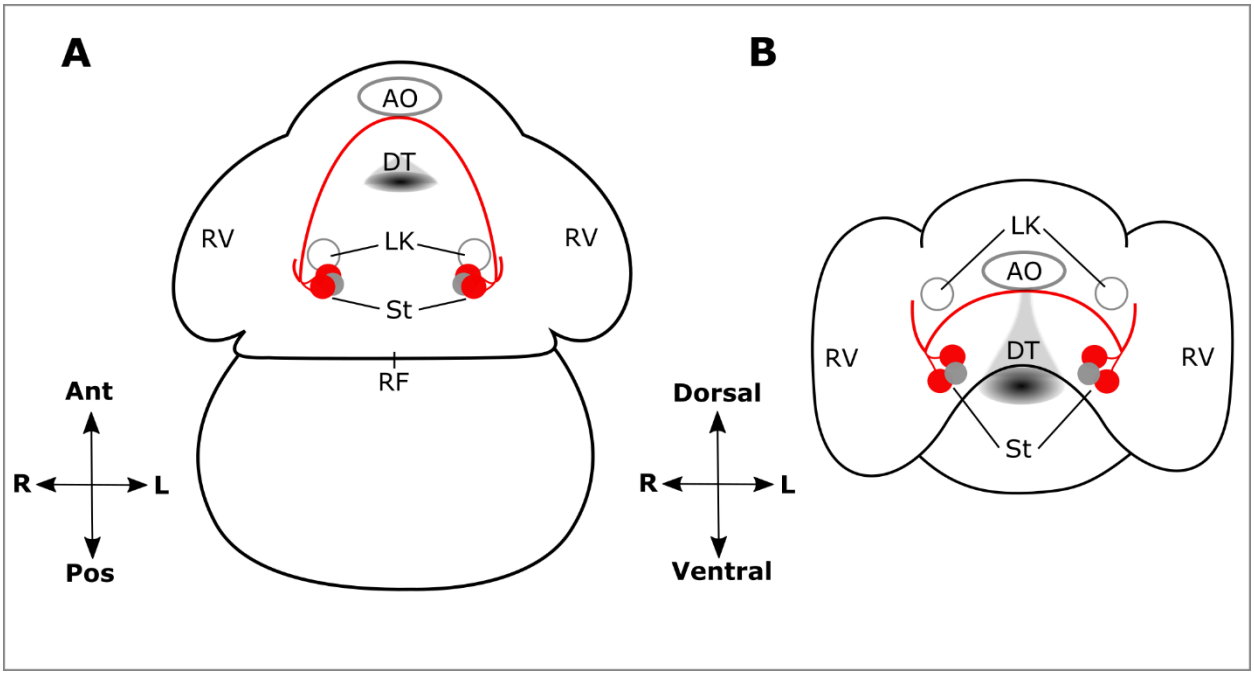
A
AO
DT
RV
LK
RV
St
RF
Ant
R
L
Pos
B
LK
AO
RV
DT
RV
St
Dorsal
R
L
Ventral

Figure 14. Schematic showing HA-LIR labelling in the late trochophore/early embryonic veliger stage of *Ilyanassa obsoleta* development (4-5 DPO): A) Ventral perspective and B) Anterior perspective. HA-LIR labelling is indicated in red showing somata in the statocysts (St) with processes projecting anterior and contralaterally passing near the apical organ (AO) and forming the static commissure. Dorsal-lateral projections from the statocysts terminate lateral to the larval kidneys; solid grey circles represent the lumen of the statocysts (LK; RV, rudimentary velum; RF, rudimentary foot; DT, digestive tract; Ant, anterior; Pos, posterior; R, right; L, left). This schematic was inspired by and adapted from Dickinson and Croll (2003).

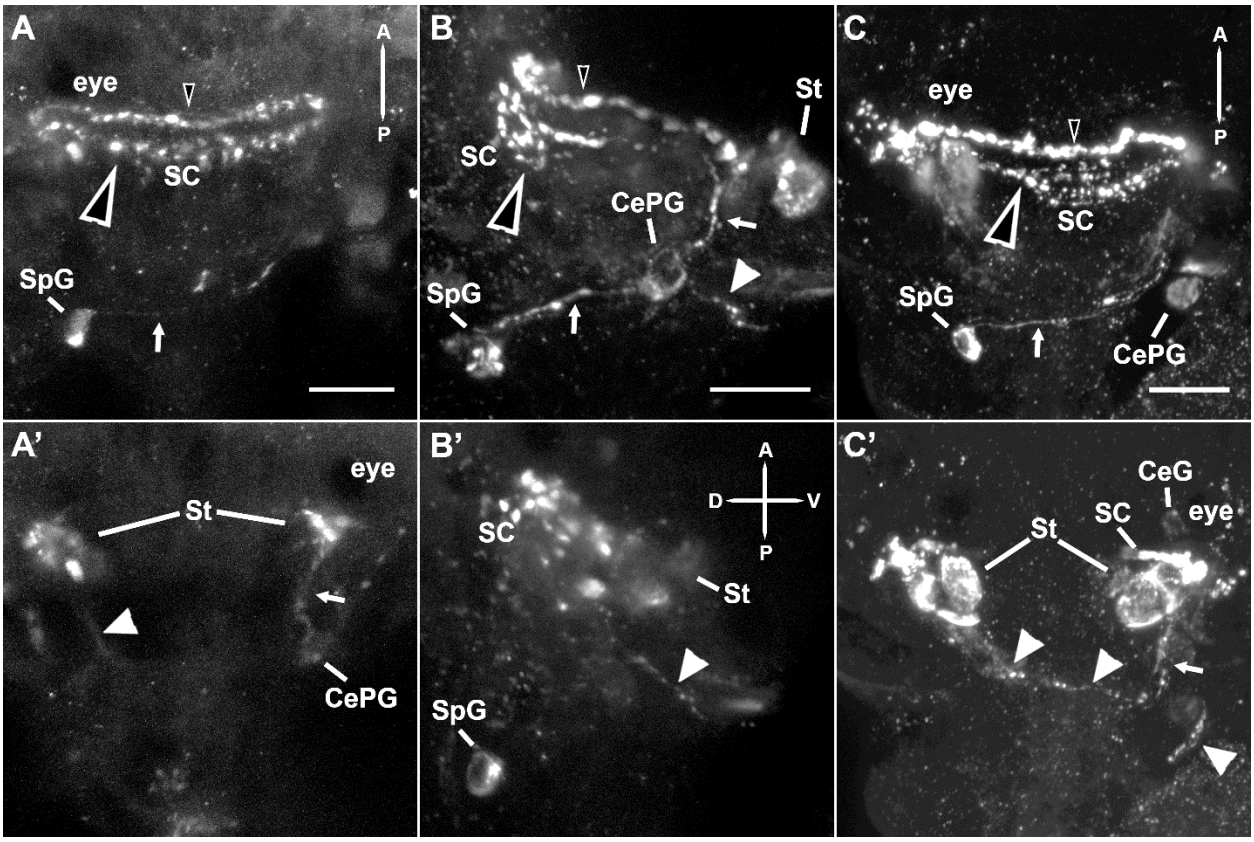
A
eye
SC
SpG
A
P
B
St
SC
CePG
SpG
C
eye
SC
SpG
CePG
A
P
A'
eye
St
CePG
B'
SC
St
SpG
A
D
V
P
C'
CeG
St
SC
eye

Figure 15. Micrographs showing histamine-like immunoreactive (HA-LIR) labelling in *Ilyanassa obsoleta* transitioning from embryonic veliger to hatchling. A-B) Embryonic veligers (7 DPO), where A) shows a sample viewed from the dorsal perspective and B) depicts a separate sample viewed from a side perspective. C) Sample viewed from the dorsal perspective at 8 DPO. Frames labelled A to C indicate superficial labelling whereas A' to C' show deep labelling of the corresponding specimen. A-B) At 7 DPO the static commissure (SC) appears as two separate blebby processes with the posterior fiber (large open arrowhead) appearing more diffuse. The posterior fiber has projections that extend posterior and contralaterally (arrows); the left fiber (large solid arrowheads) projects ventrally beneath the esophagus and the right fiber (arrows) projects dorsally above the esophagus. A cell can be found in each the right cerebral-pleural ganglion (CePG) and the supraintestinal ganglion (SpG) along the right posterior fiber. C) At 8 days post oviposition (DPO) a cell can be found in the right cerebral ganglion (CeG). The statocysts each contain three immunoreactive cell bodies (St; small open arrowhead, anterior static commissural fiber; D, dorsal; V, ventral; A, anterior; P, posterior; scale bars = 25 μm).

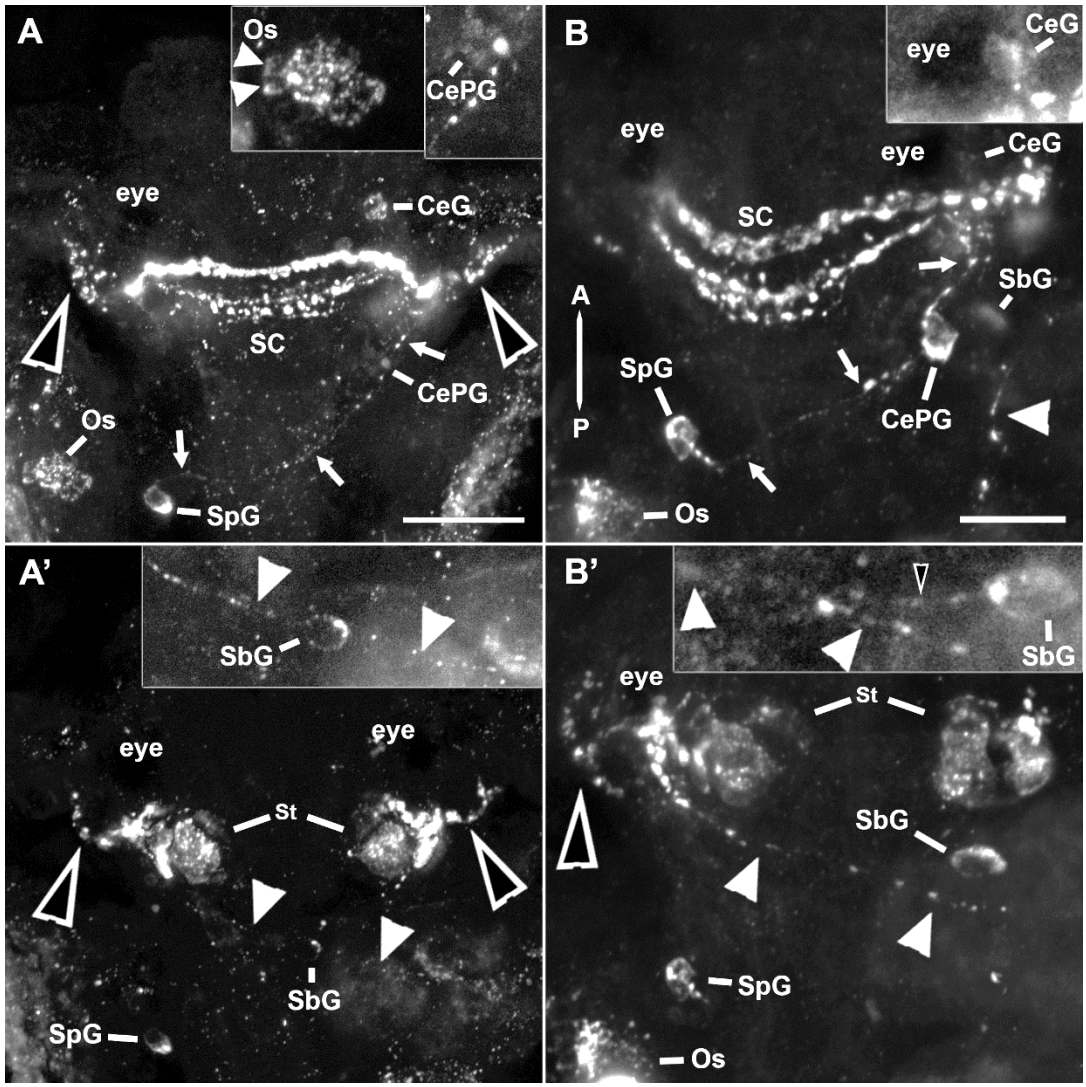
A
Os
CePG
eye
CeG
SC
CePG
Os
SpG
B
eye
CeG
eye
CeG
SC
SbG
A
P
SpG
CePG
Os
A'
SbG
eye
eye
St
SbG
SpG
B'
SbG
eye
St
SbG
SpG
Os

Figure 16. Micrographs showing histamine-like immunoreactive (HA-LIR) labelling in *Ilyanassa obsoleta* post-hatching (11-15 DPO). A-B) Specimen viewed from the dorsal perspective at 11 DPO (A; scale bar = 40 µm) and 15 DPO (B; scale bar = 25 µm). Frames labelled A to B indicate superficial labelling whereas A' to B' show deep labelling of the corresponding specimen. After hatching, a single cell becomes apparent in the right cerebral ganglion (CeG), located anterior to the static commissure (SC), and subintestinal ganglion (SbG) along the left posterior fiber (large solid arrowheads). These cells are added to the previously described cell in the cerebral-pleural (CePG) and supraintestinal ganglia (SpG) situated along the right posterior fiber (arrows). Additionally, processes extending antero-laterally from the statocysts (St) are evident (large open arrowheads). Finally, along the left side of the mantle HA-LIR punctate labelling showing 2 abutting cells (small solid arrowheads) are present, likely part of the osphradium (Os). Inlays shows digitally zoomed aspects of corresponding structures within each frame that showed faint and/or fine labelling (A = 1.6x zoom; A', B and B' = 1.7x zoom); small open arrowhead in the B' inlay reveals fiber extending to cell in the SbG (A, anterior; P, posterior).

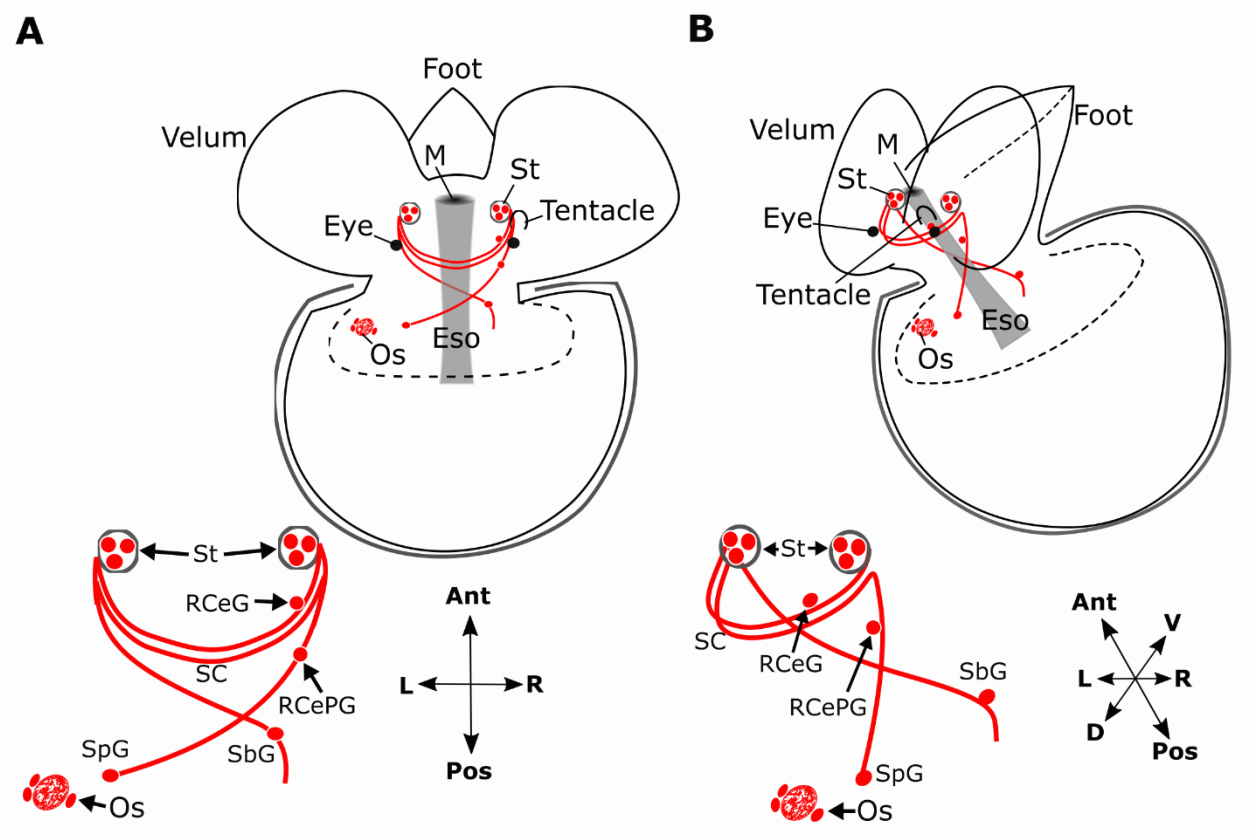
A
Foot
Velum
M
St
Tentacle
Eye
Os
Eso
St
RCeG
SC
RCePG
SpG
SbG
Os
Ant
L
R
Pos
B
Velum
Foot
M
St
Eye
Tentacle
Eso
Os
St
SC
RCeG
SbG
RCePG
SpG
Os
Ant
V
L
R
D
Pos

Figure 17. Schematic showing HA-LIR labelling in *Ilyanassa obsoleta* post-hatching (11-15 DPO): A) Dorsal perspective and B) Three dimensional angled-side perspective. Bilateral statocysts (St) each contain three immunoreactive cells with fibers projecting dorsally forming the static commissure (SC); along the static commissure, medial to the right eye is a single cell in the developing right cerebral ganglion (RCeG). Fibers are visible extending posteriorly and contralaterally from the statocysts (St) with the right posterior fiber containing a single cell in each the right cerebral-pleural ganglia (RCePG) and supraintestinal ganglion (SpG); the left posterior fiber contains a single cell in the subintestinal ganglion (SbG). Fibers projecting to the subintestinal ganglion pass ventral to the esophagus (Eso), whereas the fibers projecting to the supraintestinal ganglion pass dorsal to the esophagus (Eso), Finally, labelling of the osphradium (Os) reveals two or more cells surrounding extensive neuropil-like labelling (M, mouth; Ant, anterior; Pos, posterior; L, left; R, right; D, dorsal; V, ventral). This schematic was inspired by and adapted from Dickinson and Croll (2003).

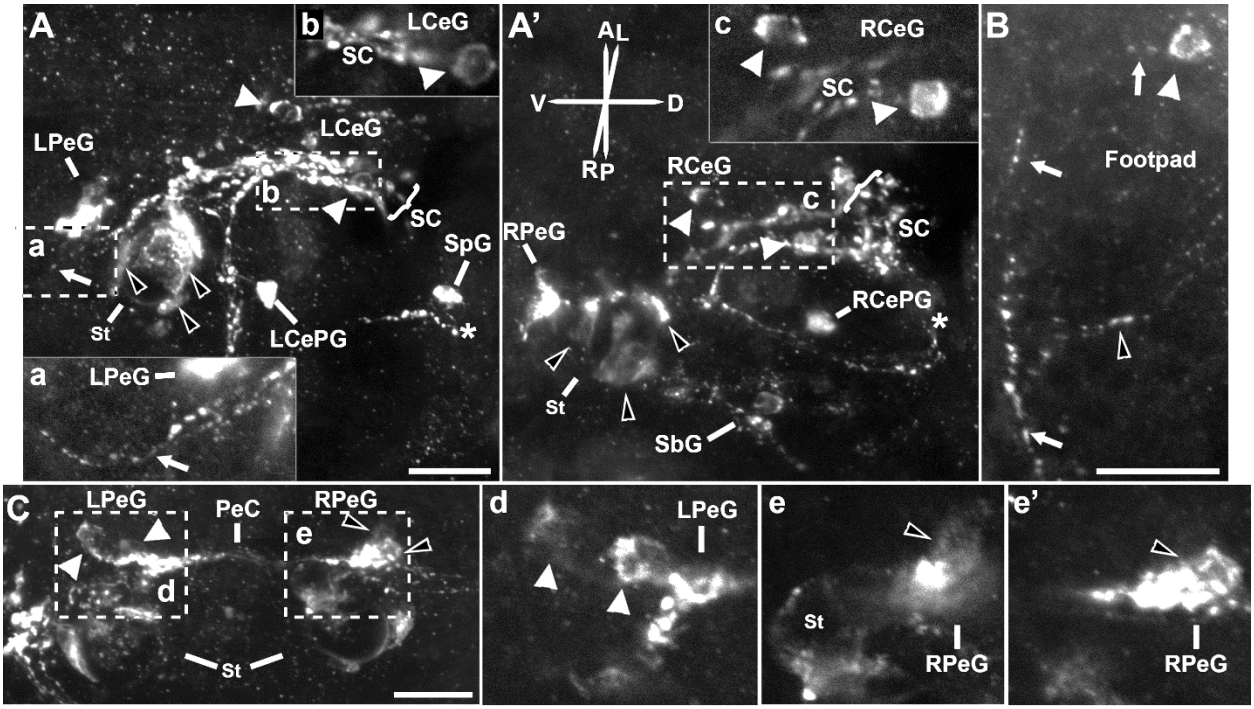
A
b
LCeG
SC
LPeG
LCeG
b
SC
a
SpG
St
LCePG
*
a
LPeG
A'
AL
V
D
RP
c
RCeG
SC
RCeG
C
SC
RPeG
RCePG
*
St
SbG
B
Footpad
C
LPeG
PeC
RPeG
e
d
St
d
LPeG
e
St
RPeG
e'
RPeG

Figure 18. Micrographs showing histamine-like immunoreactive (HA-LIR) labelling in *Ilyanassa obsoleta* free swimming veligers (22 DPO). A-A') Z-projections of the same specimen viewed from a side perspective showing shallow (A) and deep (A') labelling with points of continuation for the static commissure (SC) indicated by the curly bracket and points of continuation for the right posterior fiber indicated by the asterisk; point of continuation between frames for the left posterior fiber is obstructed by inlay a. Cells are now evident in the rudimentary pedal ganglia (PeG; L and R indicate Left and Right) anteroventral to the statocysts (St); the statocysts contain three stained somata (open arrowheads) each. Along the SC, two bilateral cells are revealed (solid arrowheads) in both the left and right cerebral ganglia (CeG). Additionally, along the left posterior fiber a single cell in each the left cerebral-pleural ganglion (LCePG) and the subintestinal ganglion (SbG) matches the single cell observed in each the right cerebral-pleural ganglion (RCePG) and supraintestinal ganglion (SpG) along the right posterior fiber. a) Inlay shows a 1.5x zoom of a HA-LIR process projecting into the footpad (arrows). b/c) inlays showing 1.5x zoom of obstructed CeG cells (A, anterior; P, posterior; V, ventral; D, dorsal; R, right; L, left). B) Anterior perspective of the right side of the foot revealing a cell (solid arrowhead) with a discontinuous blebby fiber (arrows) that fasciculates with another fiber (open arrowhead) as it projects to the central nervous system (CNS). C) Anterior perspective of pedal ganglia (PeG) and statocysts (St) showing two bilateral cells in each the LPeG (solid arrowheads) and RPeG (open arrowheads) with the pedal commissure (PeC) connecting the two ganglia; inlays d and e/e' show 2x zoom of the pedal cells where e and e' show shallow and deep labelling, respectively (scale bars = 25 μm).

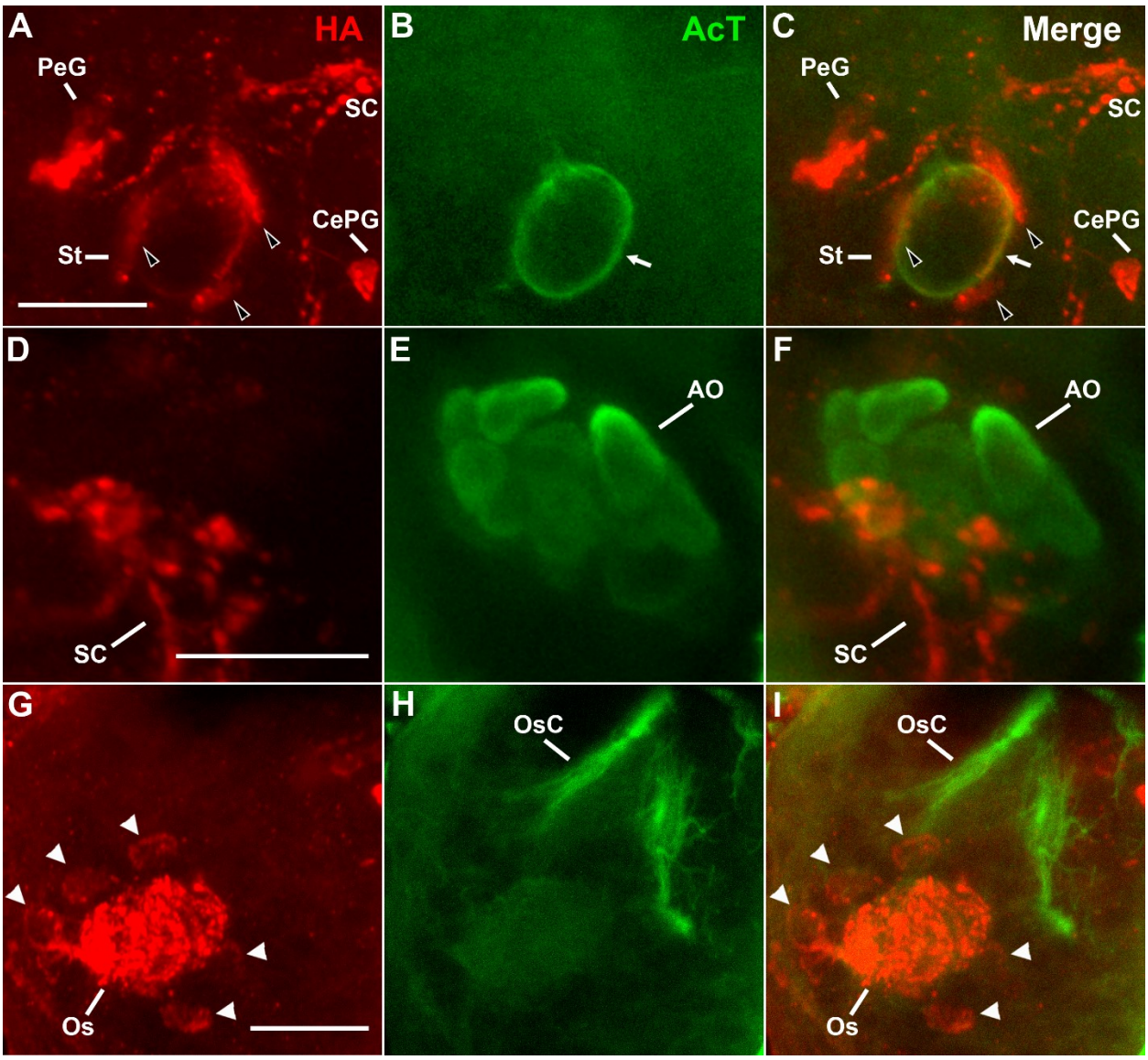
A
HA
PeG
SC
CePG
St
B
AcT
C
Merge
PeG
SC
CePG
St
D
SC
E
AO
F
AO
SC
G
Os
H
OsC
I
OsC
Os

Figure 19. Micrographs showing double labels of HA-LIR and acetylated-tubulin (AcT) labelling in the *Ilyanassa obsoleta* free swimming veliger at 22 days post oviposition (DPO). A-C) HA-LIR labelling (A) showing intense fluorescence in the pedal ganglion (PeG) anteroventral to the statocysts (St), which consist of three HA-LIR cells encapsulating the AcT-LIR (B) lumen. Merging the two channels (C) reveal the PeG immunoreactive elements as separate from the St (CePG, cerebral-pleural ganglion). D-F) HA-LIR labelling (A) of the static commissure (SC) in conjunction with AcT-LIR labelling (E) of the apical organ (AO) showing the two structures abutting (F). G-I) HA-LIR labelling (G) of the osphradium (Os) showing intensely labelled neuropil with five cells along the perimeter (solid arrowheads). AcT-LIR labelling (H) indicates ciliary tufts near the osphradium (I), thus tentatively called osphradial cilia (OsC; scale bars = 25 μm).

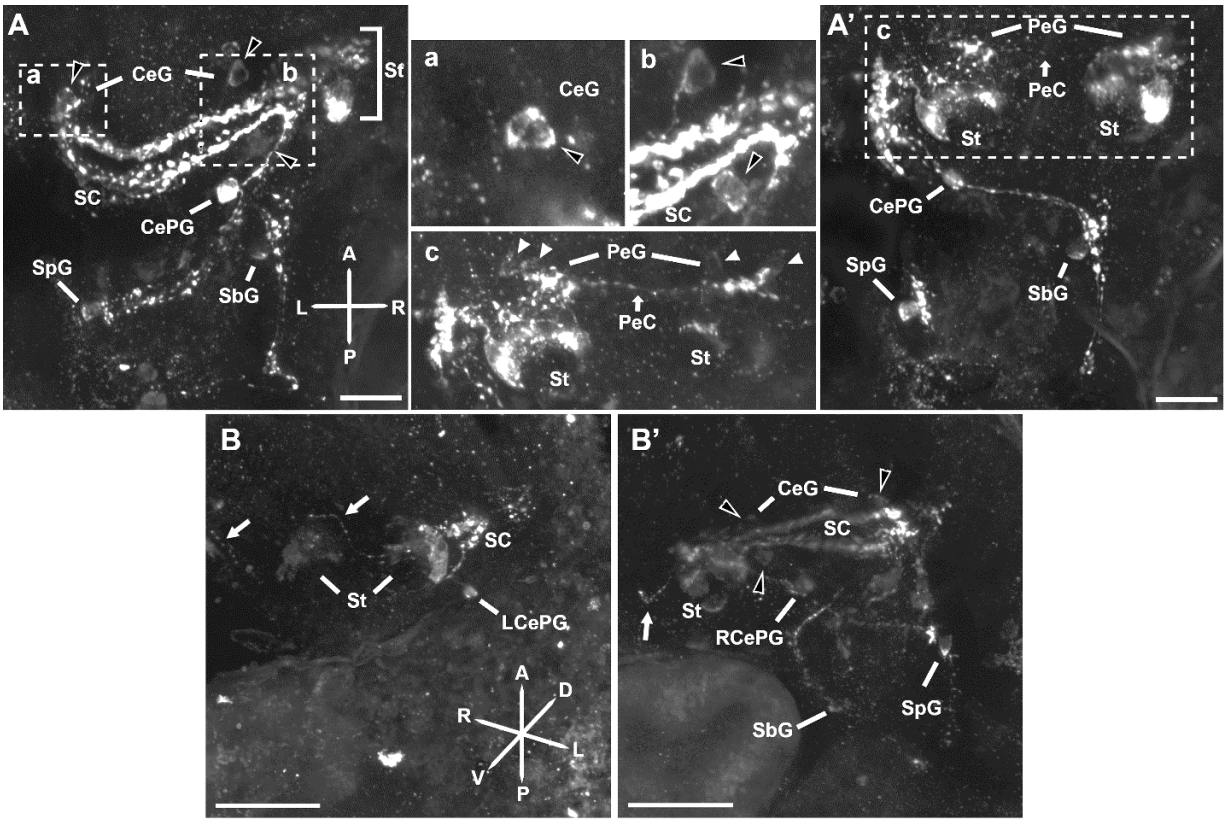
A
a
b
CeG
St
SC
CePG
SpG
SbG
A
L
R
P
a
CeG
b
SC
c
PeG
PeC
St
St
A'
c
PeG
PeC
St
St
CePG
SpG
SbG
B
SC
St
LCePG
A
D
R
L
V
P
B'
CeG
SC
St
RCePG
SpG
SbG

Figure 20. Micrographs showing histamine-like immunoreactive (HA-LIR) labelling in the *Ilyanassa obsoleta* free swimming veliger at 24-27 days post oviposition (DPO). A-A') The same specimen viewed from an anterior perspective where A) shows shallow labelling and A') shows deep labelling (scale bar = 25 μm). A) Open arrowheads indicate two bilateral cells that are visible in the cerebral ganglia (CeG) along the static commissure (SC) that runs between the statocysts (St; bracket); the left posterior cerebral cell is not visible. A fiber extends dorsal-posteriorly from the right statocyst where a cell is visible in the right cerebral-pleural ganglion (CePG). Further along this posterior loop fiber a cell is visible in the supraintestinal ganglion (SpG). A posterior loop fiber extending from the left statocyst leads to a cell in the subintestinal ganglion (SbG). a-b) Inlays showing digital zoom of the left (a; 2.8x zoom) and right (b; 2x zoom) cerebral cells from A (open arrowheads). A') Overview of ventrally located neural elements showing both statocysts (St) with the pedal commissure (PeC) and visualization of the posteriorly projecting fiber from the left statocyst where a cell is visible in the left cerebral-pleural ganglion (CePG). Further along the left posterior loop fiber a cell is visible in the subintestinal ganglion (SbG). c) Inlay showing a 1.35x zoom of the statocysts (St) and two bilateral cells (solid arrowheads) in the pedal ganglia (PeG) including a fine blebby fiber along the pedal commissure (PeC). B-B') Angled-side perspective of a second sample with B) showing shallow labelling and B') showing deep labelling. B) Shows the left statocyst (St) and cerebral-pleural ganglion (LCePG) and B') shows the right statocyst (St) and cerebral-pleural ganglion (RCePG). White arrows indicate fine fibers that project into the foot from the region around the statocysts (A, anterior; P, posterior; V, ventral; D, dorsal; R, right; L, left; scale bar = 50 μm).

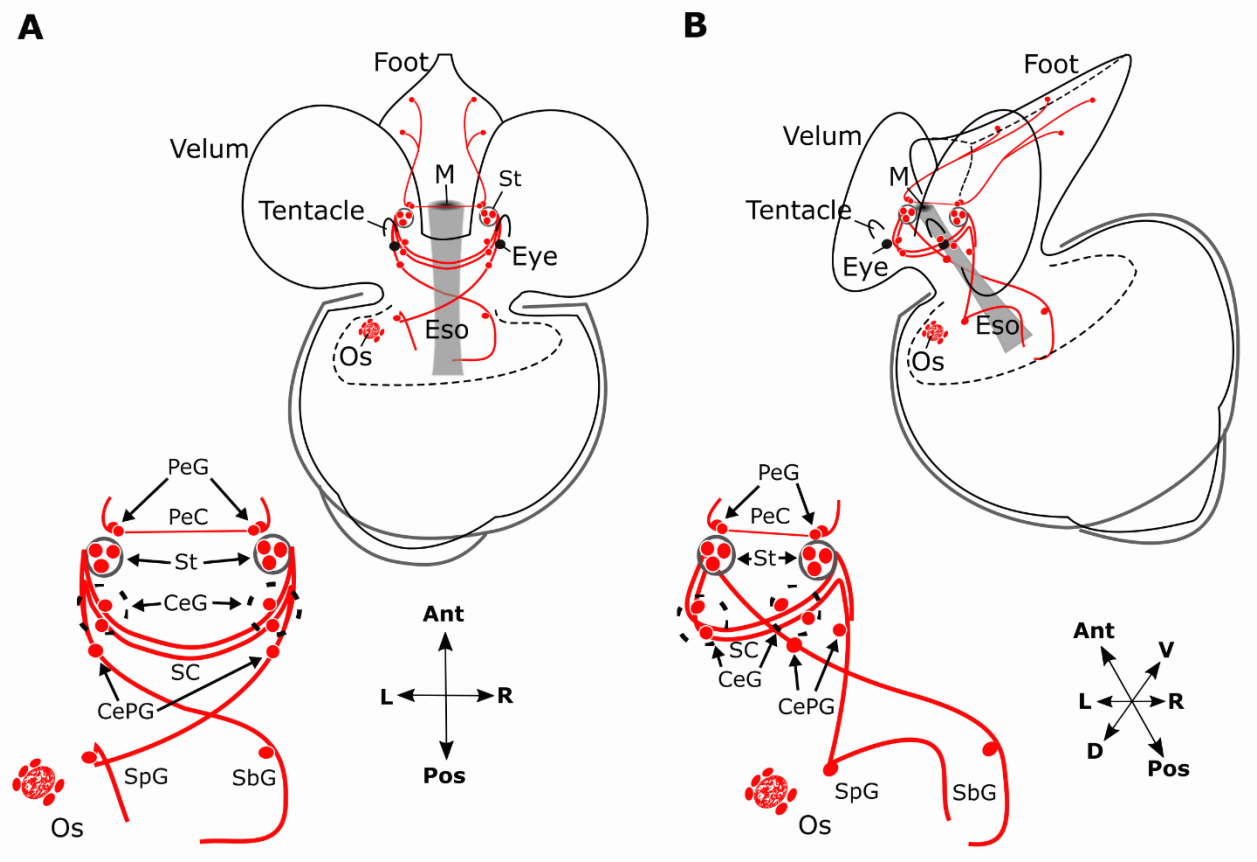
A
Foot
Velum
M
St
Tentacle
Eye
Eso
Os
PeG
PeC
St
CeG
SC
CePG
SpG
SbG
Os
Ant
L
R
Pos
B
Foot
Velum
M
Tentacle
Eye
Eso
Os
PeG
PeC
St
SC
CeG
CePG
SpG
SbG
Os
Ant
V
L
R
D
Pos

Figure 21. Schematic showing HA-LIR labelling in the free swimming *Ilyanassa obsoleta* (22-27 DPO): A) Dorsal perspective and B) Three dimensional angled-side perspective. Bilateral statocysts (St) each contain three immunoreactive cells; ventral-anterior to the statocysts (St) are the pedal ganglia (PeG) each containing two cells with fibers extending across the pedal commissure (PeC). Two bilateral cells are visi ble in the cerebral ganglia (CeG), which are located along the static commissure (SC) projecting dorsally from the statocysts. Fibers that project posteriorly from the statocysts and extend throughout the posterior loop of the central nervous system contain a bilateral cell in both the cerebral-pleural ganglia (CePG). Further along the posterior loop fibers a single cell is found in both the supraintestinal (SpG) and subintestinal (SbG) ganglia. Fibers projecting to the subintestinal ganglion pass ventral to the esophagus (Eso), whereas the fibers projecting to the supraintestinal ganglion pass dorsal to the esophagus (Eso), Finally, labelling of the osphradium (Os) reveals at least five cells surrounding extensive neuropil-like labelling (M, mouth; Ant, anterior; Pos, posterior; L, left; R, right; D, dorsal; V, ventral). This schematic was inspired by and adapted from Dickinson and Croll (2003).

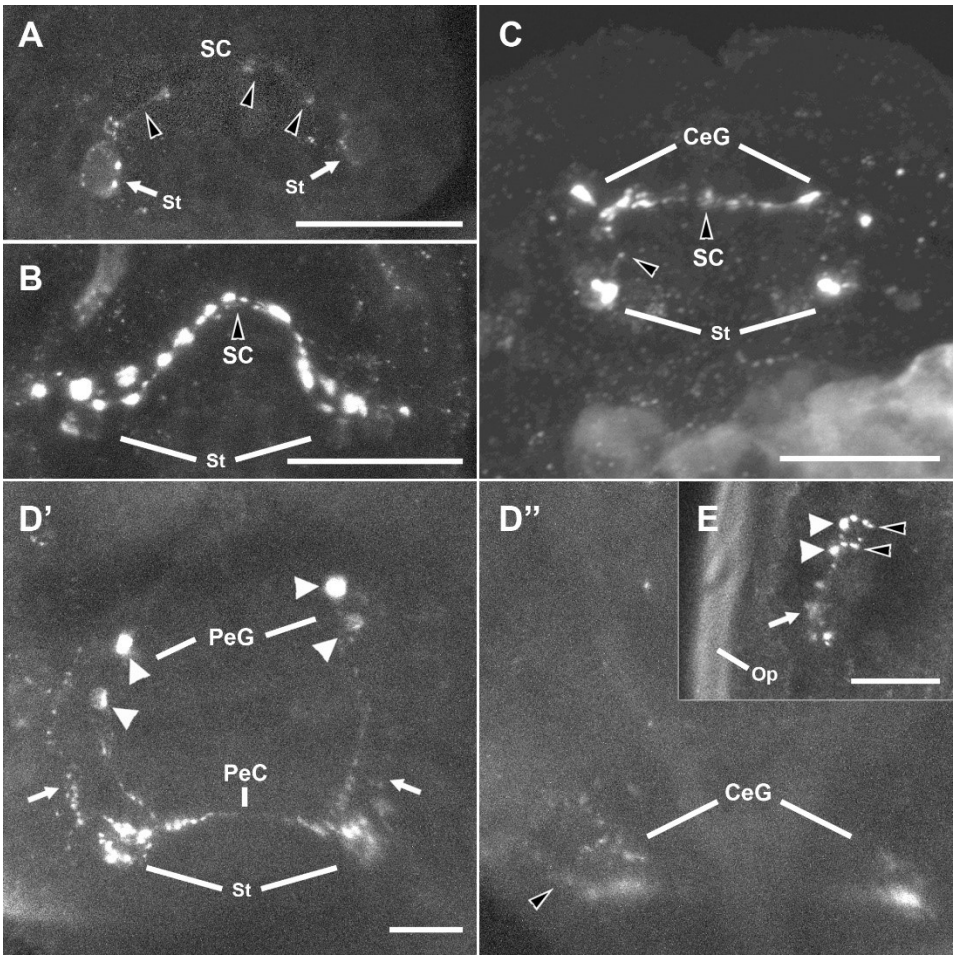
A
SC
St
St
B
SC
St
C
CeG
SC
St
D'
PeG
PeC
St
D''
CeG
E
Op

Figure 22. Micrographs showing histamine-like immunoreactive (HA-LIR) labelling in *Aplysia californica* at various stages of development from embryonic day 5 (E5) to Stage 6. A) Embryonic day 5 specimen show a single bilateral HA-LIR cell (arrows) likely part of the statocysts (St); these bilateral cells contain fine blebby processes that follow a tortuous apical path forming the static commissure (SC). B) Embryonic day 7 specimen reveal intense and blebby HA-LIR labelling of the SC that looks fragmented. C) Ventral-posterior perspective of a stage 1 hatchling veliger showing a bilaterally placed structure, likely the St, with fine blebby apical projections forming the SC; along the SC and anterior to the St is a bilaterally positioned area of intense labelling likely the rudimentary cerebral ganglia (CeG). D) Ventral view of Stage 6, competent veliger where D') shows shallow labelling and D'') shows deep labelling of the same specimen. D') Two bilateral cells (solid arrowheads) are evident anteroventral to the statocysts (St), likely part of the developing pedal ganglia (PeG), with fine blebby processes that extend toward the St and contralaterally forming the pedal commissure (PeC). Lateral to the St, blebby discontinuous processes (arrows) extend ventral into the footpad. D'') Intense labelling deep in the tissue reveals the rudimentary cerebral ganglia (CeG) with lateral projections likely to the vela (open arrowhead). E) Side perspective at Stage 6 showing the end of the lateral fibers described from D (arrows) where two relatively large blebs (solid arrowheads) are apparent with processes that turn toward the epithelium like dendrites (open arrowheads), indicating possible sensory cells in the foot (scale bars = 25 μm).

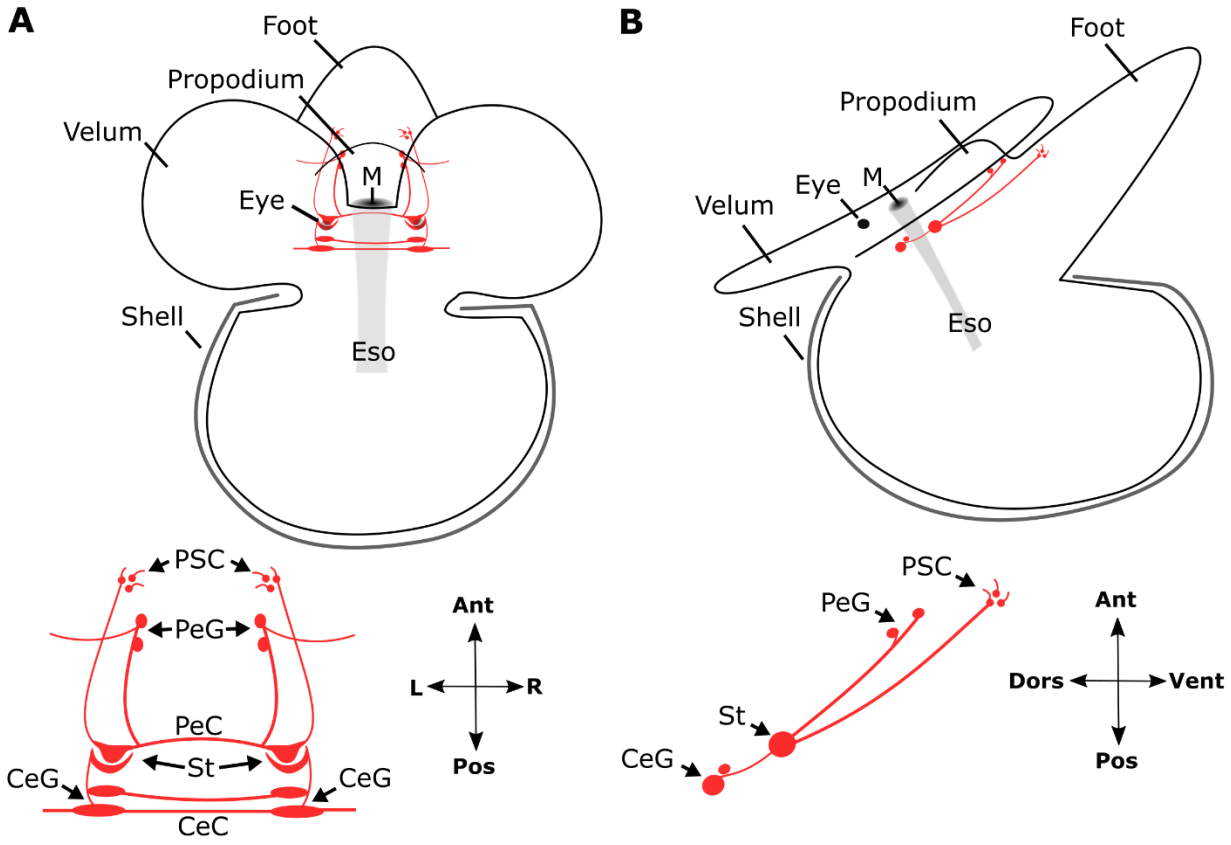
A
Foot
Propodium
Velum
Eye
M
Shell
Eso
PSC
PeG
PeC
St
CeG
CeG
CeC
Ant
L
R
Pos
B
Foot
Propodium
Velum
Eye
M
Shell
Eso
PSC
PeG
St
CeG
Ant
Dors
Vent
Pos

Figure 23. Schematic showing putative HA-LIR labelling in stage 6, metamorphically competent, *Aplysia californica*. Two bilaterally placed cells are found dorsal to the esophagus (Eso) in the cerebral ganglia (CeG) with projections ventrally to the statocysts (St) and laterally to unknown targets. Ventral to the St two bilateral cells are present that are likely part of the pedal ganglia (PeG) with dorsal projections that join the pedal commissure (PeC) and faint lateral projections; the PeC follows a path that extends between the statocysts (St). In addition to neuronal elements of the central nervous system (CNS), there are also at least three bipolar peripheral sensory cells (PSC) located bilaterally in the foot with projections entering the CNS lateral to the St (M, mouth; CeC, cerebral commissure; Ant, anterior; Pos, posterior; L, left; R, right; Dors, dorsal; Vent, ventral). This schematic was inspired by and adapted from Dickinson and Croll (2003).

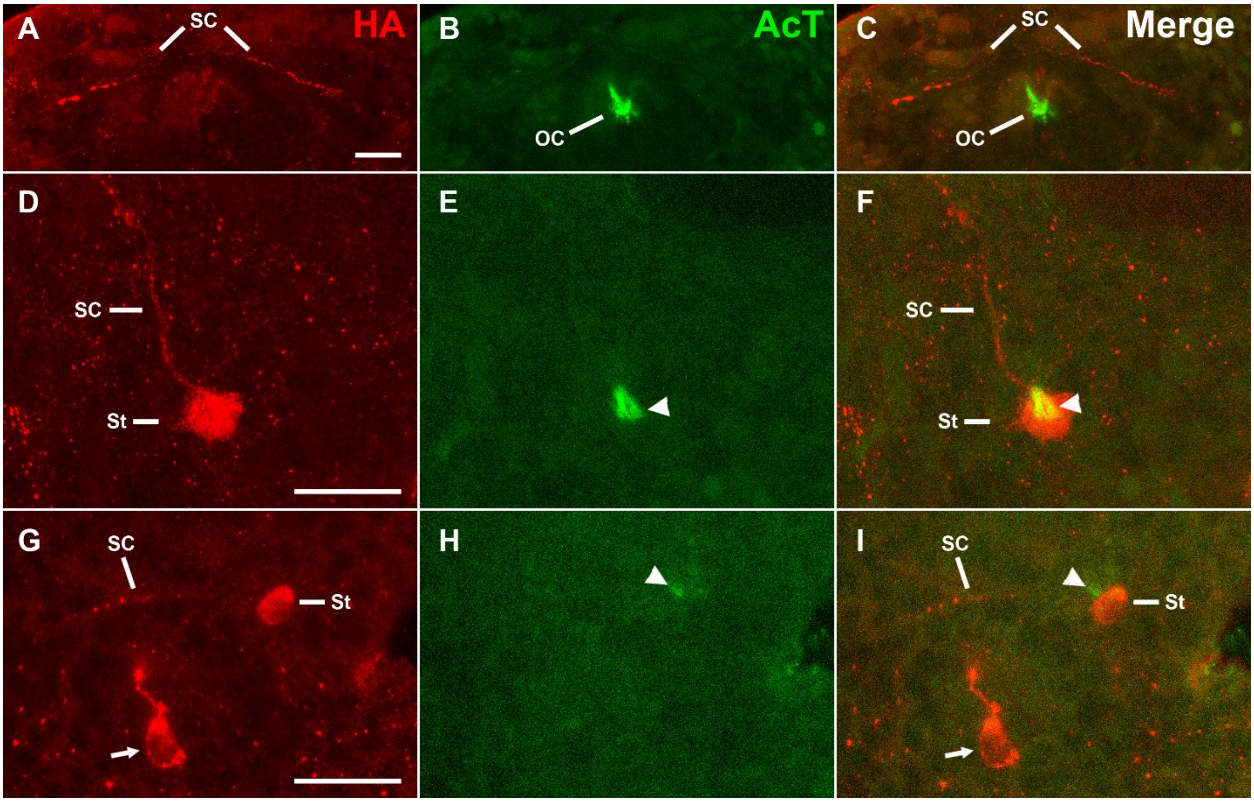
A
SC
HA
B
AcT
OC
C
SC
Merge
OC
D
SC
St
E
F
SC
St
G
SC
St
H
I
SC
St

Figure 24. Micrographs showing double labels of HA-LIR and acetylated-tubulin (AcT) labelling in early development of freshwater gastropods, *Lymnaea stagnalis* (A-F) and *Biomphalaria alexandrina* (G-I). A-C) Anterior perspective of *L. stagnalis* showing an apical HA-LIR blebby fiber, believed to be the static commissure (SC), that passes dorsal to the mouth where a patch of ACT-LIR oral cilia (OC) is identified; C) shows merged images of A and B. D-F) Side perspective of *L. stagnalis* showing a HA-LIR cell with an apical projection (SC, static commissure) likely part of the statocyst (St); AcT labelling reveals cilia (solid arrowhead) abutting the HA-LIR cell. G-I) Angled-side perspective of *B. alexandrina* showing two bilaterally placed HA-LIR cells where one is determined to be part of the statocysts (St) because it contains AcT-LIR cilia (solid arrowhead) and the other is of unknown origin (arrow). A discontinuous faint fiber is also identified that is likely part of the static commissure (SC; scale bars = 25 μm).

Chapter 5: Conclusion

The primary goal of this thesis was to expand on the current selection of neurotransmitters that have been identified and described extensively in comparative developmental studies in larvae across the animal kingdom; these previous descriptions have been used to infer evolutionary relationships and focused primarily on select biogenic amines (catecholamines and serotonin), neuropeptides (FMRFamide and enkephalin), and in some cases acetylcholine (Croll et al., 1997; Croll & Dickinson, 2004; Denes et al., 2007; Dickinson & Croll, 2003; Hay-Schmidt, 1990b, 1990a; Marlow et al., 2014; Python & Stocker, 2002; Voronezhskaya et al., 1999; Wollesen et al., 2007). The secondary goal was to describe the relevance of such neuroanatomical studies and the results presented herein in the context of current beliefs surrounding the evolutionary history of the CNS. These goals were pursued by investigating the genesis and development of octopaminergic and histaminergic neural elements during larval development of various gastropods with a focus on the marine molluscs, *I. obsoleta* and *A. californica*.

To summarize, Chapter 3 focused on octopaminergic neural elements and presented extensive evidence showing the reliability of using a DBH antibody as a marker to confirm OA positive labelling in gastropods with potential for broader comparative applications. Based on the criteria used in this thesis, results presented in Chapter 3 also indicate that OA is absent during larval development, corroborating previous research on a direct developing freshwater gastropod, *L. stagnalis* (Elekes et al., 1996). Taking into consideration past research on the physiological roles of OA in invertebrates where it has been proposed to function analogously to the vertebrate adrenergic system (Axelrod & Saavedra, 1977; Bauknecht & Jékely, 2017; David & Coulon, 1985; Roeder, 1999, 2020), these results could indicate that stress related signalling and behaviors do not appear until post-metamorphosis. Given the number of offspring produced during molluscan spawning, this could reflect an evolved life history strategy where energy is directed to behaviours that optimize growth and development at the detriment of complex stress responses in order to ensure at least a few offspring are able to survive to metamorphosis; future research looking at the relevance of OA and NE

in larva from both deuterostomes and protostomes could reveal insights into the evolutionary history of stress-related signalling in the nervous system.

Chapter 4 focused on histaminergic neural elements and provided the first early larval descriptions of HA in indirect developing marine gastropods. Results in Chapter 4 revealed an extensive network of HA positive neurons and fibers in the developing adult nervous system of larva indicating complex histaminergic signalling. As described, HA labelling first appeared in a subset of sensory cells in the statocysts at a late trochophore/early embryonic veliger stage (~4-5 DPO) corroborating studies where HA positive sensory cells have been described in the statocysts of adult gastropods (Braubach & Croll, 2004; Habib et al., 2015; Hegedűs et al., 2004b; Ohsuga et al., 2000; Soinila et al., 1990; Webber et al., 2017). These HA-LIR sensory cells contained processes that formed the static commissure, which extended through the neuropil of the apical organ (Figs 12-14). This early indication of HA and association with the AO suggests likely functionality of the statocysts in early larval development. Additionally, evidence showing early histaminergic elements during embryonic development support a previous proposal that HA positive neurons could participate in the development of the adult nervous system (Hegedűs et al., 2004a); here I propose that the early development of the statocyst and accompanying commissure could, along with previously described peptidergic fibers (Croll & Voronezhskaya, 1996; Voronezhskaya & Elekes, 1996), act as pioneering neurons for the development of the cerebral ganglia and early elements of the adult CNS. Future research could look to identify signalling molecules used in remaining sensory cells of the statocysts during development and investigate the relationship between the development of the statocysts and cerebral ganglia. If the histaminergic neural elements of the statocysts function as pioneering fibers for neurite outgrowth of the cerebral and pedal ganglia as suggested, I would suspect that neural elements arising from the statocysts would function similarly among other molluscan species; therefore, I would expect to see early development of static sensory neurons that form a commissure projecting proximal to the apical organ in other classes of mollusc other than the gastropods. Alternatively, in the absence of statocysts, I would expect similar projections of pioneering fibers that form a scaffold for neurite outgrowth of the anterior adult ganglia in other invertebrate phyla.

In addition to the statocysts, Chapter 4 described and discussed the development of HA positive neural elements in the cerebral, cerebral-pleural, supraintestinal, subintestinal and pedal ganglia as well as peripheral labelling of sensory cells in the osphradium and foot of *I. obsoleta*. These observations were also compared with results of early HA-LIR labelling in *A. californica* and *L. stagnalis* (Figs 22-24). When compared to past literature on HA signalling and function across the animal kingdom, HA represents a signalling molecule with divergent evolution. In vertebrates, HA is used predominantly for neuromodulatory roles involved with wakefulness and attention (Brown et al., 1995; Dere et al., 2003; Haas & Panula, 2003; Ishizuka & Yamatodani, 2012; Mochizuki et al., 1992; Selbach et al., 1997; Strecker et al., 2002; Tuomisto et al., 2001), whereas, it has a dominant role in sensory signalling in extant invertebrates (Braubach & Croll, 2004; Buchner et al., 1993; Habib et al., 2015; Hegedűs et al., 2004b; Nässel, 1999; Ohsuga et al., 2000; Soinila et al., 1990; Stuart et al., 2007; Webber et al., 2017; Wyeth & Croll, 2011). Hypotheses surrounding the single origination of the central nervous system among all bilateral animals, does not seem to account for this kind of divergent evolutionary processes.

The results and literature discussed in this thesis challenge the single origin hypothesis of the central nervous system. As reviewed in Chapter 1, the single origin hypothesis proposes that all nervous systems throughout Bilateria are homologous and evolved from a common ancestor that already had a consolidated central nervous system; this hypothesis is largely supported from molecular evidence indicating the conservation of developmental genes and their expression patterns in the development of body morphology but more specifically the nervous system (Arendt & Nübler-Jung, 1994, 1997; De Robertis & Sasai, 1996; Denes et al., 2007; Holley et al., 1995; Kimelman & Martin, 2012; Urbach & Technau, n.d.). The single origin hypothesis attempts to account for the degree of diversity in nervous system morphology across the animal kingdom by suggesting subsequent reduction through loss of evolutionary traits, which would have occurred up to 11 times independently throughout Bilateria (Northcutt, 2012). However, phylogenetic analyses that combine molecular and morphological traits suggests that the central nervous system could have originated up to seven times independently (Moroz, 2009). Such phylogenetic research in conjunction with studies on the evolution of body

plans and gene regulatory networks (GRNs) suggest that evidence supporting the single origin hypothesis is too narrow sighted.

Critics of the single origin hypothesis have highlighted that research on the conserved developmental genetic networks that form the basis for this hypothesis is dependant upon organisms that provide a biased perspective focusing on bilaterians with highly centralized and complex organization (Hejnol & Lowe, 2015). In fact, if one looks more broadly, the idea of conserved hox signalling mechanisms that include the observed spatial and temporal collinearity used to describe conserved anterior to posterior patterning mechanisms does not hold true for all bilaterians. For example, evidence for co-linearity of hox genes during molluscan development has been mixed with studies showing co-linearity in an apolyplacophoran (Fritsch et al., 2015), partial co-linearity in gastropods (Samadi & Steiner, 2009) and no colinear organization in bivalves (Salamanca-Díaz et al., 2021). Additionally, there are examples among deuterostomes where the conserved rules around co-linearity of Hox genes are broken (David & Mooi, 2014). Thus, indicating that the current understanding of developmental gene expression and its correlation to evolutionary history of developmental mechanisms and phenotypic expression of body plan and neural morphology is still in relatively rudimentary stages.

In fact, research on GRNs remains a rich field for investigating the structure, evolution, and conservation of GRNs across the animal kingdom. Current research into GRNs suggests that conserved developmental genes across Bilateria were likely involved in simple, relatively flat, gene signalling networks (Erwin, 2020); it is possible that through subsequent evolution these genes persisted but were co-opted into complex hierarchical gene signalling networks differentially throughout bilaterian evolution, which brought about the large diversity of body plans and morphological features observed in extant bilaterian species today (Erwin, 2020; Holland & Short, 2008). Extensive comparative studies on the structures of GRNs incorporating a strong understanding of morphological features are necessary to properly interpret molecular data on gene expression and its correlation to morphological homologies and evolutionary history of organisms.

In conclusion, the present thesis contributes to the overall conversation by expanding on our previous understanding of the gastropod larval nervous system and

potential implications for OA and HA signalling among molluscs. This research lays the framework for future comparative studies in larvae of more distantly related phyla and presents data that can be used to inform studies on GRNs and how these developmental mechanisms give rise to morphological characteristics. Molecular data have provided a powerful tool for understanding evolutionary relationships; however, the literature presented in this thesis indicates that our current knowledge surrounding GRNs and how they evolve and lead to morphological change is insufficient to rely on alone. Investigations into developmental genetic mechanisms for patterning the nervous system need to be applied more broadly in conjunction with studies on morphological characteristics to properly elucidate the evolutionary origin of the central nervous system among Bilateria.

REFERENCES

Adamo, S. A. (2012). The effects of the stress response on immune function in invertebrates: An evolutionary perspective on an ancient connection. *Hormones and Behavior*, *62*(3), 324–330. https://doi.org/10.1016/j.yhbeh.2012.02.012

Alejevski, F., Saint-Charles, A., Michard-Vanhée, C., Martin, B., Galant, S., Vasiliauskas, D., & Rouyer, F. (2019). The HisCl1 histamine receptor acts in photoreceptors to synchronize *Drosophila* behavioral rhythms with light-dark cycles. *Nature Communications*, *10*(1), 1–10. https://doi.org/10.1038/s41467-018-08116-7

Alkon, D. L. (1975). Responses of hair cells to statocyst rotation. *Journal of General Physiology*, *66*(4), 507–530. https://doi.org/10.1085/jgp.66.4.507

Antemann, V., Pass, G., & Pflüger, H. J. (2018). Octopaminergic innervation and a neurohaemal release site in the antennal heart of the locust *Schistocerca gregaria*. *Journal of Comparative Physiology A: Neuroethology, Sensory, Neural, and Behavioral Physiology*, *204*(2), 131–143. https://doi.org/10.1007/S00359-017-1213-5/FIGURES/5

Aonuma, H., Kaneda, M., Hatakeyama, D., Watanabe, T., Lukowiak, K., & Ito, E. (2017). Weak involvement of octopamine in aversive taste learning in a snail. *Neurobiology of Learning and Memory*, *141*, 189–198. https://doi.org/10.1016/J.NLM.2017.04.010

Arendt, D., & Nübler-Jung, K. (1994). Inversion of dorsoventral axis? *Nature*, *371*(6492), 26. https://doi.org/10.1038/371026a0

Arendt, D., & Nübler-Jung, K. (1997). Dorsal or ventral: Similarities in fate maps and gastrulation patterns in annelids, arthropods and chrodates. *Mechanisms of Development*, *61*(1–2), 7–21. https://doi.org/10.1016/S0925-4773(96)00620-X

Arendt, D., Tosches, M. A., & Marlow, H. (2016). From nerve net to nerve ring, nerve cord and brain-evolution of the nervous system. *Nature Reviews Neuroscience*, *17*(1), 61–72. https://doi.org/10.1038/nrn.2015.15

Atkinson, J. W. (1971). Organogenesis in normal and lobeless embryos of the marine prosobranch gastropod *Ilyanassa obsoleta*. *Journal of Morphology*, *133*(3), 339–352. https://doi.org/10.1002/JMOR.1051330307

Atkinson, J. W. (1986). An atlas of light micrographs of normal and lobeless larvae of the marine gastropod *Ilyanassa obsoleta*. *International Journal of Invertebrate Reproduction and Development*, *9*(2), 169–178. https://doi.org/10.1080/01688170.1986.10510194

Auerbach, B., & Budelmann, B. U. (1986). Evidence for acetylcholine as a neurotransmitter in the statocyst of *Octopus vulgaris*. *Cell and Tissue Research*, *243*(2), 429–436. https://doi.org/10.1007/BF00251060

Axelrod, J., & Saavedra, J. M. (1977). Octopamine. *Nature*, *265*(5594), 501–504. https://doi.org/10.1038/265501A0

Barna, J., Csoknya, M., Lázár, Z., Barthó, L., Hámori, J., & Elekes, K. (2001). Distribution and action of some putative neurotransmitters in the stomatogastric nervous system of the earthworm, *Eisenia fetida* (Oligochaeta, Annelida). *Journal of Neurocytology*, *30*(4), 313–325. https://doi.org/10.1023/A:1014456329814

Bauknecht, P., & Jékely, G. (2017). Ancient coexistence of norepinephrine, tyramine, and octopamine signaling in bilaterians. *BMC Biology*, *15*(1), 1–12. https://doi.org/10.1186/s12915-016-0341-7

Beach, G. A., Habib, M. R., El Hiani, Y., Miller, M. W., & Croll, R. P. (2019). Localization of keyhole limpet hemocyanin-like immunoreactivity in the nervous system of *Biomphalaria alexandrina*. *Journal of Neuroscience Research*, *97*(11), 1469–1482. https://doi.org/10.1002/jnr.24497

Bicker, G., Schafer, S., Ottersen, O. P., & Storm-Mathisen, J. (1988). Glutamate-like immunoreactivity in identified neuronal populations of insect nervous systems. *Journal of Neuroscience*, *8*(6), 2108–2122. https://doi.org/10.1523/JNEUROSCI.08-06-02108.1988

Bonar, D. B. (1978). Ultrastructure of a cephalic sensory organ in larvae of the gastropod *Phestilla sibogae* (Aeolidacea, Nudibrachia). *Tissue & Cell*, *10*(1), 153–165. https://doi.org/10.1016/0040-8166(78)90014-9

Braubach, O. R., & Croll, R. P. (2004). Evidence that histamine acts as a neurotransmitter in statocyst hair cells in the snail, *Lymnaea stagnalis*. *Journal of Gravitational Physiology*, *11*(3), 57–66.

Braubach, O. R., Dickinson, A. J. G., Evans, C. C. E., & Croll, R. P. (2006). Neural control of the velum in larvae of the gastropod, *Ilyanassa obsoleta*. *Journal of Experimental Biology*, *209*(23), 4676–4689. https://doi.org/10.1242/jeb.02556

Broadley, K. J. (2010). The vascular effects of trace amines and amphetamines. *Pharmacology and Therapeutics*, *125*(3), 363–375. https://doi.org/10.1016/j.pharmthera.2009.11.005

Brown, R. E., Fedorov, N. B., Haas, H. L., & Reyman, K. G. (1995). Histaminergic modulation of synaptic plasticity in area CA1 of rat hippocampal slices. *Neuropharmacology*, *34*(2), 181–190. https://doi.org/10.1016/0028-3908(94)00138-I

Buchner, E., Buchner, S., Burg, M. G., Hofbauer, A., Pak, W. L., & Pollack, I. (1993). Histamine is a major mechanosensory neurotransmitter candidate in *Drosophila melanogaster*. *Cell and Tissue Research*, *273*(1), 119–125. https://doi.org/10.1007/BF00304618

Budelmann, B. U., & Bonn, U. (1982). Histochemical evidence for catecholamines as neurotransmitters in the statocyst of *Octopus vulgaris*. *Cell and Tissue Research*, *227*(3), 475–483. https://doi.org/10.1007/BF00204779

Byrne, M., Nakajima, Y., Chee, F. C., & Burke, R. D. (2007). Apical organs in echinoderm larvae: insights into larval evolution in the Ambulacraria. *Evolution & Development*, *9*(5), 432–445. https://doi.org/10.1111/J.1525-142X.2007.00189.X

Carrigan, I. D., Croll, R. P., & Wyeth, R. C. (2015). Morphology, innervation, and peripheral sensory cells of the siphon of *Aplysia californica*. *The Journal of Comparative Neurology*, *523*(16), 2409–2425. https://doi.org/10.1002/cne.23795

Carter, J. M. (1996). Conjugation of peptides to carrier proteins via glutaraldehyde. In J. M. Walker (Ed.), *The Protein Protocols Handbook* (pp. 679–687). Humana Press. https://doi.org/10.1007/978-1-60327-259-9_117

Chia, F. -S, & Koss, R. (1979). Fine structural studies of the nervous system and the apical organ in the planula larva of the sea anemone *Anthopleura elegantissima*. *Journal of Morphology*, *160*(3), 275–297. https://doi.org/10.1002/JMOR.1051600303

Chiel, H. J., Weiss, K. R., & Kupfermann, I. (1990). Multiple roles of a histaminergic afferent neuron in the feeding behavior of *Aplysia*. *Trends in Neurosciences*, *13*(6), 223–227. https://doi.org/10.1016/0166-2236(90)90164-6

Chowański, S., Spochacz, M., Szymczak, M., & Rosiński, G. (2017). Effect of biogenic amines on the contractile activity of visceral muscles in the beetle *Tenebrio molitor*. *Bulletin of Insectology*, *70*(2), 209–220.

Churgin, M. A., McCloskey, R. J., Peters, E., & Fang-Yen, C. (2017). Antagonistic serotonergic and octopaminergic neural circuits mediate food-dependent locomotory behavior in *Caenorhabditis elegans*. *Journal of Neuroscience*, *37*(33), 7811–7823. https://doi.org/10.1523/JNEUROSCI.2636-16.2017

Coggeshall, R. E. (1969). A fine structural analysis of the statocyst in *Aplysia californica*. *Journal of Morphology*, *127*(1), 113–131. https://doi.org/10.1002/JMOR.1051270107

Conzelmann, M., Williams, E. A., Tunaru, S., Randel, N., Shahidi, R., Asadulina, A., … Jékely, G. (2013). Conserved MIP receptor-ligand pair regulates *Platynereis* larval settlement. *Proceedings of the National Academy of Sciences of the United States of America*, *110*(20), 8224–8229. https://doi.org/10.1073/pnas.1220285110

Crisp, K. M., Klukas, K. A., Gilchrist, L. S., Nartey, A. J., & Mesce, K. A. (2002). Distribution and development of dopamine- and octopamine-synthesizing neurons in the medicinal leech. *Journal of Comparative Neurology*, *442*(2), 115–129. https://doi.org/10.1002/CNE.10077

Crisp, K. M., & Mesce, K. A. (2003). To swim or not to swim: regional effects of serotonin, octopamine and amine mixtures in the medicinal leech. *Journal of Comparative Physiology A 2003 189:6*, *189*(6), 461–470. https://doi.org/10.1007/S00359-003-0424-0

Croll, R. P. (2006). Development of embryonic and larval cells containing serotonin, catecholamines, and FMRFamide-related peptides in the gastropod mollusc *Phestilla sibogae*. *Biological Bulletin*, *211*(3), 232–247. https://doi.org/10.2307/4134546

Croll, R. P., & Dickinson, A. J. G. (2004). Form and function of the larval nervous system in molluscs. *Invertebrate Reproduction and Development*, *46*(2–3), 173–187. https://doi.org/10.1080/07924259.2004.9652620

Croll, R. P., Jackson, D. L., & Voronezhskaya, E. E. (1997). Catecholamine-containing cells in larval and postlarval bivalve molluscs. *The Biological Bulletin*, *193*(2), 116–124. https://doi.org/10.2307/1542757

Croll, R. P., & Voronezhskaya, E. E. (1996). Early elements in gastropod neurogenesis. *Developmental Biology*, *173*(1), 344–347. https://doi.org/10.1006/DBIO.1996.0028

Dacey, R. G., & Bassett, J. E. (1987). Histaminergic vasodilation of intracerebral arterioles in the rat. *Journal of Cerebral Blood Flow and Metabolism*, *7*(3), 327–331. https://doi.org/10.1038/jcbfm.1987.70

Dacks, A. M., Reisenman, C. E., Paulk, A. C., & Nighorn, A. J. (2010). Histamine-immunoreactive local neurons in the antennal lobes of the *hymenoptera*. *Journal of Comparative Neurology*, *518*(15), 2917–2933. https://doi.org/10.1002/cne.22371

David, B., & Mooi, R. (2014). How Hox genes can shed light on the place of echinoderms among the deuterostomes. *EvoDevo*, *5*(1), 1–19. https://doi.org/10.1186/2041-9139-5-22

David, J. C., & Coulon, J. F. (1985). Octopamine in invertebrates and vertebrates. A review. *Progress in Neurobiology*, *24*(2), 141–185. https://doi.org/10.1016/0301-0082(85)90009-7

De Robertis, E. M., & Sasai, Y. (1996). A common plan for dorsoventral patterning in Bilateria. *Nature*, *380*, 37–40. https://doi.org/https://doi.org/10.1038/380037a0

Denes, A. S., Jékely, G., Steinmetz, P. R. H., Raible, F., Snyman, H., Prud'homme, B., … Arendt, D. (2007). Molecular architecture of annelid nerve cord supports common origin of nervous system centralization in Bilateria. *Cell*, *129*(2), 277–288. https://doi.org/10.1016/j.cell.2007.02.040

Dere, E., De Souza-Silva, M. A., Topic, B., Spieler, R. E., Haas, H. L., & Huston, J. P. (2003). Histidine-decarboxylase knockout mice show deficient nonreinforced episodic object memory, improved negatively reinforced water-maze performance, and increased neo- and ventro-striatal dopamine turnover. *Learning and Memory*, *10*(6), 510–519. https://doi.org/10.1101/lm.67603

Dickinson, A. J. G., & Croll, R. P. (2003). Development of the larval nervous system of the gastropod *Ilyanassa obsoleta*. *Journal of Comparative Neurology*, *466*(2), 197–218. https://doi.org/10.1002/cne.10863

Dickinson, A. J. G., Croll, R. P., & Voronezhskaya, E. E. (2000). Development of embryonic cells containing serotonin, catecholamines, and FMRFamide-related peptides in *Aplysia californica*. *Biological Bulletin*, *199*(3), 305–315. https://doi.org/10.2307/1543187

Dickinson, A. J. G., Nason, J., & Croll, R. P. (1999). Histochemical localization of FMRFamide, serotonin and catecholamines in embryonic *Crepidula fornicata* (Gastropoda, Prosobranchia). *Zoomorphology*, *119*(1), 49–62. https://doi.org/10.1007/s004350050080

Diefenbach, T. J., Koss, R., & Goldberg, J. I. (1998). Early development of an identified serotonergic neuron in *Helisoma trivolvis* embryos: Serotonin expression, de-expression, and uptake. *Journal of Neurobiology*, *34*(4), 361–376. https://doi.org/10.1002/(SICI)1097-4695(199803)34:4<361::AID-NEU6>3.0.CO;2-4

Dougan, D. F. H., & Wade, D. N. (1985). Octopamine receptors in the molluscan aortic bulb: Effects of clozapine and chlordimeform. *Comparative Biochemistry and Physiology Part C: Comparative Pharmacology*, *82*(1), 193–197. https://doi.org/10.1016/0742-8413(85)90228-2

Duch, C., & Pflüger, H. J. (1999). DUM neurons in locust flight: A model system for amine-mediated peripheral adjustments to the requirements of a central motor program. *Journal of Comparative Physiology - A Sensory, Neural, and Behavioral Physiology*, *184*(5), 489–499. https://doi.org/10.1007/s003590050349

Elekes, K., Eckert, M., & Rapus, J. (1993). Small sets of putative interneurons are octopamine-immunoreactive in the central nervous system of the pond snail, *Lymnaea stagnalis*. *Brain Research*, *608*(2), 191–197. https://doi.org/10.1016/0006-8993(93)91458-5

Elekes, K., Voronezhskaya, E. E., Hiripi, L., Eckert, M., & Rapus, J. (1996). Octopamine in the developing nervous system of the pond snail, *Lymnaea stagnalis* L. *Acta Biologica Hungarica*, *47*(1–4), 73–87. https://pubmed.ncbi.nlm.nih.gov/9124014/

El-Sakkary, N., Chen, S., Arkin, M. R., Caffrey, C. R., & Ribeiro, P. (2018). Octopamine signaling in the metazoan pathogen *schistosoma mansoni*: Localization, small-molecule screening and opportunities for drug development. *DMM Disease Models and Mechanisms*, *11*(7). https://doi.org/10.1242/DMM.033563/VIDEO-4

Elste, A., Koester, J., Shapiro, E., Panula, P., & Schwartz, J. H. (1990). Identification of histaminergic neurons in *Aplysia*. *Journal of Neurophysiology*, *64*(3), 736–744. https://doi.org/10.1152/JN.1990.64.3.736

Erspamer, V. (1948). Active substances in the posterior salivary glands of Octopoda. I. Enteramine-like substance. *Acta Pharmacologica et Toxicologica*, *4*(3–4), 213–223. https://doi.org/10.1111/J.1600-0773.1948.TB03344.X

Erwin, D. H. (2020). The origin of animal body plans: A view from fossil evidence and the regulatory genome. *Development*, *147*(4). https://doi.org/10.1242/dev.182899

Erwin, D. H., & Davidson, E. H. (2009). The evolution of hierarchical gene regulatory networks. *Nature Reviews Genetics*, *10*(2), 141–148. https://doi.org/10.1038/nrg2499

Evans, P. D. (1978). Octopamine: from metabolic mistake to modulator. *Trends in Neurosciences*, *1*(2), 154–157. https://doi.org/10.1016/0166-2236(78)90096-6

Farooqui, T. (2007). Octopamine-mediated neuromodulation of insect senses. *Neurochemical Research 2007 32:9*, *32*(9), 1511–1529. https://doi.org/10.1007/S11064-007-9344-7

Fernández-Montoya, J., Avendaño, C., & Negredo, P. (2018). The glutamatergic system in primary somatosensory neurons and its involvement in sensory input-dependent plasticity. *International Journal of Molecular Sciences*, *19*(1). https://doi.org/10.3390/IJMS19010069

Fritsch, M., Wollesen, T., De Oliveira, A. L., & Wanninger, A. (2015). Unexpected co-linearity of Hox gene expression in an aculiferan mollusk. *BMC Evolutionary Biology*, *15*(1), 1–17. https://doi.org/10.1186/s12862-015-0414-1

Fuchs, H. L., Gerbi, G. P., Hunter, E. J., & Christman, A. J. (2018). Waves cue distinct behaviors and differentiate transport of congeneric snail larvae from sheltered versus wavy habitats. *Proceedings of the National Academy of Sciences of the United States of America*, *115*(32), E7532–E7540. https://doi.org/10.1073/pnas.1804558115

Furness, J. B., Costa, M., & Wilson, A. J. (1977). Water-stable fluorophores, produced by reaction with aldehyde solutions, for the histochemical localization of catechol- and indolethylamines. *Histochemistry*, *52*(2), 159–170. https://doi.org/10.1007/BF00492292

Gao, W., Wiederhold, M., & Hejl, R. (1997). Development of the statocyst in the freshwater snail *Biomphalaria glabrata* (Pulmonata, Basommatophora). *Hearing Research*, *109*(1–2), 125–134. https://doi.org/10.1016/S0378-5955(97)00059-2

Glenner, H., Hansen, A. J., Sørensen, M. V., Ronquist, F., Huelsenbeck, J. P., & Willerslev, E. (2004). Bayesian inference of the metazoan phylogeny: A combined molecular and morphological approach. *Current Biology*, *14*, 1644–1649. https://doi.org/10.1016/j

Goldberg, J. L., Koehncke, N. K., Christopher, K. J., Neumann, C., & Diefenbach, T. J. (1994). Pharmacological characterization of a serotonin receptor involved in an early embryonic behavior of *Helisoma trivolvis*. *Journal of Neurobiology*, *25*(12), 1545–1557. https://doi.org/10.1002/NEU.480251207

Goodman, C. S., & Spitzer, N. C. (1979). Embryonic development of identified neurones: Differentiation from neuroblast to neurone. *Nature*, *280*(5719), 208–214. https://doi.org/10.1038/280208a0

Goosey, M. W., & Candy, D. J. (1982). The release and removal of octopamine by tissues of the locust *Schistocerca americana gregaria*. *Insect Biochemistry*, *12*(6), 681–685. https://doi.org/10.1016/0020-1790(82)90057-9

Gurdon, J. B., & Bourillot, P. Y. (2001). Morphogen gradient interpretation. *Nature*, *413*(6858), 797–803. https://doi.org/10.1038/35101500

Haas, H. L., Sergeeva, O. A., & Selbach, O. (2008). Histamine in the nervous system. *Physiological Reviews*, *88*(3), 1183–1241. https://doi.org/10.1152/physrev.00043.2007

Haas, H., & Panula, P. (2003). The role of histamine and the tuberomamillary nucleus in the nervous system. *Nature Reviews Neuroscience*, *4*(2), 121–130. https://doi.org/10.1038/nrn1034

Habib, M. R., Mohamed, A. H., Osman, G. Y., Sharaf El-Din, A. T., Mossalem, H. S., Delgado, N., … Croll, R. P. (2015). Histamine immunoreactive elements in the central and peripheral nervous systems of the snail, *Biomphalaria spp.*, intermediate host for *Schistosoma mansoni*. *PloS One*, *10*(6), e0129800. https://doi.org/10.1371/journal.pone.0129800

Hadfield, M. G., Meleshkevitch, E. A., & Boudko, D. Y. (2000). The apical sensory organ of a gastropod veliger is a receptor for settlement cues. *The Biological Bulletin*, *198*(1), 67–76. https://doi.org/10.2307/1542804

Håkanson, R., Böttcher, G., Ekblad, E., Panula, P., Simonsson, M., Dohlsten, M., … Sundler, F. (1986). Histamine in endocrine cells in the stomach - A survey of several species using a panel of histamine antibodies. *Histochemistry*, *86*(1), 5–17. https://doi.org/10.1007/BF00492340

Håkanson, R., & Owman, C. (1967). Concomitant histochemical demonstration of histamine and catecholamines in enterochromaffin-like cells of gastric mucosa. *Life Sciences*, *6*(7), 759–766. https://doi.org/10.1016/0024-3205(67)90133-6

Hamasaka, Y., & Nässel, D. R. (2006). Mapping of serotonin, dopamine, and histamine in relation to different clock neurons in the brain of *Drosophila*. *Journal of Comparative Neurology*, *494*(2), 314–330. https://doi.org/10.1002/cne.20807

Haszprunar, G. (1985). The fine morphology of the osphradial sense organs of the Mollusca. I. Gastropoda, Prosobranchia. *Philosophical Transactions of the Royal Society of London. Series B, Biological Sciences*, *307*(1133), 457–496. https://www-jstor-org.ezproxy.library.dal.ca/stable/2990171?sid=primo&seq=1

Haszprunar, G. (1987). The fine morphology of the osphradial sense organs of the Mollusca. III. Placophora and Bivalvia. *Philosophical Transactions of the Royal Society of London. B, Biological Sciences*, *315*(1169), 37–61. https://doi.org/10.1098/RSTB.1987.0002

Hay-Schmidt, A. (1990a). Catecholamine-containing, serotonin-like and neuropeptide FMRFamide-like immunoreactive cells and processes in the nervous system of the pilidium larva (Nemertini). *Zoomorphology*, *109*, 231–244. https://link.springer.com/content/pdf/10.1007/BF00312190.pdf

Hay-Schmidt, A. (1990b). Distribution of catecholamine-containing, serotonin-like and neuropeptide FMRFamide-like immunoreactive neurons and processes in the nervous system of the actinotroch larva of *Phoronis muelleri* (Phoronida). *Cell and Tissue Research*, *259*(1), 105–118. https://doi.org/10.1007/BF00571435

Hegedűs, E., Kaslin, J., & Elekes, K. (2004a). Embryogenesis of the histaminergic system in the pond snail, *Lymnaea stagnalis* L.: An immunocytochemical and biochemical study. *Acta Biologica Hungarica*, *55*(1–4), 301–313. https://doi.org/10.1556/ABiol.55.2004.1-4.36

Hegedűs, E., Kaslin, J., Hiripi, L., Kiss, T., Panula, P., & Elekes, K. (2004b). Histaminergic neurons in the central and peripheral nervous system of gastropods (*Helix*, *Lymnaea*): an immunocytochemical, biochemical, and electrophysiological approach. *The Journal of Comparative Neurology*, *475*(3), 391–405. https://doi.org/10.1002/cne.20171

Hejnol, A., & Lowe, C. J. (2015). Embracing the comparative approach: How robust phylogenies and broader developmental sampling impacts the understanding of nervous system evolution. *Philosophical Transactions of the Royal Society B: Biological Sciences*, *370*(1684). https://doi.org/10.1098/rstb.2015.0045

Hillier, N. K., & Kavanagh, R. M. B. (2015). Differential octopaminergic modulation of olfactory receptor neuron responses to sex pheromones in *Heliothis virescens*. *PLoS ONE*, *10*(12), 1–15. https://doi.org/10.1371/journal.pone.0143179

Hindinger, S., Schwaha, T., & Wanninger, A. (2013). Immunocytochemical studies reveal novel neural structures in nemertean pilidium larvae and provide evidence for incorporation of larval components into the juvenile nervous system. *Frontiers in Zoology*, *10*(1), 1–13. https://doi.org/10.1186/1742-9994-10-31

Hiripi, L., Vehovszky, Á., Juhos, S., & Elekes, K. (1998). An octopaminergic system in the CNS of the snails, *Lymnaea stagnalis* and *Helix pomatia*. *Philosophical Transactions of the Royal Society B: Biological Sciences*, *353*(1375), 1621–1629. https://doi.org/10.1098/rstb.1998.0314

Hiroi, T., Imaoka, S., & Funae, Y. (1998). Dopamine formation from tyramine by CYP2D6. *Biochemical and Biophysical Research Communications*, *249*(3), 838–843. https://doi.org/10.1006/BBRC.1998.9232

Hirth, F. (2010). On the origin and evolution of the tripartite brain. *Brain, Behavior and Evolution*, *76*(1), 3–10. https://doi.org/10.1159/000320218

Hirth, F., Kammermeier, L., Frei, E., Walldorf, U., Noll, M., & Reichert, H. (2003). An urbilaterian origin of the tripartite brain: Developmental genetic insights from *Drosophila*. *Development*, *130*(11), 2365–2373. https://doi.org/10.1242/dev.00438

Histamine Antibody | Immunostar. (n.d.). Retrieved March 25, 2022, from https://www.immunostar.com/product/histamine-antibody/

Holland, L. Z. (2015). Evolution of basal deuterostome nervous systems. *Journal of Experimental Biology*, *218*(4), 637–645. https://doi.org/10.1242/jeb.109108

Holland, L. Z., & Short, S. (2008). Gene duplication, co-option and recruitment during the origin of the vertebrate brain from the invertebrate chordate brain. *Brain, Behavior and Evolution*, *72*(2), 91–105. https://doi.org/10.1159/000151470

Holland, N. D. (2003). Early central nervous system evolution: An era of skin brains? *Nature Reviews Neuroscience*, *4*(8), 617–627. https://doi.org/10.1038/nrn1175

Holland, P. W. H. (2013). Evolution of homeobox genes. *Wiley Interdisciplinary Reviews: Developmental Biology*, *2*(1), 31–45. https://doi.org/10.1002/wdev.78

Holley, S. A., Jackson, P. D., Sasai, Y., Lu, B., De Robertis, E. M., Hoffmann, F. M., & Ferguson, E. L. (1995). A conserved system for dorsal-ventral patterning in insects and vertebrates involving *sog* and *chordin*. *Nature*, *376*(6537), 249–253. https://doi.org/10.1038/376249a0

Hong, S. T., Bang, S., Paik, D., Kang, J., Hwang, S., Jeon, K., … Kim, J. (2006). Histamine and its receptors modulate temperature-preference behaviors in *Drosophila*. *The Journal of Neuroscience*, *26*(27), 7245–7256. https://doi.org/10.1523/JNEUROSCI.5426-05.2006

Ibrahim, K. E., Couch, M. W., Williams, C. M., Fregly, M. J., & Midgley, J. M. (1985). m-Octopamine: Normal occurrence with p-octopamine in mammalian sympathetic nerves. *Journal of Neurochemistry*, *44*(6), 1862–1867. https://doi.org/10.1111/j.1471-4159.1985.tb07180.x

Ishizuka, T., & Yamatodani, A. (2012). Integrative role of the histaminergic system in feeding and taste perception. *Frontiers in Systems Neuroscience*, *6*, 44. https://doi.org/10.3389/fnsys.2012.00044

Jackson, A. R., MacRae, T. H., & Croll, R. P. (1995). Unusual distribution of tubulin isoforms in the snail *Lymnaea stagnalis*. *Cell and Tissue Research*, *281*(3), 507–515. https://doi.org/10.1007/BF00417868

Jin, H., Koyama, T., Hatanaka, Y., Akiyama, S., Takayama, F., & Kawasaki, H. (2006). Histamine-induced vasodilation and vasoconstriction in the mesenteric resistance artery of the rat. *European Journal of Pharmacology*, *529*(1–3), 136–144. https://doi.org/10.1016/j.ejphar.2005.10.060

Joh, T. H., & Hwang, O. (1987). Dopamine beta-hydroxylase: Biochemistry and molecular biology. *Annals of the New York Academy of Sciences*, *493*(1), 342–350. https://doi.org/10.1111/J.1749-6632.1987.TB27217.X

Joyce, A., & Vogeler, S. (2018). Molluscan bivalve settlement and metamorphosis: Neuroendocrine inducers and morphogenetic responses. *Aquaculture*, *487*(October 2017), 64–82. https://doi.org/10.1016/j.aquaculture.2018.01.002

Jung, J. W., Kim, J. H., Pfeiffer, R., Ahn, Y. J., Page, T. L., & Kwon, H. W. (2013). Neuromodulation of olfactory sensitivity in the peripheral olfactory organs of the American cockroach, *Periplaneta americana*. *PLoS ONE*, *8*(11), 1–11. https://doi.org/10.1371/journal.pone.0081361

Juorio, A. V., & Molinoff, P. B. (1974). The normal occurrence of octopamine in neural tissues of the octopus and other cephalopods. *Journal of Neurochemistry*, *22*(2), 271–280. https://doi.org/10.1111/j.1471-4159.1974.tb11590.x

Jutel, M., Watanabe, T., Klunker, S., Akdis, M., Thomet, O. A. R., Malolepszy, J., … Akdis, C. A. (2001). Histamine regulates T-cell and antibody responses by differential expression of H1 and H2 receptors. *Nature*, *413*(6854), 420–425. https://doi.org/10.1038/35096564

Kammermeier, L., & Reichert, H. (2001). Common developmental genetic mechanisms for patterning invertebrate and vertebrate brains. *Brain Research Bulletin*, *55*(6), 675–682. https://doi.org/10.1016/S0361-9230(01)00559-7

Kempf, S. C., Page, L. R., & Pires, A. (1997). Development of serotonin-like immunoreactivity in the embryos and larvae of nudibranch mollusks with emphasis on the structure and possible function of the apical sensory organ. *Journal of Comparative Neurology*, *386*(3), 507–528. https://doi.org/10.1002/(SICI)1096-9861(19970929)386:3<507::AID-CNE12>3.0.CO;2-7

Kimelman, D., & Martin, B. L. (2012). Anterior-posterior patterning in early development: Three strategies. *Wiley Interdisciplinary Reviews: Developmental Biology*, *1*(2), 253–266. https://doi.org/10.1002/wdev.25

Konings, P. N. M., Vullings, H. G. B., Geffard, M., Buijs, R. M., Diederen, J. H. B., & Jansen, W. F. (1988). Immunocytochemical demonstration of octopamine-immunoreactive cells in the nervous system of *Locusta migratoria* and *Schistocerca gregaria*. *Cell and Tissue Research*, *251*(2), 371–379. https://doi.org/10.1007/BF00215846

Kononenko, N., Kiss, T., & Elekes, K. (2012). The neuroanatomical and ultrastructural organization of statocyst hair cells in the pond snail, *Lymnaea stagnalis*. *Acta Biologica Hungarica*, *63*(SUPPL. 1), 99–113. https://doi.org/10.1556/ABiol.63.2012.Suppl.1.10

Koss, R., Diefenbach, T. J., Kuang, S., Doran, S. A., & Goldberg, J. I. (2003). Coordinated development of identified serotonergic neurons and their target ciliary cells in *Helisoma trivolvis* embryos. *Journal of Comparative Neurology*, *457*(4), 313–325. https://doi.org/10.1002/cne.10512

Kriegstein, A. R. (1977a). Development of the nervous system of *Aplysia californica*. *Proceedings of the National Academy of Sciences of the United States of America*, *74*(1), 375–378. https://doi.org/10.1073/pnas.74.1.375

Kriegstein, A. R. (1977b). Stages in the post-hatching development of *Aplysia californica*. *Journal of Experimental Zoology*, *199*(2), 275–288. https://doi.org/10.1002/jez.1401990212

Kurita, Y., & Wada, H. (2011). Evidence that gastropod torsion is driven by asymmetric cell proliferation activated by TGF-β signalling. *Biology Letters*, *7*(5), 759. https://doi.org/10.1098/RSBL.2011.0263

Lacalli, T. C. (1981). Structure and development of the apical organ in trochophores of *Spirobranchus polycerus*, *Phyllodoce maculata* and *Phyllodoce mucosa* (Polychaeta). *Proceedings of the Royal Society of London. Series B, Biological Sciences*, *212*(1189), 381–402. https://www.jstor.org/stable/35660

Lacalli, T. C. (1995). Dorsoventral axis inversion. *Nature*, *373*(6510), 110–111. https://doi.org/10.1038/373110c0

Lappin, T. R. J., Grier, D. G., Thompson, A., & Halliday, H. L. (2006). HOX genes: Seductive science, mysterious mechanisms. *Ulster Medical Journal*, *75*(1), 23–31.

Larroux, C., Fahey, B., Degnan, S. M., Adamski, M., Rokhsar, D. S., & Degnan, B. M. M. (2007). The NK homeobox gene cluster predates the origin of Hox genes. *Current Biology*, *17*(8), 706–710. https://doi.org/10.1016/j.cub.2007.03.008

Lemus, R., & Karol, M. H. (2008). Conjugation of Haptens. In M. G. Jones & P. Lympany (Eds.), *Methods in molecular medicine* (Vol. 138). Humana Press. https://doi.org/10.1007/978-1-59745-366-0_14

Lewis, E. B. (1978). A gene complex controlling segmentation in *Drosophila*. *Nature*, *276*(5688), 565–570. https://doi.org/10.1038/276565a0

Lewis, E. J., & Asnani, L. P. (1992). Soluble and membrane-bound forms of dopamine beta-hydroxylase are encoded by the same mRNA. *Journal of Biological Chemistry*, *267*(1), 494–500. https://doi.org/10.1016/S0021-9258(18)48522-5

Lichtneckert, R., & Reichert, H. (2005). Insights into the urbilaterian brain: Conserved genetic patterning mechanisms in insect and vertebrate brain development. *Heredity*, *94*(5), 465–477. https://doi.org/10.1038/sj.hdy.6800664

Lin, M. F., & Leise, E. M. (1996). Gangliogenesis in the prosobranch gastropod *Ilyanassa obsoleta*. *Journal of Comparative Neurology*, *374*(2), 180–193. https://doi.org/10.1002/(SICI)1096-9861(19961014)374:2<180::AID-CNE2>3.0.CO;2-Z

Lindberg, D. R., & Sigwart, J. D. (2015). What is the molluscan osphradium? A reconsideration of homology. *Zoologischer Anzeiger*, *256*, 14–21. https://doi.org/10.1016/j.jcz.2015.04.001

Lowe, C. J., Wu, M., Salic, A., Evans, L., Lander, E., Stange-Thomann, N., … Kirschner, M. (2003). Anteroposterior patterning in hemichordates and the origins of the chordate nervous system. *Cell*, *113*(7), 853–865. https://doi.org/10.1016/S0092-8674(03)00469-0

Madeira, F., Park, Y. M., Lee, J., Buso, N., Gur, T., Madhusoodanan, N., … Lopez, R. (2019). The EMBL-EBI search and sequence analysis tools APIs in 2019. *Nucleic Acids Research*, *47*(W1), W636–W641. https://doi.org/10.1093/NAR/GKZ268

Marlow, H. Q., Srivastava, M., Matus, D. Q., Rokhsar, D., & Martindale, M. Q. (2009). Anatomy and development of the nervous system of *Nematostella vectensis*, an anthozoan cnidarian. *Developmental Neurobiology*, *69*(4), 235–254. https://doi.org/10.1002/dneu.20698

Marlow, H., Tosches, M. A., Tomer, R., Steinmetz, P. R., Lauri, A., Larsson, T., & Arendt, D. (2014). Larval body patterning and apical organs are conserved in animal evolution. *BMC Biology*, *12*, 1–17. https://doi.org/10.1186/1741-7007-12-7

Marois, R., & Croll, R. P. (1992). Development of serotoninlike immunoreactivity in the embryonic nervous system of the snail *Lymnaea stagnalis*. *Journal of Comparative Neurology*, *322*(2), 255–265. https://doi.org/10.1002/CNE.903220211

McCain, E. R. (1992). Cell interactions influence the pattern of biomineralization in the *Ilyanassa obsoleta* (mollusca) embryo. *Developmental Dynamics*, *195*(3), 188–200. https://doi.org/10.1002/aja.1001950305

McCune, A. R., & Schimenti, J. C. (2012). Using genetic networks and homology to understand the evolution of phenotypic traits. *Current Genomics*, *13*(1), 74–84. https://doi.org/10.2174/138920212799034785

Mercer, A. R., & Menzel, R. (1982). The effects of biogenic amines on conditioned and unconditioned responses to olfactory stimuli in the honeybee *Apis mellifera*. *Journal of Comparative Physiology □ A*, *145*(3), 363–368. https://doi.org/10.1007/BF00619340

Metcalfe, D. D., Baram, D., & Mekori, Y. A. (1997). Mast cells. *Physiological Reviews*, *77*(4), 1033–1079. https://doi.org/10.1152/PHYSREV.1997.77.4.1033

Miyamoto, N., Nakajima, Y., Wada, H., & Saito, Y. (2010). Development of the nervous system in the acorn worm *Balanoglossus simodensis*: insights into nervous system evolution. *Evolution & Development*, *12*(4), 416–424. https://doi.org/10.1111/J.1525-142X.2010.00428.X

Mochizuki, T., Yamatodani, A., Okakura, K., Horii, A., Inagaki, N., & Wada, H. (1992). Circadian rhythm of histamine release from the hypothalamus of freely moving rats. *Physiology & Behavior*, *51*(2), 391–394. https://doi.org/10.1016/0031-9384(92)90157-W

Moroz, L. L. (2009). On the independent origins of complex brains and neurons. *Brain, Behavior and Evolution*, *74*(3), 177–190. https://doi.org/10.1159/000258665

Nagy, L., & Hiripi, L. (2002). Role of tyrosine, DOPA and decarboxylase enzymes in the synthesis of monoamines in the brain of the locust. *Neurochemistry International*, *41*(1), 9–16. https://doi.org/10.1016/S0197-0186(01)00141-3

Nässel, D. R. (1999). Histamine in the brain of insects: A review. *Microscopy Research and Technique*, *44*(2–3), 121–136. https://doi.org/10.1002/(SICI)1097-0029(19990115/01)44:2/3<121::AID-JEMT6>3.0.CO;2-F

Nezlin, L., Moroz, L., Elofsson, R., & Sakharov, D. (1994a). Immunolabeled neuroactive substances in the osphradium of the pond snail *Lymnaea stagnalis*. *Cell and Tissue Research*, *275*(2), 269–275. https://doi.org/10.1007/BF00319424

Nezlin, L. P., Elofsson, R., & Sakharov, D. A. (1994b). Transmitter-specific subsets of sensory elements in the prosobranch osphradium. *Biological Bulletin*, *187*(2), 174–184. https://doi.org/10.2307/1542240

Nielsen, C. (1985). Animal phylogeny in the light of the trochaea theory. *Biological Journal of the Linnean Society*, *25*(3), 243–299. https://doi.org/10.1111/J.1095-8312.1985.TB00396.X

Nielsen, C. (1999). Origin of the chordate central nervous system and the origin of chordates. *Development Genes and Evolution*, *209*(3), 198–205. https://doi.org/10.1007/s004270050244

Nielsen, C. (2004). Trochophora larvae: Cell-lineages, ciliary bands, and body regions. 1. Annelida and Mollusca. *Journal of Experimental Zoology Part B: Molecular and Developmental Evolution*, *302*(1), 35–68. https://doi.org/10.1002/jez.b.20001

Nielsen, C. (2005). Trochophora larvae: Cell-lineages, ciliary bands and body regions. 2. Other groups and general discussion. *Journal of Experimental Zoology Part B: Molecular and Developmental Evolution*, *304*(5), 401–447. https://doi.org/10.1002/jez.b.21050

Nielsen, C. (2018). Origin of the trochophora larva. *Royal Society Open Science*, *5*(7). https://doi.org/10.1098/rsos.180042

Nielsen, C., Brunet, T., & Arendt, D. (2018). Evolution of the bilaterian mouth and anus. *Nature Ecology and Evolution*, *2*(9), 1358–1376. https://doi.org/10.1038/s41559-018-0641-0

Nielsen, C., & Norrevang, A. (1985). The trochaea theory: an example of life cycle phylogeny. *The Origin and Relationships of Lower Invertebrates*, 28–41.

Northcutt, R. G. (2012). Evolution of centralized nervous systems: Two schools of evolutionary thought. *Proceedings of the National Academy of Sciences of the United States of America*, *109*(SUPPL.1), 10626–10633. https://doi.org/10.1073/pnas.1201889109

Ohsuga, K., Kurokawa, M., & Kuwasawa, K. (2000). Mosaic arrangement of SCPb-, FMRFamide-, and histamine-like immunoreactive sensory hair cells in the statocyst of the gastropod mollusc *Pleurobranchaea japonica*. *Cell and Tissue Research*, *300*(1), 165–172. https://doi.org/10.1007/S004410000186

Omond, S. E. T., Hale, M. W., & Lesku, J. A. (2022). Neurotransmitters of sleep and wakefulness in flatworms. *Sleep*. https://doi.org/10.1093/SLEEP/ZSAC053

Orchard, I., & Lange, A. B. (1984). Cyclic AMP in locust fat body: Correlation with octopamine and adipokinetic hormones during flight. *Journal of Insect Physiology*, *30*(12), 901–904. https://doi.org/10.1016/0022-1910(84)90066-0

Page, L. R. (2003). Gastropod ontogenetic torsion: Developmental remnants of an ancient evolutionary change in body plan. *Journal of Experimental Zoology Part B: Molecular and Developmental Evolution*, *297*(1), 11–26. https://doi.org/10.1002/jez.b.12

Page, L. R., & Parries, S. C. (2000). Comparative study of the apical ganglion in planktotrophic caenogastropod larvae: Ultrastructure and immunoreactivity to serotonin. *Journal of Comparative Neurology*, *418*(4), 383–401. https://doi.org/10.1002/(SICI)1096-9861(20000320)418:4<383::AID-CNE2>3.0.CO;2-B

Papaefthimiou, C., & Theophilidis, G. (2011). Octopamine—A single modulator with double action on the heart of two insect species (*Apis mellifera macedonica* and *Bactrocera oleae*): Acceleration vs. inhibition. *Journal of Insect Physiology*, *57*(2), 316–325. https://doi.org/10.1016/J.JINSPHYS.2010.11.022

Pedrozo, H. A., Schwartz, Z., Luther, M., Dean, D. D., Boyan, B. D., & Wiederhold, M. L. (1996). A mechanism of adaptation to hypergravity in the statocyst of *Aplysia californica*. *Hearing Research*, *102*(1–2), 51–62. https://doi.org/10.1016/S0378-5955(96)00147-5

Pflüger, H. J., & Stevenson, P. A. (2005). Evolutionary aspects of octopaminergic systems with emphasis on arthropods. *Arthropod Structure and Development*, *34*(3), 379–396. https://doi.org/10.1016/j.asd.2005.04.004

Phillips, T. (2008). Gradient-based DNA transcription control in animals. *Nature Education*, *1*(1), 179. https://www.nature.com/scitable/topicpage/gradient-based-dna-transcription-control-in-animals-1062/

Prinz, C., Zanner, R., & Gratzl, M. (2003). Physiology of gastric enterochromaffin-like cells. *Annual Review of Physiology*, *65*(3), 371–382. https://doi.org/10.1146/annurev.physiol.65.092101.142205

Pryce, K., Samuel, D., Lagares, E., Myrthil, M., Bess, F., Harris, A., … Catapane, E. J. (2015). Presence of octopamine and an octopamine receptor in *Crassostrea virginica*. *In Vivo*, *37*(1), 16. /pmc/articles/PMC4652596/

Python, F., & Stocker, R. F. (2002). Immunoreactivity against choline acetyltransferase, γ-aminobutyric acid, histamine, octopamine, and serotonin in the larval chemosensory system of *Drosophila melanogaster*. *Journal of Comparative Neurology*, *453*(2), 157–167. https://doi.org/10.1002/cne.10383

Raven, Ch. P. (1966). Morphogenesis: The analysis of molluscan development. In J. E. Harris & E. W. Yemm (Eds.), *International Series of Monographs on Pure and Applied Biology* (Vol. 8, Issue 5). Pergamon Press. http://hdl.handle.net/2027/uc1.b4339746

Ravhe, I. S., Krishnan, A., & Manoj, N. (2021). Evolutionary history of histamine receptors: Early vertebrate origin and expansion of the H3-H4 subtypes. *Molecular Phylogenetics and Evolution*, *154*, 106989. https://doi.org/10.1016/J.YMPEV.2020.106989

Rawlinson, K. A. (2010). Embryonic and post-embryonic development of the polyclad flatworm *Maritigrella crozieri*; implications for the evolution of spiralian life history traits. *Frontiers in Zoology*, *7*(1), 1–25. https://doi.org/10.1186/1742-9994-7-12/FIGURES/9

Render, J. (1997). Cell fate maps in the *Ilyanassa obsoleta* embryo beyond the third division. *Developmental Biology*, *189*(2), 301–310. https://doi.org/10.1006/DBIO.1997.8654

Rentzsch, F., Fritzenwanker, J. H., Scholz, C. B., & Technau, U. (2008). FGF signalling controls formation of the apical sensory organ in the cnidarian *Nematostella vectensis*. *Development*, *135*(10), 1761–1769. https://doi.org/10.1242/dev.020784

Robertson, H. A. (1981). Octopamine--after a decade as a putative neuroregulator. *Essays in Neurochemistry and Neuropharmacology*, *5*, 47–73. https://pubmed.ncbi.nlm.nih.gov/6112146/

Roeder, T. (1999). Octopamine in invertebrates. *Progress in Neurobiology*, *59*(5), 533–561. https://doi.org/10.1016/S0301-0082(99)00016-7

Roeder, T. (2003). Metabotropic histamine receptors - Nothing for invertebrates? *European Journal of Pharmacology*, *466*(1–2), 85–90. https://doi.org/10.1016/S0014-2999(03)01553-X

Roeder, T. (2020). The control of metabolic traits by octopamine and tyramine in invertebrates. *Journal of Experimental Biology*, *223*(7). https://doi.org/10.1242/jeb.194282

Romero, L. M., & Gormally, B. M. G. (2019). How truly conserved is the "well-conserved" vertebrate stress response? *Integrative and Comparative Biology*, *59*(2), 273–281. https://doi.org/10.1093/ICB/ICZ011

Rudolf, R., & Straka, T. (2019). Nicotinic acetylcholine receptor at vertebrate motor endplates: Endocytosis, recycling, and degradation. *Neuroscience Letters*, *711*, 134434. https://doi.org/10.1016/J.NEULET.2019.134434

Ryan, J. F., & Baxevanis, A. D. (2007). Hox, Wnt, and the evolution of the primary body axis: Insights from the early-divergent phyla. *Biology Direct*, *2*. https://doi.org/10.1186/1745-6150-2-37

Saavedra, J. M., Brownstein, M. J., Carpenter, D. O., & Axelrod, J. (1974). Octopamine: Presence in single neurons of *Aplysia* suggests neurotransmitter function. *Science*, *185*(4148), 364–365. https://doi.org/10.1126/SCIENCE.185.4148.364

Sachse, S., Peele, P., Silbering, A. F., Gühmann, M., & Galizia, C. G. (2006). Role of histamine as a putative inhibitory transmitter in the honeybee antennal lobe. *Frontiers in Zoology*, *3*, 1–7. https://doi.org/10.1186/1742-9994-3-22

Salamanca-Díaz, D. A., Calcino, A. D., De Oliveira, A. L., & Wanninger, A. (2021). Non-collinear Hox gene expression in bivalves and the evolution of morphological novelties in mollusks. *Scientific Reports*, *11*(1), 1–12. https://doi.org/10.1038/s41598-021-82122-6

Samadi, L., & Steiner, G. (2009). Involvement of Hox genes in shell morphogenesis in the encapsulated development of a top shell gastropod (*Gibbula varia L.*). *Development Genes and Evolution*, *219*(9–10), 523–530. https://doi.org/10.1007/s00427-009-0308-6

Sandmeier, E., Hale, T. I., & Christen, P. (1994). Multiple evolutionary origin of pyridoxal-5′-phosphate-dependent amino acid decarboxylases. *European Journal of Biochemistry*, *221*(3), 997–1002. https://doi.org/10.1111/J.1432-1033.1994.TB18816.X

Santagata, S. (2011). Evaluating neurophylogenetic patterns in the larval nervous systems of brachiopods and their evolutionary significance to other bilaterian phyla. *Journal of Morphology*, *272*(10), 1153–1169. https://doi.org/10.1002/jmor.10975

Satterlie, R. A., & Andrew Cameron, R. (1985). Electrical activity at metamorphosis in larvae of the sea urchin *Lytechinus pictus* (Echinoidea: Echinodermata). *Journal of Experimental Zoology*, *235*(2), 197–204. https://doi.org/10.1002/JEZ.1402350206

Sayin, S., De Backer, J. F., Siju, K. P., Wosniack, M. E., Lewis, L. P., Frisch, L. M., … Grunwald Kadow, I. C. (2019). A neural circuit arbitrates between persistence and withdrawal in hungry *Drosophila*. *Neuron*, *104*(3), 544-558.e6. https://doi.org/10.1016/j.neuron.2019.07.028

Scaros, A. T., Andouche, A., Baratte, S., & Croll, R. P. (2020). Histamine and histidine decarboxylase in the olfactory system and brain of the common cuttlefish *Sepia officinalis* (Linnaeus, 1758). *Journal of Comparative Neurology*, *528*(7), 1095–1112. https://doi.org/10.1002/cne.24809

Schneider, H., Budhiraja, P., Walter, I., Beltz, B. S., Peckol, E., & Kravitz, E. A. (1996). Developmental expression of the octopamine phenotype in lobsters, *Homarus americanus*. *Journal of Comparative Neurology*, *371*(1), 3–14. https://doi.org/10.1002/(SICI)1096-9861(19960715)371:1<3::AID-CNE1>3.0.CO;2-7

Selbach, O., Brown, R. E., & Haas, H. L. (1997). Long-term increase of hippocampal excitability by histamine and cyclic AMP. *Neuropharmacology*, *36*(11–12), 1539–1548. https://doi.org/10.1016/S0028-3908(97)00144-5

Shen, K., & Cowan, C. W. (2010). Guidance molecules in synapse formation and plasticity. *Cold Spring Harbor Perspectives in Biology*, *2*(4), 1842–1843. https://doi.org/10.1101/CSHPERSPECT.A001842

Sinakevitch, I. G., Geffard, M., Pelhate, M., & Lapied, B. (1994). Octopamine-like immunoreactivity in the dorsal unpaired median (DUM) neurons innervating the accessory gland of the male cockroach *Periplaneta americana*. *Cell and Tissue Research*, *276*(1), 15–21. https://doi.org/10.1007/BF00354779

Sinigaglia, C., Busengdal, H., Lerner, A., Oliveri, P., & Rentzsch, F. (2015). Molecular characterization of the apical organ of the anthozoan *Nematostella vectensis*. *Developmental Biology*, *398*(1), 120. https://doi.org/10.1016/J.YDBIO.2014.11.019

Sly, B. J., Snoke, M. S., & Raff, R. A. (2003). Who came first-larvae or adults? Origins of bilaterian metazoan larvae Life history modes and metazoan phylogeny. *J. Dev. Biol*, *47*, 623–632. www.ijdb.ehu.es

Smarandache-Wellmann, C. R. (2016). Arthropod neurons and nervous system. *Current Biology*, *26*(20), R960–R965. https://doi.org/10.1016/J.CUB.2016.07.063

Soinila, S., Mpitsos, G. J., & Panula, P. (1990). Comparative study of histamine immunoreactivity in nervous systems of *Aplysia* and *Pleurobranchaea*. *The Journal of Comparative Neurology*, *298*(1), 83–96. https://doi.org/10.1002/cne.902980107

Strausfeld, N. J., & Hirth, F. (2015). Introduction to 'Origin and evolution of the nervous system.' *Philosophical Transactions of the Royal Society B: Biological Sciences*, *370*(1684), 20150033. https://doi.org/10.1098/rstb.2015.0033

Strecker, R. E., Nalwalk, J., Dauphin, L. J., Thakkar, M. M., Chen, Y., Ramesh, V., … McCarley, R. W. (2002). Extracellular histamine levels in the feline preoptic/anterior hypothalamic area during natural sleep-wakefulness and prolonged wakefulness: An in vivo microdialysis study. *Neuroscience*, *113*(3), 663–670. https://doi.org/10.1016/S0306-4522(02)00158-6

Stuart, A. E., Borycz, J., & Meinertzhagen, I. A. (2007). The dynamics of signaling at the histaminergic photoreceptor synapse of arthropods. *Progress in Neurobiology*, *82*(4), 202–227. https://doi.org/10.1016/j.pneurobio.2007.03.006

Sutherby, J., Giardini, J. L., Nguyen, J., Wessel, G., Leguia, M., & Heyland, A. (2012). Histamine is a modulator of metamorphic competence in *Strongylocentrotus purpuratus* (Echinodermata: Echinoidea). *BMC Developmental Biology*, *12*. https://doi.org/10.1186/1471-213X-12-14

Swanson, R. L., Byrne, M., Prowse, T. A. A., Mos, B., Dworjanyn, S. A., & Steinberg, P. D. (2012). Dissolved histamine: A potential habitat marker promoting settlement and metamorphosis in sea urchin larvae. *Marine Biology*, *159*(4), 915–925. https://doi.org/10.1007/s00227-011-1869-2

Swanson, R. L., Williamson, J. E., De Nys, R., Kumar, N., Bucknall, M. P., & Steinberg, P. D. (2004). Induction of settlement of larvae of the sea urchin *Holopneustes purpurascens* by histamine from a host alga. *Biological Bulletin*, *206*(3), 161–172. https://doi.org/10.2307/1543640

Thangam, E. B., Jemima, E. A., Singh, H., Baig, M. S., Khan, M., Mathias, C. B., Church, M. K., & Saluja, R. (2018). The role of histamine and histamine receptors in mast cell-mediated allergy and inflammation: The hunt for new therapeutic targets. *Frontiers in Immunology*, *9*, 1873. https://doi.org/10.3389/fimmu.2018.01873

Tomlinson, S. G. (1987). Intermediate stages in the embryonic development of the gastropod *Ilyanassa obsoleta*: A scanning electron microscope study. *International Journal of Invertebrate Reproduction and Development*, *12*(3), 253–280. https://doi.org/10.1080/01688170.1987.10510325

Tuomisto, L., Lozeva, V., Valjakka, A., & Lecklin, A. (2001). Modifying effects of histamine on circadian rhythms and neuronal excitability. *Behavioural Brain Research*, *124*(2), 129–135. https://doi.org/10.1016/S0166-4328(01)00222-4

Urbach, R., & Technau, G. (n.d.). *Dorsoventral Patterning of the Brain: A Comparative Approach - Madame Curie Bioscience Database - NCBI Bookshelf*. Madame Curie Bioscience Database. Retrieved March 26, 2022, from https://www.ncbi.nlm.nih.gov/books/NBK6006/

van Kessel, S. P., Frye, A. K., El-Gendy, A. O., Castejon, M., Keshavarzian, A., van Dijk, G., & El Aidy, S. (2019). Gut bacterial tyrosine decarboxylases restrict levels of levodopa in the treatment of Parkinson's disease. *Nature Communications*, *10*(1), 1–11. https://doi.org/10.1038/s41467-019-08294-y

Vehovszky, Á., Elliott, C. J. H., Voronezhskaya, E. E., Hiripi, L., & Elekes, K. (1998). Octopamine: A new feeding modulator in *Lymnaea*. *Philosophical Transactions of the Royal Society B: Biological Sciences*, *353*(1375), 1631–1643. https://doi.org/10.1098/rstb.1998.0315

Vehovszky, Á., Szabó, H., & Elliott, C. J. H. (2005). Octopamine increases the excitability of neurons in the snail feeding system by modulation of inward sodium current but not outward potassium currents. *BMC Neuroscience*, *6*. https://doi.org/10.1186/1471-2202-6-70

Voronezhskaya, E. E., & Elekes, K. (1996). Transient and sustained expression of FMRFamide-like immunoreactivity in the developing nervous system of *Lymnaea stagnalis* (Mollusca, Pulmonata). *Cellular and Molecular Neurobiology*, *16*(6), 661–676. https://doi.org/10.1007/BF02151903

Voronezhskaya, E. E., Hiripi, L., Elekes, K., & Croll, R. P. (1999). Development of catecholaminergic neurons in the pond snail, *Lymnaea stagnalis*: I. Embryonic development of dopamine-containing neurons and dopamine-dependent behaviors. *The Journal of Comparative Neurology*, *404*(3), 285–296. https://doi.org/10.1002/(SICI)1096-9861(19990215)404:3

Voronezhskaya, E. E., Khabarova, M. Y., & Nezlin, L. P. (2004). Apical sensory neurones mediate developmental retardation induced by conspecific environmental stimuli in freshwater pulmonate snails. *Development*, *131*(15), 3671–3680. https://doi.org/10.1242/dev.01237

Voronezhskaya, E. E., & Khabarova, M. Yu. (2003). Function of the apical sensory organ in the development of invertebrates. *Doklady Biological Sciences: Proceedings of the Academy of Sciences of the USSR, Biological Sciences Sections*, *390*(1/6), 231–234. https://doi.org/10.1023/A:1024453416281

Wada, H., Saiga, H., Satoh, N., & Holland, P. W. H. (1998). Tripartite organization of the ancestral chordate brain and the antiquity of placodes: insights from ascidian Pax-2/5/8, Hox and Otx genes. *Development*, *125*(6), 1113–1122. https://doi.org/10.1242/DEV.125.6.1113

Wada, H., & Satoh, N. (2001). Patterning the protochordate neural tube. *Current Opinion in Neurobiology*, *11*(1), 16–21. https://doi.org/10.1016/S0959-4388(00)00168-9

Wagner, G. P. (2007). The developmental genetics of homology. *Nature Reviews Genetics*, *8*(6), 473–479. https://doi.org/10.1038/nrg2099

Wang, X., Li, J., Dong, G., & Yue, J. (2014). The endogenous substrates of brain CYP2D. *European Journal of Pharmacology*, *724*(1), 211–218. https://doi.org/10.1016/j.ejphar.2013.12.025

Wanninger, A. (2009). Shaping the things to come: Ontogeny of lophotrochozoan neuromuscular systems and the tetraneuralia concept. *Biological Bulletin*, *216*(3), 293–306. https://doi.org/10.2307/25548161

Wanninger, A., Ruthensteiner, B., & Haszprunar, G. (2000). Torsion in *Patella caerulea* (Mollusca, Patellogastropoda): Ontogenetic process, timing, and mechanisms. *Invertebrate Biology*, *119*(2), 177–187. https://doi.org/10.1111/J.1744-7410.2000.TB00006.X

Wanninger, A., & Wollesen, T. (2019). The evolution of molluscs. *Biological Reviews*, *94*(1), 102–115. https://doi.org/10.1111/BRV.12439

Watanabe, H., Fujisawa, T., & Holstein, T. W. (2009). Cnidarians and the evolutionary origin of the nervous system. *Development Growth and Differentiation*, *51*(3), 167–183. https://doi.org/10.1111/j.1440-169X.2009.01103.x

Webber, M. P., Thomson, J. W. S., Buckland-Nicks, J., Croll, R. P., & Wyeth, R. C. (2017). GABA-, histamine-, and FMRFamide-immunoreactivity in the visual, vestibular and central nervous systems of *Hermissenda crassicornis*. *Journal of Comparative Neurology*, *525*(16), 3514–3528. https://doi.org/10.1002/cne.24286

Weiss, K. R., Shapiro, E., & Kupfermann, I. (1986). Modulatory synaptic actions of an identified histaminergic neuron on the serotonergic metacerebral cell of *Aplysia*. *Journal of Neuroscience*, *6*(8), 2393–2402. https://doi.org/10.1523/jneurosci.06-08-02393.1986

Wiederhold, M. L., Sharma, J. S., Driscoll, B. P., & Harrison, J. L. (1990). Development of the statocyst in *Aplysia californica* I. Observations on statoconial development. *Hearing Research*, *49*(1–3), 63–78. https://doi.org/10.1016/0378-5955(90)90095-7

Wiederhold, M. L., Sheridan, C. E., & Smith, N. K. (1986). Statoconia formation in molluscan statocysts. *Scanning Electron Microscopy*, *Pt 2*, 781–792. https://pubmed.ncbi.nlm.nih.gov/11539732/

Williamson, R. (1989). Electrophysiological evidence for cholinergic and catecholaminergic efferent transmitters in the statocyst of octopus. *Comparative Biochemistry and Physiology Part C: Comparative Pharmacology*, *93*(1), 23–27. https://doi.org/10.1016/0742-8413(89)90004-2

Wollesen, T., Wanninger, A., & Klussmann-Kolb, A. (2007). Neurogenesis of cephalic sensory organs of *Aplysia californica*. *Cell and Tissue Research*, *330*(2), 361–379. https://doi.org/10.1007/S00441-007-0460-0/FIGURES/10

Wurst, W., & Bally-Cuif, L. (2001). Neural plate patterning: upstream and downstream of the isthmic organizer. *Nature Reviews Neuroscience*, *2*(2), 99–108. https://doi.org/10.1038/35053516

Wyeth, R. C., & Croll, R. P. (2011). Peripheral sensory cells in the cephalic sensory organs of *Lymnaea stagnalis*. *The Journal of Comparative Neurology*, *519*(10), 1894–1913. https://doi.org/10.1002/cne.22607

Yamauchi, K., & Ogasawara, M. (2019). The role of histamine in the pathophysiology of asthma and the clinical efficacy of antihistamines in asthma therapy. *International Journal of Molecular Sciences*, *20*(7). https://doi.org/10.3390/ijms20071733

Yang, Z., Yu, Y., Zhang, V., Tian, Y., Qi, W., & Wang, L. (2015). Octopamine mediates starvation-induced hyperactivity in adult *Drosophila*. *Proceedings of the National Academy of Sciences of the United States of America*, *112*(16), 5219–5224. https://doi.org/10.1073/pnas.1417838112

Young, A. P., Beach, G. A., Croll, R. P., Jackson, D. J., & Wyeth, R. C. (2022). Tyrosine hydroxylase messenger RNA corroborates protein localization in the nervous system of the pond snail, *Lymnaea stagnalis*. *Invertebrate Biology*, e12367. https://doi.org/10.1111/IVB.12367

Young, C. M. (2003). *Atlas of Marine Invertebrate Larvae* (M. A. Sewell & M. E. Rice, Eds.). Academic Press. https://doi.org/10.1046/J.1365-2109.2003.00819.X

Zaitseva, O. v. (2001). The structural organization of the statocyst sensory system in nudibranch mollusks. *Neuroscience and Behavioral Physiology*, *31*(1), 111–117. https://doi.org/10.1023/A:1026646902656

Zhu, H., Xu, G., Zhang, K., Kong, X., Han, R., Zhou, J., & Ni, Y. (2016). Crystal structure of tyrosine decarboxylase and identification of key residues involved in conformational swing and substrate binding. *Scientific Reports*, *6*(February), 1–10. https://doi.org/10.1038/srep27779